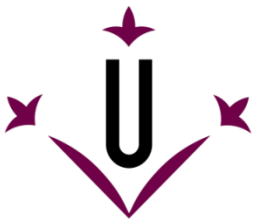

Universitat de Lleida

Document downloaded from:

http://hdl.handle.net/10459.1/68382

The final publication is available at:

https://doi.org/10.1007/s13595-019-0824-0

Copyright

(c) INRA and Springer-Verlag France SAS, part of Springer Nature, 2019

A general method for the classification of forest stands using species composition and vertical and horizontal structure

Miquel De Cáceres[1], Santiago Martín-Alcón[1], José R. González-Olabarria[1], Lluís Coll[1,2]

[1] Forest Science and Technology Centre of Catalonia (CTFC), Solsona 25280 Spain

[2] Department of Agriculture and Forest Engineering (EAGROF), University of Lleida, 25198 Lleida, Spain. Email address: lluis.coll@ctfc.cat

* Corresponding address: miquelcaceres@gmail.com

Key message: We present a novel approach to define pure- and mixed-forest typologies from the comparison of pairs of forest plots in terms of species identity, diameter and height of their trees.

Abstract

Context: Forest typologies are useful for many purposes, including forest mapping, assessing habitat quality, studying forest dynamics or defining sustainable management strategies. Quantitative typologies meant for forestry applications normally focus on horizontal and vertical structure of forest plots as main classification criteria, with species composition often playing a secondary role. The selection of relevant variables is often idiosyncratic and influenced by a priori expectations of the forest types to be distinguished.

Aims and methods: Here we present a general framework to define forest typologies where the dissimilarity between forest stands is assessed using coefficients that integrate the information of species composition with the univariate distribution of tree diameters or heights or the bivariate distribution of tree diameters and heights. We illustrate our proposal with a classification of forests plots in Catalonia (NE Spain) using available forest inventory data.

Results: The number of subtypes obtained using the tree diameter distribution for the calculation of dissimilarity where often the same as those obtained from the tree height distribution or to those using the bivariate distribution. However, classifications obtained using the three approaches where often different in terms of forest plot membership.

Conclusion: The proposed classification framework is particularly suited to define forest typologies from forest inventory data and allows taking advantage of the bivariate distribution of diameters and heights if both variables are measured. It can provide support to the development of typologies in situations where fine-scale variability of topographic, climatic and legacy management factors leads to fine-scale variation in forest structure and composition, including uneven-aged and mixed stands.

Keywords: dissimilarity coefficients, forest plot, forest typology, mixed forests, stand structure

Introduction

Vegetation classifications are powerful tools to describe, summarize and represent the variation of vegetation across space and time (De Cáceres et al. 2015). The development and use of typologies in forestry can be traced back to the birth of forest science, because forest types have traditionally helped foresters to summarize site and stand quality, a prerequisite for predicting potential growth or timber yield (Cajander 1949). Nowadays, forest typologies are important tools for assessing and monitoring the state of forest ecosystems at several scales (Corona 2016). They are useful for many purposes, such as assessing habitat quality or the vulnerability to disturbances, anticipating forest dynamics or mapping forest resources for the definition of sustainable stand-oriented management strategies (e.g., James and Wamer 1982; Bebi et al. 2001; Bruciamacchie 2001; Barbati et al. 2007, 2014). In addition, combining detailed forest typologies with three-dimensional remote sensing data has recently shown its potential for mapping variations on developmental stages, post-disturbance regeneration patterns or even the change of management activities on forested landscapes (Falkowski et al. 2009; Bottalico et al. 2014; Martín-Alcón et al. 2015; Valbuena et al. 2016, 2017).

Forest typologies can be rather informal qualitative descriptions, sometimes complemented with profile diagrams to make them easier to communicate (O'Hara et al. 1996; Larsen and Nielsen 2007). Alternatively, they can be defined quantitatively and the resulting forest classes be differentiated using formal assignment rules (e.g. classification trees) on the basis of chosen thresholds for relevant variables (e.g., Bebi et al. 2001; Bruciamacchie 2001; Giannetti et al. 2018). Quantitative assignment rules can be defined by expert knowledge, after preliminary inspection of the main axes of variation of potential variables (e.g., Aunós et al. 2007), but a more data-driven approach involves two steps: (1) to define homogeneous groups of forest plots using unsupervised classification methods (i.e., hierarchical or non-hierarchical clustering); (2) to define assignment rules by means of supervised classification (e.g., discriminant analysis, classification trees or neural networks), using the classification produced in the first step as training data (Reque and Bravo 2008; Martín-Alcón et al. 2012; De Cáceres and Wiser 2012). The first step of the data-driven approach requires deciding how to measure the *resemblance* between forest plots, i.e. deciding which structural and compositional

67 variables are relevant and how to combine their information in a resemblance (dissimilarity or
68 similarity) coefficient.

69 Fine-grained quantitative forest typologies normally focus on structure as main classification
70 criteria (e.g., basal area, canopy cover, the distribution of tree diameters and heights, stocking density
71 or wood volume) (Faith et al. 1985; McElhinny et al. 2005). Very often, the chosen variables are
72 expressed in different units (e.g., basal area vs. dominant height) and/or are partially correlated (e.g.
73 basal area vs. mean quadratic diameter), which requires employing variable standardization or factor
74 analysis prior to the calculation of distances between forest stands (e.g., Reque and Bravo 2008;
75 Martín-Alcón et al. 2012; Casals et al. 2015). Besides the need to represent both horizontal and
76 vertical structure, there are no standard choices of relevant variables and procedures to define
77 typologies, which results in variable choices being rather idiosyncratic to each classification analysis.
78 In addition, the scope of typologies is often restricted to forests where a single target species is
79 dominating or has minimum abundance (in terms of basal area or number of individuals). For
80 example, in Spain quantitative forest typologies have focused on silver fir (*Abies alba* Mill.), beech
81 (*Fagus sylvatica* L.), sessile oak (*Quercus petraea* Matt.) or mountain pine (*Pinus uncinata* Ram.)
82 forests (Aunós et al. 2007; Reque and Bravo 2008; Martín-Alcón et al. 2012). The role of other tree
83 species than the target ones is only accounted for implicitly, by considering variables such as the
84 percentage of the total basal area corresponding to the target species or the ratio of the average size
85 for individuals of the target species compared to others (Aunós et al. 2007; Reque and Bravo 2008).
86 Although coarse forest typologies exist simultaneously addressing variation in structure and
87 composition (e.g., Godinho-Ferreira et al. 2005; Barbati et al. 2014), quantitative classifications
88 addressing in detail the compositional and structural variation of mixed-forests are rare (Ngo Bieng et
89 al. 2006). This may seem surprising, since mixed forests occupy almost one-fourth (23%) of the
90 European's forested land (FOREST EUROPE et al. 2011) and their importance is progressively
91 increasing in response to the growing complexity of societal demands (Bravo-Oviedo et al. 2014).
92 Adopting similarity or dissimilarity coefficients designed to account for multiple structural and

93 compositional attributes would allow defining fine forest typologies in different contexts (even-aged
94 vs. uneven-aged, pure vs. mixed) in a more consistent way.

95 Ecologists have long compared the composition of plant or animal communities using species
96 presence-absence or abundance data (i.e. cover or density values) and multivariate resemblance
97 coefficients (Legendre and Legendre 2012). However, the usefulness of this type of coefficients in
98 forestry is rather limited, due to the inability to simultaneously consider the vertical and horizontal
99 structure of stands. At most, compositional coefficients have been used for the classification of stands
100 in terms of the composition within canopy and understory layers separately (Youngblood 1993). De
101 Cáceres et al. (2013) presented a general framework to compare ecological communities that takes
102 into account size structure and composition simultaneously, and illustrated their approach for the
103 comparison of forest stands in terms of diameter distribution and tree species identity. While this
104 framework has been successfully applied to describe and typify the structure and composition of
105 Anatolian black pine forests (Yılmaz et al. 2018) and to assess the amount structural and
106 compositional variation within forests (Yao et al. 2019), its full potential for the definition of forest
107 typologies remains to be explored. Moreover, when characterizing and/or differentiating forest stands
108 from a forestry perspective both the distribution of tree diameters and tree heights may be relevant,
109 because the provision of several forest goods (e.g., timber quantity and quality) and services (e.g., soil
110 protection or habitat quality) depends on the distribution of these two variables. Although the two are
111 often correlated, general frameworks to measure the resemblance between forest stands could take
112 into account the joint bivariate distribution of diameters and heights.

113 The objectives of this article are twofold. First, we introduce an extension of the De Cáceres et
114 al. (2013) framework to allow considering two size variables (namely height and diameter), instead of
115 only one, when calculating the resemblance between forest stands. Second, we illustrate the
116 usefulness of this approach to define typologies of different kinds, including pure vs. mixed stands or
117 even-aged vs. uneven-aged stands. In the following section, we first review the conceptual and
118 mathematical aspects of the framework of De Cáceres et al. (2013), describe its extension to consider
119 two size variables, and present a small simulation study that illustrates the behaviour of the proposed

dissimilarity coefficients. Then, we use our dissimilarity framework and unsupervised clustering techniques to derive pure- and mixed-forest typologies from forest inventory data. When doing that, we compare the results obtained using the bivariate distribution of tree diameters and heights with those obtained using one of the two marginal distributions only. Finally, we discuss the advantages and limitations of the resemblance framework, including potential applications beyond the definition of typologies.

Resemblance between forest stands in terms of structure and composition

Original framework

The framework of De Cáceres et al. (2013) allows defining and calculating the dissimilarity between forest stands in a flexible way, depending on the variable choices made by the user regarding three aspects of stand organization (Pommerening 2002):

a. *Abundance* (i.e. horizontal structure): A non-negative variable to represent the space occupied by plants, such as density, (projected) crown cover or basal area.
b. *Size* (i.e. vertical structure): A (continuous or ordinal) variable to represent plant size, such as tree diameter or plant height.
c. *Composition*: A categorization of plants, such as species composition, growth forms or other functional distinction.

Choices for (a) and (b) imply specifying a distribution of the total abundance into size classes (e.g., overall density or basal area into tree diameter or height classes). Instead of using this size distribution directly, however, the framework operates on the basis of cumulative values. The *cumulative abundance profile* (CAP) is a function taking a size value as input and returning the cumulative abundance of plants whose size is equal to or larger than the input value. For example, if tree diameter is chosen as the size variable and basal area as the abundance variable, the CAP value is the cumulative basal area corresponding to trees as thick as or thicker than the input diameter (see Fig. 1).

145 CAP is a non-increasing function whose value is always maximal for the smallest value of the size
146 variable (e.g., the cumulative basal area corresponding to the smallest diameter class is equal to the
147 basal area of the stand).

148 The procedure to calculate the resemblance between a pair of forest stands can be summarized
149 in three steps: (1) calculating the CAP for each tree species (or compositional class) in each of the two
150 stands; (2) comparing the CAPs of the two stands for each species; (3) pooling the result of CAP
151 comparisons across species with an appropriate dissimilarity coefficient. The details of the three steps
152 are as follows (De Cáceres et al. 2013):

153 Step 1 – Calculation of CAP, following the definition given above, is done for each k species
154 and for each of the two stands separately. The importance accorded to differences in stand horizontal
155 structure (a), vertical structure (b) and composition (c) will depend on the variables and/or
156 transformations chosen to represent these aspects when building CAPs. For example, dividing trees
157 into angiosperm and gymnosperms, instead of using species composition, will decrease the
158 importance of compositional vs. structural differences. Similarly, the importance of vertical structure
159 can be modulated by changing the resolution of diameter or height bins (Yao et al. 2019). Unequal
160 widths of diameter or height bins can be used to modulate the importance accorded to differences in
161 abundance across tree size (e.g., using diameter quadratic bins will increase the importance of
162 differences in saplings). Finally, the role of horizontal structure can be modulated by transforming
163 CAPs prior to their comparison. For example, a square root transformation applied to cumulative
164 abundance values will decrease the importance of differences in horizontal structure with respect to
165 the other aspects (De Cáceres et al. 2013).

166 Step 2 –The comparison of the two CAPs for a given species k – CAP_{1k} and CAP_{2k} – is done by
167 integrating the comparison of cumulative abundance values along the values of the structural variable.
168 This comparison leads to distinguishing between three regions in the diagram that shows the two
169 CAPs: A_k, the areas where the two profiles overlap; B_k, the areas where CAP_{1k} exceeds CAP_{2k}; and C_k,

the areas where CAP_{2k} exceeds CAP_{1k} (Fig. 1b). If θ is the size variable, the three quantities are mathematically calculated using:

$$
\begin{aligned}
A_k &= \int_{\theta=0}^{\infty} \min(\mathrm{CAP}_{1k}(\theta), \mathrm{CAP}_{2k}(\theta)) \cdot d\theta \\
B_k &= \int_{\theta=0}^{\infty} (\mathrm{CAP}_{1k}(\theta) - \min(\mathrm{CAP}_{1k}(\theta), \mathrm{CAP}_{2k}(\theta))) \cdot d\theta \\
C_k &= \int_{s=0}^{\infty} (\mathrm{CAP}_{2j}(\theta) - \min(\mathrm{CAP}_{1k}(\theta), \mathrm{CAP}_{2k}(\theta))) \cdot d\theta
\end{aligned}
\tag{1}
$$

While eq. 1 assumes a continuous size variable, if one employs a discrete size variable (i.e., height or diameter bins) to define CAPs, then A_k, B_k and C_k are calculated replacing integrals in eq. 1 by summations across size classes.

Step 3 – The species-wise comparison of pairs of CAPs results in values A_k, B_k and C_k for each species k. At this point, compositional resemblance coefficients typical of community ecology can be calculated, provided they can be decomposed into quantities analogous to A_k, B_k and C_k (Tamás et al. 2001). Although several coefficients where presented in De Cáceres et al. (2013), we focus here on D_{man} and D_{bray}, which are generalizations of the Manhattan (or city-block) distance and the Percentage difference (alias Bray-Curtis) dissimilarity (Odum 1950; Bray and Curtis 1957), respectively. The Manhattan distance calculated across all species (from $k = 1$ to $k = p$ species or compositional classes) is:

$$
D_{man} = \sum_{k=1}^{p} (B_k + C_k) \tag{2}
$$

and the corresponding generalization of the Bray-Curtis dissimilarity is:

$$
D_{bray} = \frac{\sum_{k=1}^{p} (B_k + C_k)}{\sum_{k=1}^{p} (2A_k + B_k + C_k)} \tag{3}
$$

The main difference between D_{man} and D_{bray} is that the latter involves a normalizing factor that relativizes the dissimilarity between the two stands to the [0-1] interval. For example, in the single-species case of the CAPs represented in Fig. 1b, $D_{man} = 31.8$ and $D_{bray} = 0.265$.

190 *Extension of the framework*

191 With the aim of comparing forest stands in terms of their observed bivariate distribution of tree
192 heights and diameters, we define here the *cumulative abundance surface* (CAS) as a function taking a
193 *pair* of values of size variables and returning the cumulative abundance of individuals whose sizes are
194 equal to or larger than the values given. If one takes height and diameter as size variables and basal
195 area as abundance measure, the CAS function will return the basal area of trees as tall as or taller than
196 the input height value and, at the same time, whose diameter is as thick as or thicker than the input
197 diameter value (Fig. 2a-b). Like the marginal distributions of any bivariate joint distribution, CAS can
198 be marginalized into the CAPs of its two size variables (Fig. 2c-d).

199 The calculation of resemblance between stands is analogous to the original procedure but
200 replacing the role of CAPs by CASs. In Step 1 one calculates the CAS for each species in each stand.
201 The comparison of CAS_{1k} and CAS_{2k} for a given species k (Step 2) is done by integrating the
202 comparison of cumulative abundance values across the plane defined by the two size variables. In this
203 case the intersection of the two surfaces defines three volumes: A_k –the volume common to the two
204 cumulative surfaces; B_k – the volume that occurs in CAS_{1k} but not in CAS_{2k}; and C_k – the volume that
205 occurs in CAS_{2k} but not in stand CAS_{1k}. If θ and φ are the two size variables, the three quantities are:

206
$$A_k = \int_{\theta=0}^{\infty}\int_{\varphi=0}^{\infty} \min(\mathrm{CAS}_{1k}(\theta,\varphi), \mathrm{CAS}_{2k}(\theta,\varphi)) \cdot d\theta \cdot d\varphi$$
$$B_k = \int_{\theta=0}^{\infty}\int_{\varphi=0}^{\infty} (\mathrm{CAS}_{1k}(\theta,\varphi) - \min(\mathrm{CAS}_{1k}(\theta,\varphi), \mathrm{CAS}_{2k}(\theta,\varphi))) \cdot d\theta \cdot d\varphi \quad (4)$$
$$C_k = \int_{\theta=0}^{\infty}\int_{\varphi=0}^{\infty} (\mathrm{CAS}_{2k}(\theta,\varphi) - \min(\mathrm{CAS}_{1k}(\theta,\varphi), \mathrm{CAS}_{2k}(\theta,\varphi))) \cdot d\theta \cdot d\varphi$$

207 As before, we require the resemblance indices (Step 3) to be a function of A_k, B_k and C_k for each
208 species. In particular, D_{man} and D_{bray} (eqs. 2 and 3) can be calculated without modification. Functions
209 to build CASs and to calculate the resemblance coefficients D_{man} and D_{bray} have been included in the
210 R package 'vegclust' (De Cáceres et al. 2010).

211 *Simulation study*

We simulated tree data using Johnson's Sbb distribution (Johnson 1949; Schreuder and Hafley 1977) to study whether D_{man} and D_{bray} can reflect differences in terms of total basal area, tree diameter distribution and tree height distribution (see details in Appendix S1). We did not include differences in composition because they were already studied in De Cáceres et al. (2013). In a first experiment we simulated 25 different stands by crossing five treatments in stand basal area (5, 10, 15, 20 and 25 m^2/ha; labeled '1' to '5') with five treatments in size distribution (labeled 'a' to 'e'), assuming that when stands had trees larger in diameter those trees were also taller (i.e., in treatment 'a' mean dbh/height was 5cm/4m; in 'b' 12cm/5m; up to 80cm/20m in 'e'). In a second experiment we simulated stands having all the same basal area (25 m^2/ha) but differing in height distribution, diameter distribution, or both. In this case we crossed five treatments in diameter distribution (labeled 'a' to 'e') with five treatments in tree height distribution (labeled '1' to '5'). Thus, stands could be composed of short and thin trees, tall and thin trees, short and thick trees, or tall and thick trees; with intermediates situations being also covered. For every stand, we simulated tree individuals until the target basal area was met.

The CAS for each stand was built taking basal area as abundance variable and tree diameter and tree height as size variables. We then calculated the resemblance between all pairs of the 25 stands using either D_{man} or D_{bray}. Kruskal's non-metric multidimensional scaling was used to display each of the resulting dissimilarity matrices in a two-dimensional scatter plot (Fig. 3). Both coefficients were responsive to variations in stand basal area, tree height distribution and tree diameter distribution, and the resulting resemblance matrices satisfactorily preserved the ordering of stands along the simulated gradients of the two experiments. Nevertheless, the behaviour of D_{man} and D_{bray} differed in the magnitude of dissimilarity values for stands having low basal area. CASs enclose a larger volume when either the basal area of the stand increases or when trees are larger (see Figs. S1.2 and S1.4), which leads to larger values of A_k, B_k and C_k when comparing CASs in those situations. Since D_{man} does not have a normalizing factor in its formula the resulting distance value were affected by differences in CAS volume. The choice of a dissimilarity index should be made in relation to the problem at hand (Legendre and De Cáceres 2013). After inspecting the results of the simulation study,

239 we concluded that D_{man} is more appropriate than D_{bray} for forestry applications because it better
240 represents the differences in the distribution of wood volume across species or tree sizes.

241 **Definition of forest types in Catalonia using forest inventory data**

242 Here we illustrate the usefulness of the framework presented in the previous section to define forest
243 typologies on the basis of differences in stand composition and structure. Starting from forest
244 inventory data, we generated a classification system for forests in Catalonia (NE of Spain) with two
245 classification levels. Forest types of the first (coarser) level were defined using species dominance as
246 single classification criterion whereas the definition of subtypes of the second (finer) level included
247 both composition and structure as classification criteria. To evaluate the effect of considering the
248 bivariate distribution of diameters and heights vs. considering one of the two marginal distributions
249 alone, we compare the typologies obtained using the extended (CAS) framework with the typologies
250 obtained using the original (CAP) framework.

251 *Data preparation*

252 We compiled 10,546 plot records of the Third Spanish Forest Inventory (NFI3) in Catalonia (DGCN
253 2005). NFI3 plots consist of four nested circular subplots (of radius 5, 10, 15 and 25 m). For each
254 subplot, species identity, height (cm) and diameter at breast height (dbh, cm) of a living tree are
255 recorded only if its diameter is larger than a threshold (7.5, 12.5, 22.5 and 42.5 cm, respectively). For
256 example, between 15 m and 25 m radius only trees larger than 42.5 cm are recorded. In subplots of 5
257 m radius, the number of saplings (2.5 cm ≤ dbh ≤ 7.5 cm) per species and their average height is also
258 recorded. We calculated the basal area per hectare (m^2/ha) corresponding to each measured tree by
259 multiplying the normal section of the tree by a density factor that depended on the subplot indicated
260 by its dbh. We focused on forests dominated by the twelve most prevalent tree species in the region:
261 Aleppo pine (*Pinus halepensis* Mill.), Black pine (*P. nigra* Arnold), Scots pine (*Pinus sylvestris* L.),
262 Mountain pine (*Pinus uncinata* Ram.), Stone pine (*Pinus pinea* L.), Maritime pine (*Pinus pinaster*
263 Aiton), European fir (*Abies alba* Mill.), Holm oak (*Quercus ilex* L.), Cork oak (*Q. suber* L.), Downy
264 oak (*Quercus humilis* Mill.), Portuguese oak (*Quercus faginea* Lam.) and European beech (*Fagus*

sylvatica L.). We discarded from the data set a total of 3,168 forest plots where tree species other than those mentioned accounted for more than 20% of basal area or more than 20% of all individuals.

Level 1 – Dominance-based forest types

With the remaining 7,378 plots we first defined forest types depending on species dominance. A given plot was considered to be dominated by one of the twelve tree species if that species alone accounted simultaneously for more than 80% of basal area and more than 80% of tree density. Similarly, the plot was considered as being co-dominated by two species if each of them alone accounted for between 20% and 80% of basal area or density and altogether they accounted for more than 80% of both variables. Forest types defined in this way were only considered valid if they had at least 10 plots assigned to them, to ensure a minimum number of class members. Among the 7,378 plots evaluated, 4,337 were dominated by a single species whereas 2,034 were co-dominated by two species (see Table 1). The remaining 1,007 plots were considered as showing intermediate dominance patterns and were discarded for the definition of forest subtypes. We calculated the non-parametric (Spearman's ρ) correlation between tree diameters and tree heights of each species in each forest plot. Average correlations were rather high for forests dominated by *Abies alba* but much lower for those dominated by oak species like *Quercus ilex* or *Q. faginea* (Table 1).

Level 2 – Forest subtypes

For each dominance-based forest type, we considered the definition of subtypes according to both composition and structure. We generated subtypes using either the extended (CAS) framework or the original (CAP) framework. CASs for each plot and species were built using basal area as abundance variable and taking tree diameter and height as size variables. In order to increase the sensitivity of dissimilarities with respect to recruitment stages, diameter bins were finer to distinguish thin trees than to distinguish thick trees: dbh limits (in cm) for class r were defined as $4 + [(0.5\cdot(r\text{-}1))^2, (0.5\cdot r)^2]$ cm. The resulting bins were: 4 – 6.25 cm, 6.25 – 9 cm, 9 – 12.25 cm, 12.25 – 16 cm, 16 – 20.25 cm, etc. Height classes were defined using 100 cm bins. CAPs were built in the same way as for CASs, taking either tree diameter or tree height as (single) size variable (these will be referred to as CAP(d)

291 or CAP(h), respectively). We evaluated the dissimilarity between pairs of plots using D_{man} (eq. 2),
292 with B_k and C_k calculated from either CAS pairs, CAP(d) pairs or CAP(h) pairs. The correlation
293 between the three resulting dissimilarity matrices was almost always above 0.85 (see Table S2.1 in
294 Appendix S2), indicating a large degree of agreement in the three ways of assessing resemblance
295 between forest stands (but see classification results below). To illustrate how choices regarding the
296 dissimilarity metric and the definition of diameter and height bins may affect the dissimilarity
297 between forest plots, we include in Fig. 4 the results of a small sensitivity analysis using the 434
298 forest plots dominated by *Pinus nigra*. They indicate that the dissimilarity metric (D_{man} or D_{bray}) is the
299 most critical choice (Fig. 4b). After that, including or not the height or diameter distributions (i.e.
300 splitting abundance data into height or diameter bins) leads to markedly different dissimilarity values.
301 Whether bins are more or less finely defined is of lower importance, especially beyond a certain level
302 of resolution (D3-D4 or H3-H4 in Fig.4c).

303 For each dominance-based forest type and each of the three approaches, partitions of different
304 numbers of clusters (from 2 to 12) were obtained as follows. Starting from the square matrix
305 containing distances between pairs of plots, an initial partition was generated by cutting the
306 dendrogram produced by Ward's hierarchical clustering (Ward 1963). Then we used the clustering
307 algorithm Partitioning Around Medoids (Kaufman and Rousseuw 1990) to refine this initial partition.
308 A cluster medoid is defined as the object (i.e. a plot) having the minimal sum of distances to all the
309 other objects in the cluster. We evaluated the final partitions corresponding to different numbers of
310 clusters using Silhouette analysis (Kaufman and Rousseuw 1990). For each forest type, we selected
311 the partition with the maximum number of clusters (subtypes) as long as the average cluster Silhouette
312 was larger than 0.20 and all clusters had at least 10 plots assigned to them. Subtypes were not defined
313 if no partition fulfilled these requirements.

314 The number of subtypes recognized for each dominance-based forest type under each of the
315 three approaches is indicated in Table 2. In general, the number of subtypes depended on the total
316 number of plots included in the dominance-based forest type. For example, pure *P. halepensis* forests,
317 the most frequent type, were subdivided into the largest number of subtypes, whereas only two

318 subtypes were recognized for forests dominated by *A. alba* or *P. pinaster*, both species with low
319 prevalence in the study area. Forests co-dominated by two-species followed the same rule. While six
320 CAS-based subtypes were recognized for the common *P. halepensis – Q. ilex* forests, several other
321 mixed forests were represented by too few plots to be divided into subtypes. Clearly, those
322 dominance-based forest types less represented in the study area were described in less detail.

323 For 19 out of 36 dominance-based types, the number of subtypes distinguished using the CAS
324 framework was equal to the number of subtypes distinguished using either CAP(d) or CAP(h) (Table
325 2). However, the overall number of subtypes was 133 using CAS, 124 using CAP(h) and 100 using
326 CAP(d), indicating a slightly greater diversity of bivariate distributions and height distributions,
327 compared to the diversity of diameter distributions. We calculated the Rand Index (Hubert and Arabie
328 1985) to compare the classifications into subtypes obtained under each approach. This index allows
329 comparing classifications with different numbers of groups and is ranged between 0 (indicating a
330 match between the two classifications no greater than would be expected by chance) and 1 (indicating
331 a perfect match). Surprisingly, the agreement between approaches was rather low for several forest
332 types (Table 2). A high level of agreement was obtained for forests dominated by *Pinus pinea* or
333 *Pinus pinaster*, probably due to a simplicity of forest structures derived from management, but in the
334 remaining cases the agreement was moderate or even low. In particular, the subtypes obtained using
335 either CAS, CAP(d) or CAP(h) were rather different for forests dominated by *Pinus uncinata*, *Pinus*
336 *sylvestris*, *Quercus ilex*, *Q. suber* and *Q. humilis*, indicating a high degree of complexity in forest
337 structures.

338 *Interpretation of CAS forest subtypes*

339 The characterization of all CAS-based subtypes is given in tables (structural statistics) and figures
340 (density and basal area distributions across diameter and height classes) of Appendices S3 and S4 of
341 Supplementary Material. Examining the distribution of density along tree size classes allowed us to
342 interpret subtypes from silvicultural and ecological perspectives. The distinction between subtypes of
343 single-species forests could arise due to a higher density only, without substantial differences in tree

diameter or height distribution; or be due to differences in the distribution of one or both size variables. For instance, among the forest stands dominated by *P. nigra* (Fig. 5 and Table S3.2) four subtypes (PN1, PN2, PN4 and PN5) had diameter and height distributions that indicated different stages of development of even-aged forests, whereas a fifth subtype (PN3) included greater horizontal and vertical irregularity (i.e., uneven-aged stands). Among the even-aged subtypes, PN2 and PN4 reflected similar developmental stages but were noticeably different with regard to stand density. For its part, subtype PN5 not only involved the most mature stand development stage among even-aged forests, but could also be described as a mature and densely stocked uneven-aged stand.

Forests co-dominated by two species with similar degree of shade-tolerance included subtypes where both species had similar contribution to total basal area and subtypes when either one species or the other was more abundant than the other, but often with the two species having similar tree size distributions. For example, the interpretation of subtypes co-dominated by *P. sylvestris* and *P. uncinata* (Fig. 6 and Table S4.10) led to the identification of one young and one more mature stand subtypes, both with similar occupancy of the two species (PSPU1 and PSPU2), and other two mature subtypes, one dominated by *P. sylvestris* (PSPU3), the other by *P. uncinata* (PSPU4). Similar interpretations could be made for pine-pine mixed forests (e.g. *P. nigra – P. sylvestris*, *P. halepensis – P. pinea* or *P. halepensis – P. nigra*) and oak-oak mixed forests (e.g. *Q. ilex – Q. humilis*). In forests co-dominated by two species showing different degrees of shade-tolerance, trees of the shade-intolerant species were generally of larger size than trees of the shade-tolerant species. However, situations where the shade-tolerant species dominated the stand were also identified (see Appendix S4). For example, the six subtypes co-dominated by *P. halepensis* and *Q. ilex* (Fig. 7 and Table S4.3) reflected structural and compositional differences that in some cases indicated different successional stages between the shade-intolerant and the shade-tolerant species. A first subtype (PHQI1) matched with young and open stands co-dominated by the two species. Four of other subtypes (PHQI2, PHQI3, PHQI5 and PHQI6) showed a dominant layer of *P. halepensis* over a non-negligible layer of *Q. ilex*. These subtypes were differentiated by the size and density of pines. The remaining subtype (PHQI4) suggested a more advanced successional stage in which *Q. ilex*, although growing in a lower

371 stratum, had already become dominant in terms of basal area. We reached similar interpretations for
372 several pine-oak mixed forests (i.e. combinations between *P. halepensis*, *P. nigra*, *P. sylvestris* or *P.*
373 *pinea*, on one side, and *Q. ilex*, *Q. suber*, *Q. humilis*, or *Q. faginea*, on the other), but also for other
374 kinds of mixed forests (e.g. *P. sylvestris – F. sylvatica* or *P. uncinata – A. alba*).

375 **Discussion**

376 The approach presented here attempts to simplify the task of determining the resemblance between
377 forest stands. Instead of requiring the selection of multiple variables, often having different units and
378 therefore being difficult to consider simultaneously, our approach allows the analyst to compare the
379 vertical and horizontal structure of forest plots by performing a small set of choices (one or two size
380 variables, an abundance variable and a compositional resolution). Similarly to other approaches based
381 on the Lorenz curves (Valbuena et al. 2013), our approach tries to exploit all the information in the
382 uni- or bivariate distribution of diameters and heights. Thanks to the flexibility of dissimilarity indices
383 based on CAPs and CASs, our approach allows comparing and classifying forest stands of very
384 different kinds. Therefore, even if its spatial grain is the forest plot, the same framework can be
385 applied consistently for large areas if combined with data from large-scale forest surveys such as
386 national forest inventories. Thus, it could be used to complement coarse forest typologies (Barbati et
387 al. 2014) with finer classification levels.

388 One of the main advantages of our approach is its flexibility with regard to the kind of input
389 data that it accepts and the number of ways to analyse it. Multiple choices can be made for size (i.e.,
390 vertical structure) and abundance (i.e., horizontal structure) variables, as well as for the definition of
391 compositional classes. Here we used height and diameter, which seem natural choices of size
392 variables when comparing forest plots using individual tree data. Comparisons between forest stands
393 can be done using both variables and cumulative abundance surfaces (CASs), if both variables have
394 been measured, or using cumulative abundance profiles (CAPs) if only one of them is available. If, for
395 a given forest data set, the vertical structure is defined as vegetation strata, one can adapt the method
396 by defining the highest stratum reached by plants as the size variable. Our approach is also flexible

with respect to the variable chosen to represent horizontal structure (e.g., basal area, projected cover or number of individuals). For example, if forest data consists of records from Airborne LiDAR, one could classify them into forest types choosing height classes as size variable and the number of first LiDAR returns corresponding to each height class as abundance (i.e. horizontal structure) variable. With regard to compositional classes, species taxonomic identity seems a natural choice, but other classes such as functional groups could be used instead. If the presence of dead trees, such as standing snags or fallen logs is deemed relevant (e.g. if forest types need to represent successional stages or habitat quality for wildlife; McComb & Lindenmayer 1999), one can add compositional classes to represent them (diameter and height/length of the dead tree could still be used as size variables). Another source of flexibility comes from the possibility of altering the scale of the size variables or the abundance variable. For example, in our application with forest inventory data we defined quadratic diameter bins, but linear or logarithmic bins would also be possible.

We found that tree diameters did not strongly correlate (monotonically) with heights in our forest inventory data. Further, classifications obtained using the CAS framework where often not very similar to classifications obtained using the original framework (CAP), even if the number of subtypes recognized was often the same. Taking into account the bivariate distribution of diameters and heights may better accommodate to the complexity of forest structures than univariate distributions. However, the observed higher overall number of subtypes could be an artefact derived from inaccuracies in the estimation of tree sizes. Although we focused here on how dissimilarities are defined, other important choices for the definition of typologies are those of the unsupervised classification algorithm and its parameters. With the chosen values for average Silhouette (0.2) and minimum membership (10 plots), the number of subtypes of some forests, like those of *Pinus halepensis*, is probably too high for practical use. Larger values of these thresholds would led to fewer subtypes in these cases, but could compromise the recognition of subtypes less represented in the forest inventory data. Practitioners are welcome to search for parameter combinations that produce interpretable and operational typologies.

While general and flexible, our approach has limitations in the kind of structural variables that can be included (McElhinny et al. 2005). Because it focuses on the structure provided by plants (i.e.

424 trees, shrubs and even herbs), it does not accommodate easily to other structural features such as litter
425 cover or ground cover. Species diversity and variations in plant dimensions are fully represented in
426 our approach, but spacing between plants is only represented in terms of density (Pommerening
427 2002). Unlike in Ngo Bieng et al. (2006), patterns of spatial clumping or segregation of plants are not
428 taken into account for the definition of forest types. Another limitation of the classification approach
429 employed here is that it does not produce determination keys easy to apply for field sampling or
430 assignment rules for mapping with remote sensing data (Valbuena et al. 2013). Supervised
431 classification might be needed to produce membership rules for mapping or keys for field
432 determination. Finally, our approach relies on a sufficiently accurate estimation of the uni- or
433 bivariate distribution of tree diameters and heights in the input data. Limitations derived from field
434 sampling protocols, such as a small plot size or the nested plot structure of our forest inventory data,
435 may be a source of error in the estimation of dissimilarities and the resulting forest classes (Nanos and
436 de Luna 2017).

437 In our opinion the approach presented here allows the description and classification of forest
438 stands (i.e. through forest plot data) at a sufficient level of detail to facilitate forest planning and
439 decision-making in biogeographic contexts where fine-scale variability of topographic, climatic and
440 land-use factors leads to large variability in forest structure and composition (e.g., Bruciamacchie
441 2001). In particular, it allows classifying mixed-forests according to structural attributes over large
442 areas, which remained a difficult and challenging task until now. The compositional and structural
443 typologies obtained using our approach can provide forest managers with critical information for the
444 efficient organization of silvicultural operations in time and space. For example, they could be used to
445 develop type-based management guidelines aiming to either maintain a certain stock and size
446 distribution of trees (e.g., Gove 2004) or emulate natural succession (e.g., Attiwill 1994). If necessary,
447 the structural and compositional dissimilarity between the managed stand and specific forest types
448 could be used to accurately monitor deviations from planned sequences. Finally, our approach could
449 also be used in the study of forest dynamics (De Cáceres et al. 2019). The definition of a forest
450 typology from consecutive surveys of permanent forest plots could provide critical information on the

prevalence of regressive and successional series across a study area, and allow the evaluation of the most important factors driving such changes, including the role of disturbances.

References

Attiwill PM (1994) The disturbance of forest ecosystems: the ecological basis for conservative management. For Ecol Manage 63:247–300. doi: 10.1016/0378-1127(94)90114-7

Aunós A, Martínez E, Blanco R (2007) Tipología selvícola para los abetales españoles de Abies alba Mill. Investig Agrar Sist y Recur For 16:52–64

Barbati A, Corona P, Marchetti M (2007) A forest typology for monitoring sustainable forest management: The case of European Forest Types. Plant Biosyst 141:93–103. doi: 10.1080/11263500601153842

Barbati A, Marchetti M, Chirici G, Corona P (2014) European Forest Types and Forest Europe SFM indicators: Tools for monitoring progress on forest biodiversity conservation. For Ecol Manage 321:145–157. doi: 10.1016/j.foreco.2013.07.004

Bebi P, Kienast F, Schönenberger W (2001) Assessing structures in mountain forests as a basis for investigating the forests' dynamics and protective function. For Ecol Manage 145:3–14. doi: 10.1016/S0378-1127(00)00570-3

Bottalico F, Travaglini D, Chirici G, et al (2014) Classifying silvicultural systems (coppices vs. high forests) in mediterranean oak forests by airborne laser scanning data. Eur J Remote Sens 47:437–460. doi: 10.5721/EuJRS20144725

Bravo-Oviedo A, Pretzsch H, Ammer C, et al (2014) European mixed forests: Definition and research perspectives. For Syst 23:518–533. doi: 10.5424/fs/2014233-06256

Bray RJ, Curtis JT (1957) An ordination of the upland forest communities of southern Wisconsin. Ecol Monogr 27:325–349

Bruciamacchie M (2001) Les typologies de peuplements, 20 ans après. Rev For Fr III:449–458

Cajander AK (1949) Forest types and their significance. Acta For Fenn 56:1–71

Casals P, Camprodon J, Caritat A, et al (2015) Forest structure of mediterranean yew (Taxus baccata L.) populations and neighbor effects on juvenile yew performance in the NE Iberian Peninsula.

For Syst 24:. doi: 10.5424/fs/2015243-07469

Corona P (2016) Consolidating new paradigms in large-scale monitoring and assessment of forest ecosystems. Environ Res 144:8–14. doi: 10.1016/j.envres.2015.10.017

De Cáceres M, Chytrý M, Agrillo E, et al (2015) A comparative framework for broad-scale plot-based vegetation classification. Appl Veg Sci 18:543–560. doi: 10.1111/avsc.12179

De Cáceres M, Coll L, Legendre P, et al (2019) Trajectory analysis in community ecology. Ecol Monogr. doi: 10.1002/ecm.1350

De Cáceres M, Font X, Oliva F (2010) The management of vegetation classifications with fuzzy clustering. J Veg Sci 21:1138–1151. doi: 10.1111/j.1654-1103.2010.01211.x

De Cáceres M, Legendre P, He F (2013) Dissimilarity measurements and the size structure of ecological communities. Methods Ecol Evol 4:1167–1177. doi: 10.1111/2041-210X.12116

De Cáceres M, Wiser SK (2012) Towards consistency in vegetation classification. J Veg Sci 23:387–393. doi: 10.1111/j.1654-1103.2011.01354.x

DGCN (2005) Tercer Inventario Forestal Nacional (1997-2007): Catalunya. Dirección General de Conservación de la Naturaleza, Ministerio de Medio Ambiente, Madrid

Faith D, Austin M, Belbin L, Margules C (1985) Numerical classification of profile attributes in environmental studies. J Environ Manage 20:73–85

Falkowski MJ, Evans JS, Martinuzzi S, et al (2009) Characterizing forest succession with lidar data: An evaluation for the Inland Northwest, USA. Remote Sens Environ 113:946–956. doi: 10.1016/j.rse.2009.01.003

FOREST EUROPE, UNECE, FAO (2011) State of Europe's Forests 2011. Status and Trends in Sustainable Forest Management in Europe

Giannetti F, Barbati A, Mancini LD, et al (2018) European Forest Types: toward an automated classification. Ann For Sci 75:. doi: 10.1007/s13595-017-0674-6

Godinho-Ferreira P, Azevedo A, Rego F (2005) Carta da Tipologia Florestal de Portugal Continental. Silva Lusit 13:1–34

Gove JH (2004) Structural stocking guides: a new look at an old friend. Can J For Res 34:1044–1056. doi: 10.1139/x03-272

506 Hubert L, Arabie P (1985) Comparing partitions. J Classif 2:193–218
507 James FC, Wamer NO (1982) Relationships between temperate forest bird communities and
508 vegetation structure. Ecology 63:159–171
509 Johnson NL (1949) Bivariate distributions based on simple translation system. Biometrika 36:297–
510 304
511 Kaufman L, Rousseuw PJ (1990) Finding Groups in Data: An Introduction to Cluster Analysis. New
512 York: Willey & Sons Inc.
513 Larsen JB, Nielsen AB (2007) Nature-based forest management-Where are we going?. Elaborating
514 forest development types in and with practice. For Ecol Manage 238:107–117. doi:
515 10.1016/j.foreco.2006.09.087
516 Legendre P, De Cáceres M (2013) Beta diversity as the variance of community data: dissimilarity
517 coefficients and partitioning. Ecol Lett 16:951–963. doi: 10.1111/ele.12141
518 Legendre P, Legendre L (2012) Numerical Ecology, 3rd Eng. Elsevier Science BV., Amsterdam, NL
519 Martín-Alcón S, Coll L, Aunós A (2012) A broad-scale analysis of the main factors determining the
520 current structure and understory composition of Catalonian sub-alpine (Pinus uncinata Ram.)
521 forests. Forestry 85:225–236. doi: 10.1093/forestry/cpr067
522 Martín-Alcón S, Coll L, De Cáceres M, et al (2015) Combining aerial LiDAR and multispectral
523 imagery to assess postfire regeneration types in a Mediterranean forest. Can J For Res 45:856–
524 866
525 McElhinny C, Gibbons P, Brack C, Bauhus J (2005) Forest and woodland stand structural complexity:
526 Its definition and measurement. For Ecol Manage 218:1–24. doi: 10.1016/j.foreco.2005.08.034
527 Nanos N, de Luna SS (2017) Fitting diameter distribution models to data from forest inventories with
528 concentric plot design. For Syst 26:1–13. doi: 10.5424/fs/2017262-10486
529 Ngo Bieng MA, Ginisty C, Goreaud F, Perot T (2006) First typology of oak and Scots pine mixed
530 stands in Orléans Forest (France), based on the canopy spatial structure. New Zeal J For Sci
531 36:325–346
532 O'Hara KL, Latham P a, Hessburg P, Smith BG (1996) A structural classification for Inland
533 Northwest forest vegetation. West J Appl For 11:97–102

534 Odum EP (1950) Bird populations of the Highlands (North Carolina) Plateau in relation to plant
535 succession and avian invasion. Ecology 31:587–605
536 Pommerening A (2002) Approaches to quantifying forest structures. Forestry 75:305–324. doi:
537 10.1093/forestry/75.3.305
538 Reque JA, Bravo F (2008) Identifying forest structure types using National Forest Inventory Data: the
539 case of sessile oak forest in the Cantabrian range. Investig Agrar Sist y Recur For 17:105–113
540 Schreuder HT, Hafley WL (1977) Bivariate distribution for describing stand structure of tree heights
541 and diameters. Biometrics 33:471–478
542 Tamás J, Podani J, Csontos P (2001) An extension of presence/absence coefficients to abundance
543 data: a new look at absence. J Veg Sci 12:401–410. doi: 10.2307/3236854
544 Valbuena R, Maltamo M, Mehtätalo L, Packalen P (2017) Key structural features of Boreal forests
545 may be detected directly using L-moments from airborne lidar data. Remote Sens Environ
546 194:437–446. doi: 10.1016/j.rse.2016.10.024
547 Valbuena R, Maltamo M, Packalen P (2016) Classification of multilayered forest development classes
548 from low-density national airborne lidar datasets. Forestry 89:392–401. doi:
549 10.1093/forestry/cpw010
550 Valbuena R, Packalen P, Mehtätalo L, et al (2013) Characterizing forest structural types and
551 shelterwood dynamics from Lorenz-based indicators predicted by airborne laser scanning. Can J
552 For Res 43:1063–1074
553 Ward JH (1963) Hierarchical grouping to optimize an objective function. J Am Stat Assoc 58:236–
554 244
555 Yao J, Zhang C, De Cáceres M, et al (2019) Variation in compositional and structural components of
556 community assemblage and its determinants. J Veg Sci. doi: 10.1111/jvs.12708
557 Yılmaz OY, Yılmaz H, Akyüz YF (2018) Effects of the overstory on the diversity of the herb and
558 shrub layers of Anatolian black pine forests. Eur J For Res 137:433–445. doi: 10.1007/s10342-
559 018-1114-3
560 Youngblood A (1993) Community type classification of forest vegetation in young, mixed stands,
561 interior Alaska. Res. Pap. PNW-RP-458. Portland, OR: U.S. Department of Agriculture, Forest

562 Service, Pacific Northwest Research Station. 49 p.

563

564

565 **TABLES**

566 **Table 1**: Forest types (12 single-species forests and 26 two-species forests) defined by dominance
567 criteria, number of NFI3 plots assigned to them.

Forest type	N	Average ρ(H, DBH)	Forest type	N	Average ρ(H, DBH)
Single-species forests (12)			**Two-species forests (cont.)**		
Pinus halepensis	1,297	0.666	*P. nigra – Q. ilex*	110	0.662/0.481
Pinus nigra	434	0.761	*P. nigra – Q. humilis*	90	0.795/0.588
Pinus sylvestris	679	0.694	*P. nigra – Q. faginea*	53	0.712/0.693
Pinus uncinata	431	0.741	*P. sylvestris – P. uncinata*	117	0.681/0.736
Pinus pinea	60	0.622	*P. sylvestris – A. alba*	19	0.616/0.890
Pinus pinaster	40	0.622	*P. sylvestris – Q. ilex*	143	0.635/0.612
Abies alba	42	0.831	*P. sylvestris – Q. humilis*	134	0.668/0.551
Quercus ilex	798	0.569	*P. sylvestris – Q. faginea*	24	0.685/0.624
Quercus suber	178	0.701	*P. sylvestris – F. sylvatica*	31	0.609/0.615
Quercus humilis	189	0.671	*P. uncinata – A. alba*	38	0.722/0.769
Quercus faginea	95	0.612	*P. pinea – P. pinaster*	14	0.457/0.712
Fagus sylvatica	94	0.740	*P. pinea – Q. ilex*	69	0.525/0.640
Total	**4,337**		*P. pinea – Q. suber*	44	0.616/0.650
			P. pinaster – Q. ilex	12	0.653/0.048
Two-species forests (26)			*P. pinaster – Q. suber*	33	0.565/0.646
P. halepensis – P. nigra	94	0.714/0.792	*A. alba – F. sylvatica*	30	0.855/0.612
P. halepensis – P. pinea	74	0.622/0.665	*Q. ilex – Q. suber*	113	0.618/0.668
P. halepensis – Q. ilex	341	0.670/0.597	*Q. ilex – Q. humilis*	152	0.608/0.565
P. halepensis – Q. humilis	29	0.610/0.638	*Q. ilex – Q. faginea*	45	0.601/0.610
P. halepensis – Q. faginea	41	0.665/0.440	*Q. suber – Q. humilis*	10	0.711/0.865
P. nigra – P. sylvestris	174	0.741/0.665	**Total**	**2,034**	

568

569

570 **Table 2**: Number of forest subtypes (clusters) in classifications based on CAP(d) (i.e., using diameter
571 distribution alone), classifications based on CAP(h) (i.e., using height distribution alone) and
572 classifications based on CAS (i.e., taking into account the bivariate distribution of diameters and
573 heights). The adjusted Rand (Hubert & Arabie 1984) index evaluates the degree of agreement
574 between the membership matrices issued from each classification approach. Adjusted Rand values
575 corresponding to line 'Total' were calculated after pooling the membership matrices corresponding to
576 the different dominance-based types.

a) Single-species forests (12)	**Number of subtypes**			**Adjusted Rand index**		
Forest type	**CAP(d)**	**CAP(h)**	**CAS**	**CAP(d) vs. CAP(h)**	**CAP(d) vs. CAS**	**CAP(h) vs. CAS**
Pinus halepensis	7	12	12	0.545	0.460	0.464
Pinus nigra	5	6	5	0.631	0.513	0.621
Pinus sylvestris	3	5	6	0.326	0.374	0.529
Pinus uncinata	4	5	10	0.571	0.319	0.398
Pinus pinea	3	3	3	0.616	0.886	0.704
Pinus pinaster	2	2	2	0.900	0.900	1.000
Abies alba	3	2	2	0.602	0.472	0.647
Quercus ilex	3	8	11	0.387	0.324	0.498
Quercus suber	4	4	7	0.436	0.424	0.487
Quercus humilis	3	3	3	0.781	0.391	0.369
Quercus faginea	2	2	2	0.873	0.791	0.751
Fagus sylvatica	2	3	3	0.467	0.378	0.648
Total	**41**	**55**	**68**	**0.579**	**0.509**	**0.567**

577

b) Two-species forests (26)	**Number of subtypes**			**Adjusted Rand index**		
Forest type	**CAP(d)**	**CAP(h)**	**CAS**	**CAP(d) vs. CAP(h)**	**CAP(d) vs. CAS**	**CAP(h) vs. CAS**
P. halepensis – P. nigra	3	3	3	0.624	0.481	0.672
P. halepensis – P. pinea	3	4	4	0.573	0.519	0.809
P. halepensis – Q. ilex	4	5	6	0.455	0.470	0.439
P. halepensis – Q. humilis	2	2	1	0.508		
P. halepensis – Q. faginea	3	3	2	0.565	0.455	0.455
P. nigra – P. sylvestris	3	6	5	0.509	0.477	0.563
P. nigra – Q. ilex	3	3	4	0.890	0.774	0.753
P. nigra – Q. humilis	3	4	3	0.465	0.521	0.556
P. nigra – Q. faginea	2	2	2	0.533	0.716	0.533
P. sylvestris – P. uncinata	4	4	4	0.463	0.760	0.517
P. sylvestris – A. alba	1	1	1			
P. sylvestris – Q. ilex	2	3	3	0.378	0.480	0.601
P. sylvestris – Q. humilis	2	5	2	0.318	0.854	0.339
P. sylvestris – Q. faginea	2	2	2	0.681	0.681	1.000
P. sylvestris – F. sylvatica	2	1	1			
P. uncinata – A. alba	2	2	2	1.000	1.000	1.000
P. pinea – P. pinaster	1	1	1			

P. pinea – Q. ilex	2	3	4	0.477	0.543	0.583
P. pinea – Q. suber	2	2	2	0.821	0.909	0.738
P. pinaster – Q. ilex	1	1	1			
P. pinaster – Q. suber	2	2	1	0.765		
A. alba – F. sylvatica	1	2	2			0.425
Q. ilex – Q. suber	2	2	3	0.796	0.201	0.209
Q. ilex – Q. humilis	3	3	4	0.824	0.519	0.560
Q. ilex – Q. faginea	3	2	1	0.489		
Q. suber – Q. humilis	1	1	1			
Total	**59**	**69**	**65**	**0.702**	**0.708**	**0.673**

578

579

FIGURE CAPTIONS

Fig. 1. Example of calculation of resemblance between a pair of monospecific stands using the CAP framework: (a) Distribution of trees in diameter 5-cm classes in the two stands; (b) CAPs for the two stands, using diameter as size variable and basal area as abundance variable. Values of A_k, B_k and C_k are indicated in each of three areas resulting from the intersection of CAPs.

Fig. 2. Example of the construction of a CAS and its marginal CAPs for diameters and heights from individual tree data. Panel (a) is a scatterplot of diameter and height values in a 20 × 20 m forest plot. Panel (b) shows the cumulative abundance surface (CAS) calculated after deciding the limits of bins for heights and diameters. Panels (c) and (d) contain the CAPs that result from marginalizing the CAS.

Fig. 3: Non-metric multidimensional scaling (nMDS) of the dissimilarity matrix obtained using either D_{man} or D_{bray} for simulated stands varying in (a) stand basal area vs. average tree size, or (b) average diameter vs. average height. Labels in (a) indicate forest stands simulated using combinations of tree size distribution (a-e) and stand basal area (1-5). Labels in (b) indicate forest stands simulated using combinations of diameter distribution (a-e) and height distribution (1-5). Edges indicate stands that are contiguous along treatment sequences.

Fig. 4: Sensitivity analysis regarding the effect of dissimilarity metric and the resolution of diameter and height bins on the dissimilarities between plots. Dissimilarities between the 434 forest plots dominated by *Pinus nigra* were calculated using 50 combinations of dissimilarity metric (either D_{man} or D_{bray}; filled circles and diamonds, respectively) and five degrees of resolution in the definition of diameter bins (D0 to D4) and height bins (H0 to H5). Panel (a) shows bin definitions graphically, along with the symbol sizes (for diameters) and gray tones (for heights) used in the remaining panels (b-d). Panel (b) shows a metric MDS representation in two dimensions (stress = 0.068) of the correlation between the 50 different dissimilarity matrices. Panels (c) and (d) show the MDS representation when focusing on the 25 combinations corresponding to D_{man} (stress = 0.099) and when focusing on those corresponding to D_{bray} (stress = 0.131), respectively.

606 **Fig. 5**: Five subtypes of forests dominated by *Pinus nigra* (PN), ordered by increasing stand's basal
607 area (see Table 2). For each subtype we show the distribution of basal area (m^2/ha) among 1-m height
608 classes and 5-cm diameter classes (first and second columns, respectively) and the distribution of
609 density (ind./ha) among height and dbh classes (third and fourth columns, respectively).

610 **Fig. 6**: Four subtypes of forests co-dominated by *P. sylvestris* (PS) and *P. uncinata* (PU) (both shade-
611 intolerant species), ordered by increasing basal area (see Table 3). For each subtype and species we
612 show the distribution of basal area (m^2/ha) among 1 m height classes and 5 cm diameter classes (first
613 and second columns, respectively) and the distribution of density (ind./ha) among height and dbh
614 classes (third and fourth columns, respectively).

615 **Fig. 7**: Six subtypes of forests co-dominated by *P. halepensis* (PH; shade-intolerant) and *Q. ilex* (QI;
616 shade-tolerant), ordered by increasing basal area (see Table 4). For each subtype and species we show
617 the distribution of basal area (m^2/ha) among 1 m height classes and 5 cm diameter classes (first and
618 second columns, respectively) and the distribution of density (ind./ha) among height and dbh classes
619 (third and fourth columns, respectively).

620

621 **FIGURES**

622 **Fig. 1**.

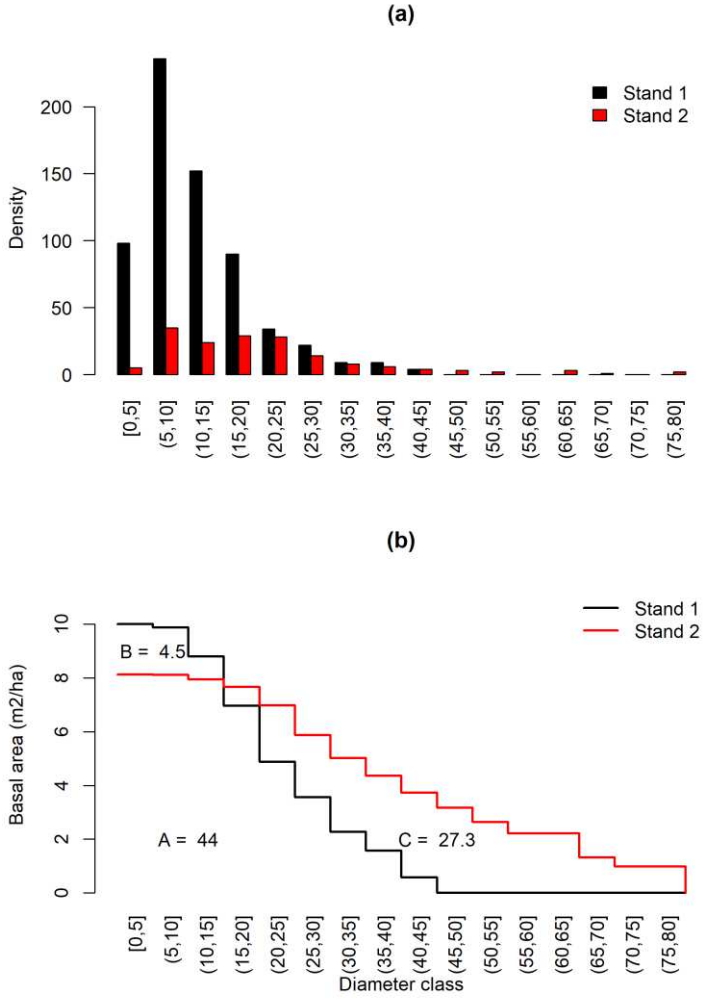

623

624

625 **Fig. 2**.

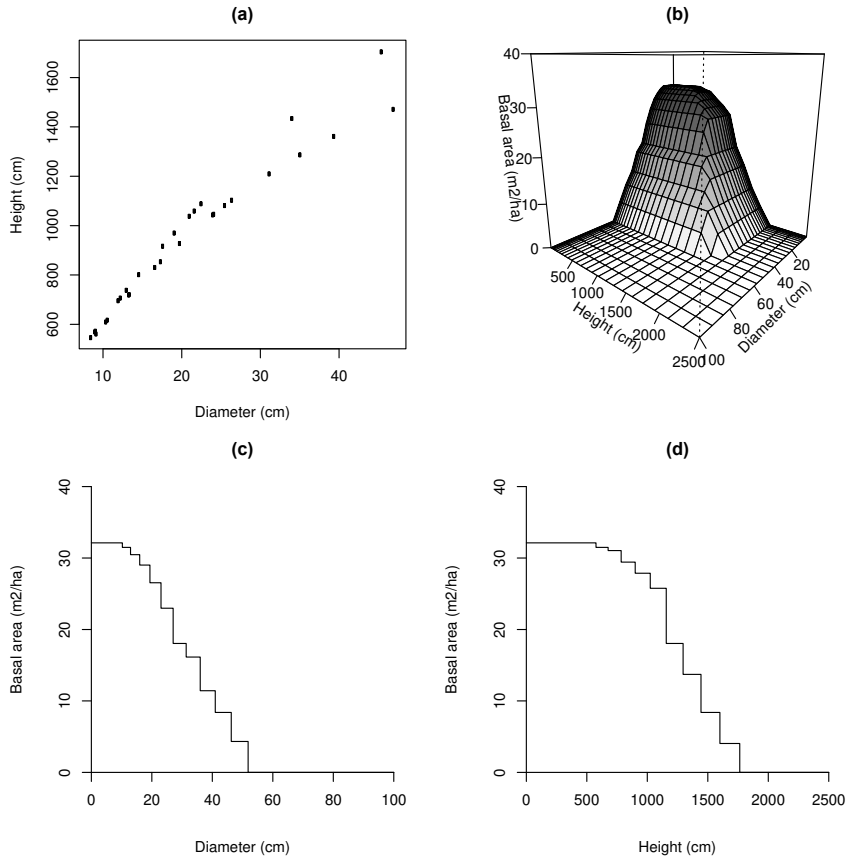

626

627

628 **Fig. 3**.

629

a)

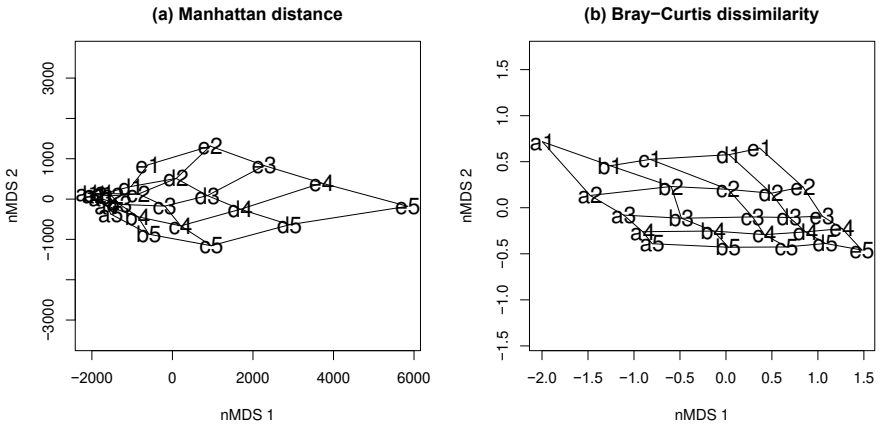

b)

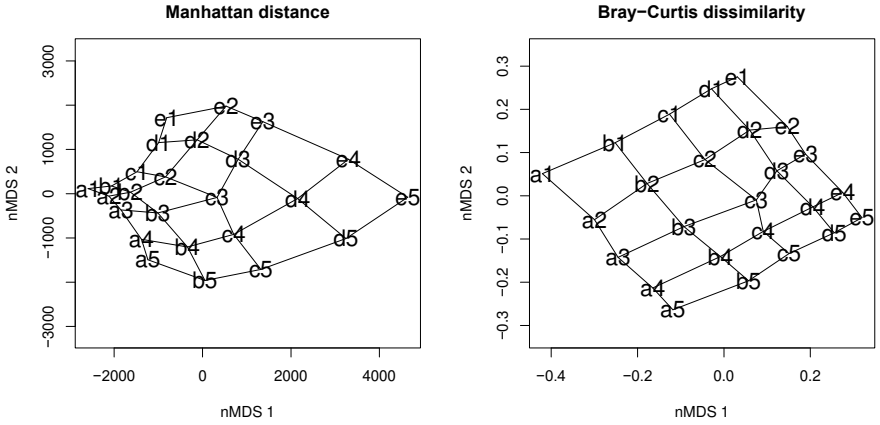

630 **Fig. 4.**

631

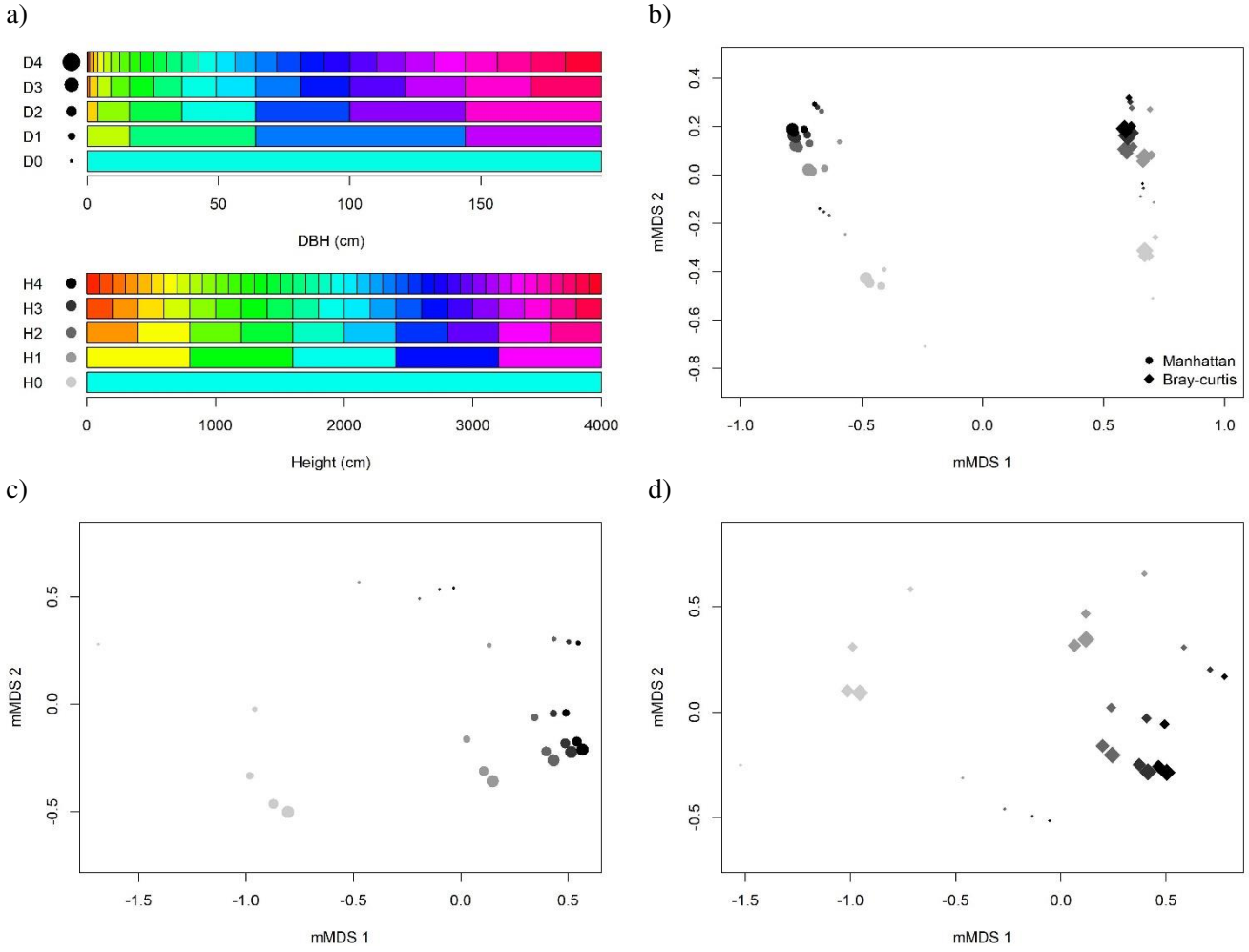

632

633

Fig. 5.

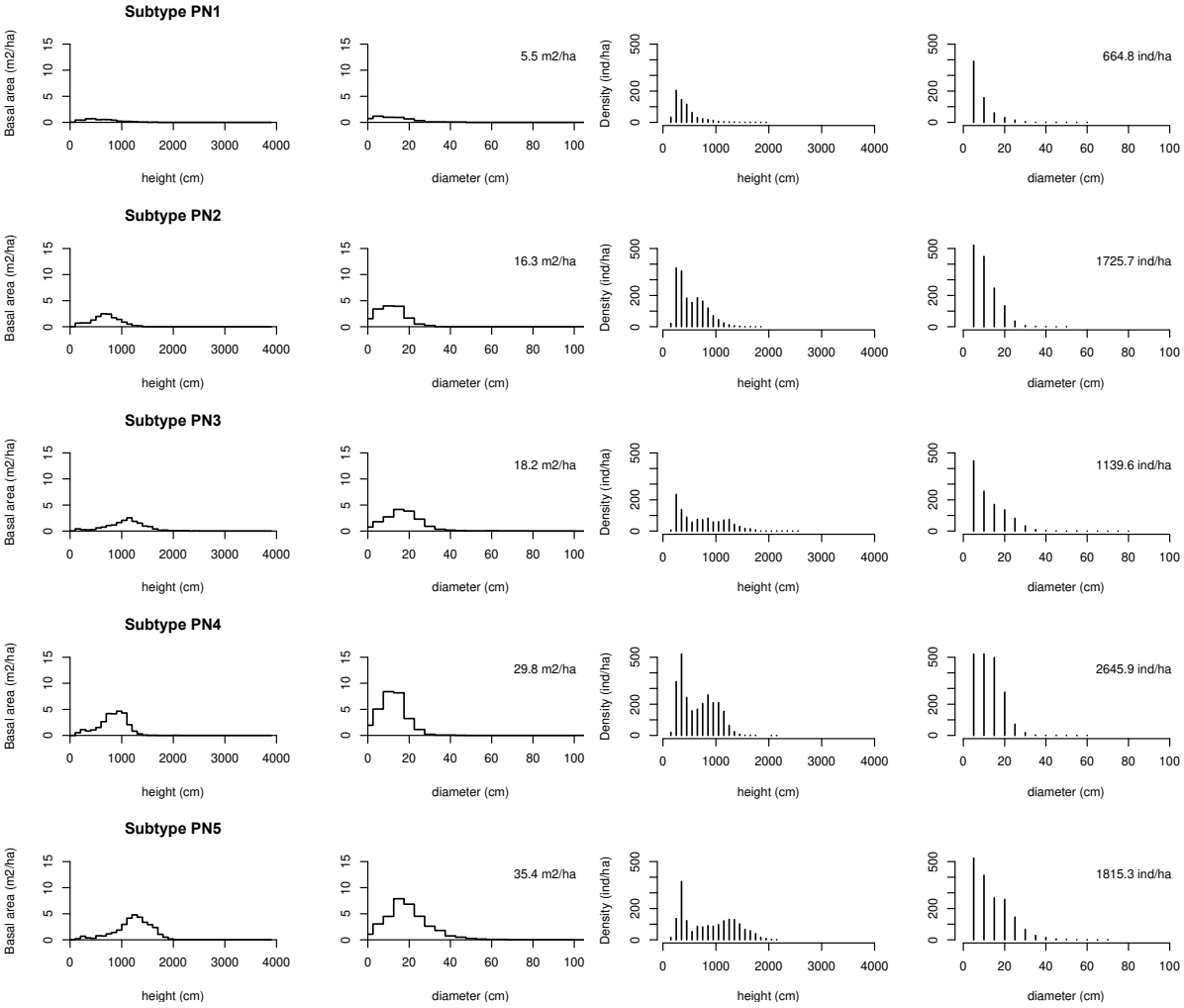
Subtype PN1
Basal area (m2/ha)
height (cm)
5.5 m2/ha
diameter (cm)
Density (ind/ha)
height (cm)
664.8 ind/ha
diameter (cm)
Subtype PN2
16.3 m2/ha
1725.7 ind/ha
Subtype PN3
18.2 m2/ha
1139.6 ind/ha
Subtype PN4
29.8 m2/ha
2645.9 ind/ha
Subtype PN5
35.4 m2/ha
1815.3 ind/ha

637 **Fig. 6**.

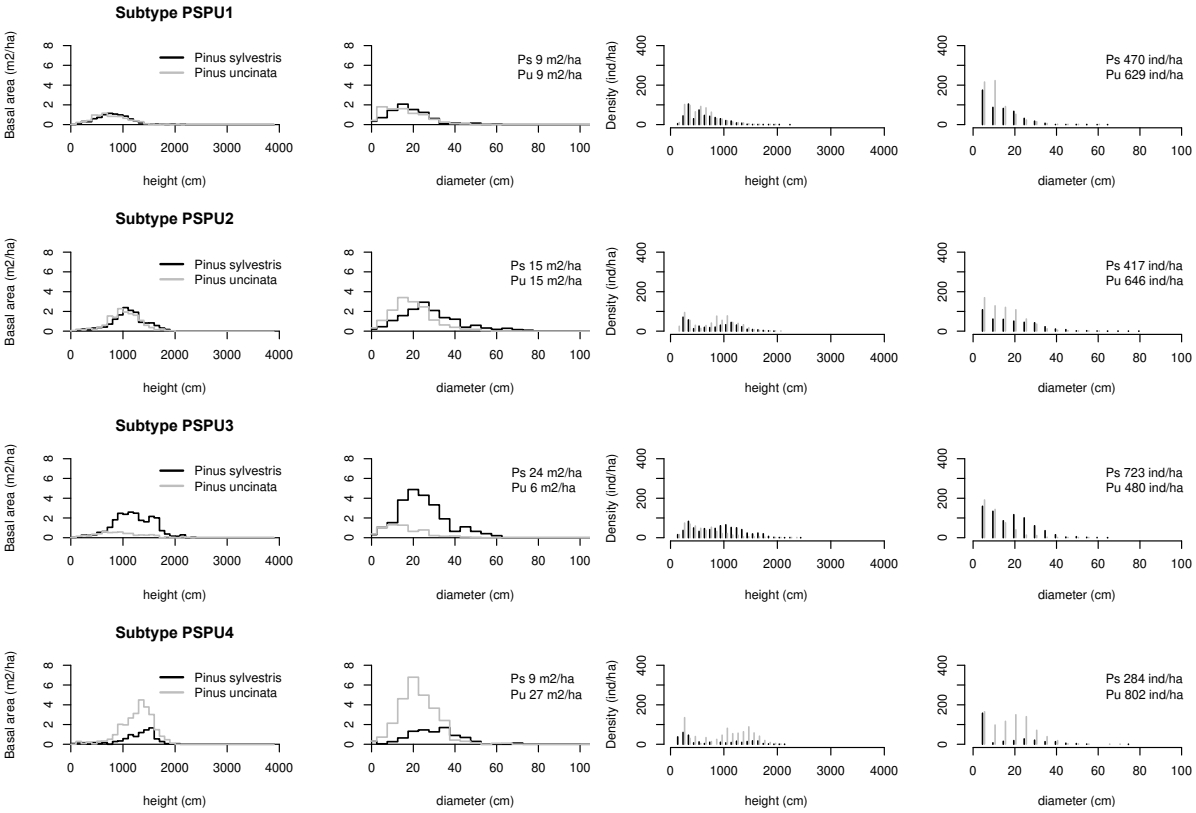

638

639

640 **Fig. 7**.

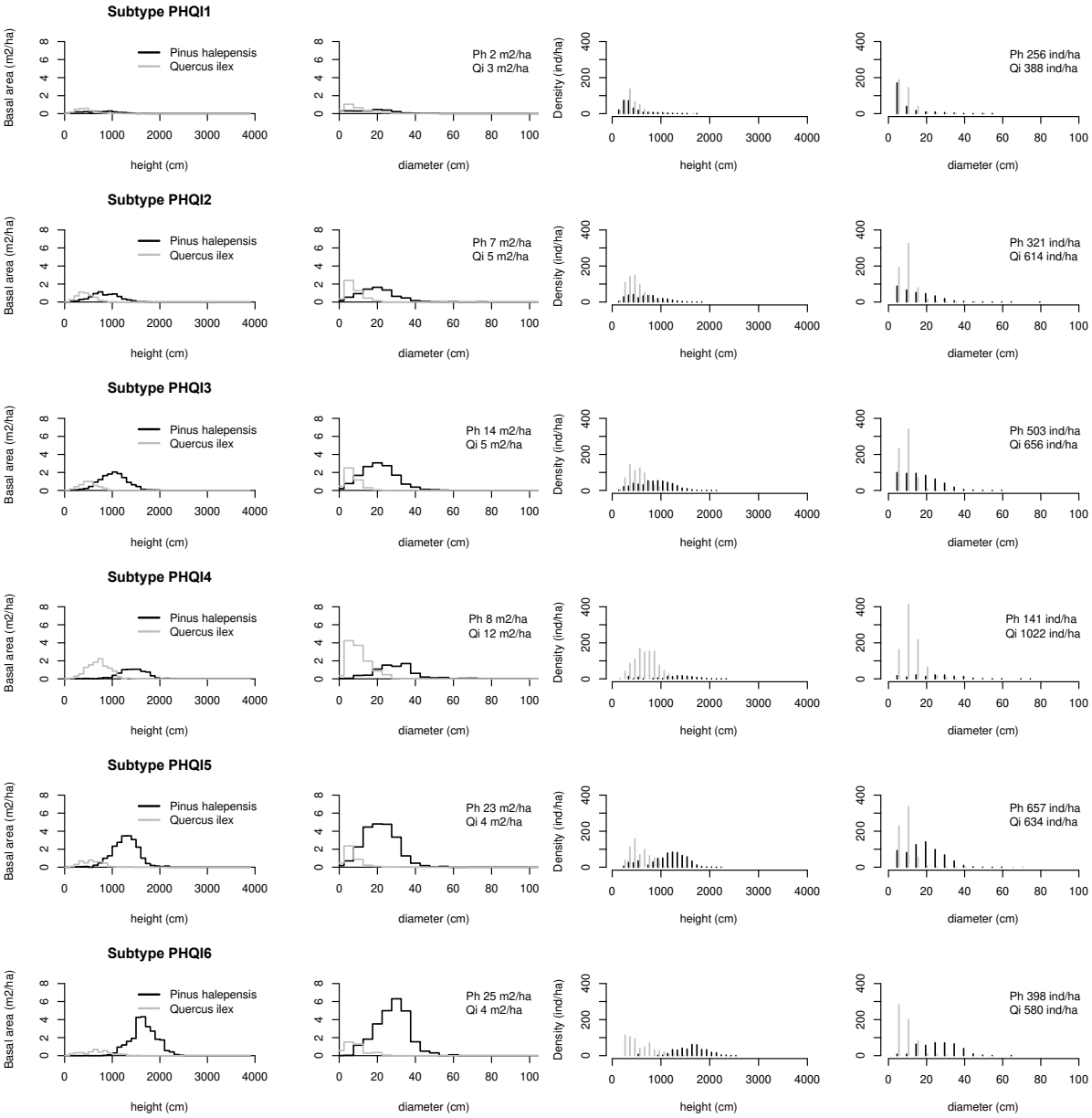

641

642

643

Supplementary Material

Appendix S1. Simulation study

Simulated treatments

We simulated forest tree data using Johnson's Sbb distribution (Johnson 1949; Schreuder & Hafley 1977) to study the appropriateness of D_{man} and D_{bray} to reflect differences in terms of total basal area, tree diameter distribution and tree height distribution. For simplicity, we did not include differences in composition; these were considered in De Cáceres et al. (2013). In all simulations some parameters of the Sbb distribution were fixed ($\rho = 0.8$, $\delta_1 = \delta_2 = 1.5$). We changed parameters γ_1 and γ_2 of the Sbb distribution to simulate variations in the distribution of tree diameter and tree height. Five treatments were considered for each size variable (see Fig. S1.1). Five treatments of stand basal area were also considered: 5, 10, 15, 20 and 25 m^2/ha. For each simulated stand we generated tree individuals until to the stand's target basal area was met.

Fig. S1.1 Marginal probability density functions for tree diameters and tree heights obtained by setting different values for Sbb parameters γ_1 and γ_2, respectively.

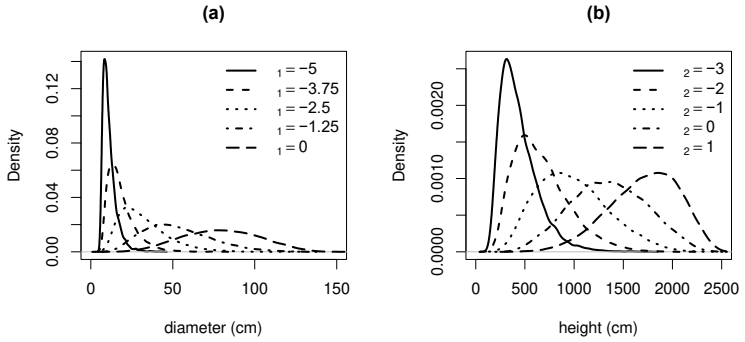

First simulation experiment

In a first experiment we generated 25 different stands by crossing the five treatments in stand basal area (labeled '1' to '5') with five treatments in tree size distribution (labeled 'a' to 'e'), assuming that when trees were larger in diameter they were also larger in height (i.e., in treatment 'a' γ_1 = -5 and γ_2 = -3; in 'b' γ_1 = -3.75 and γ_2 = -2; etc.). Thus, simulated stands were composed of few small individuals, many small individuals, few large individuals or many large individuals; with intermediate situations being also covered. The CAS for each plot was build using basal area as abundance variable and tree diameter and tree height as size variables. We defined quadratic diameter bins, meaning that more classes were defined to distinguish thin trees than to distinguish thick trees. Specifically, diameter limits (in cm) for class r were defined as $4 + [(0.5\cdot(r\text{-}1))^2, (0.5\cdot r)^2]$ cm. The

669 resulting classes were: 4 – 6.25 cm, 6.25 – 9 cm, 9 – 12.25 cm, 12.25 – 16 cm, 16 – 20.25 cm etc.
670 Height classes were defined linearly using 100 cm bins. Fig. S1.2 shows the CAS corresponding to
671 each of the 25 simulated stands.

672 **Fig. S1.2**. Cumulative abundance surfaces (CASs) corresponding to the 25 simulated forest stands of
673 the first experiment. Each of the five rows corresponds to the bivariate distributions of diameter and
674 height presented in Fig. S1.1. Columns differ in the stand's basal area simulated (5, 10, 15, 20 and 25
675 m^2/ha).

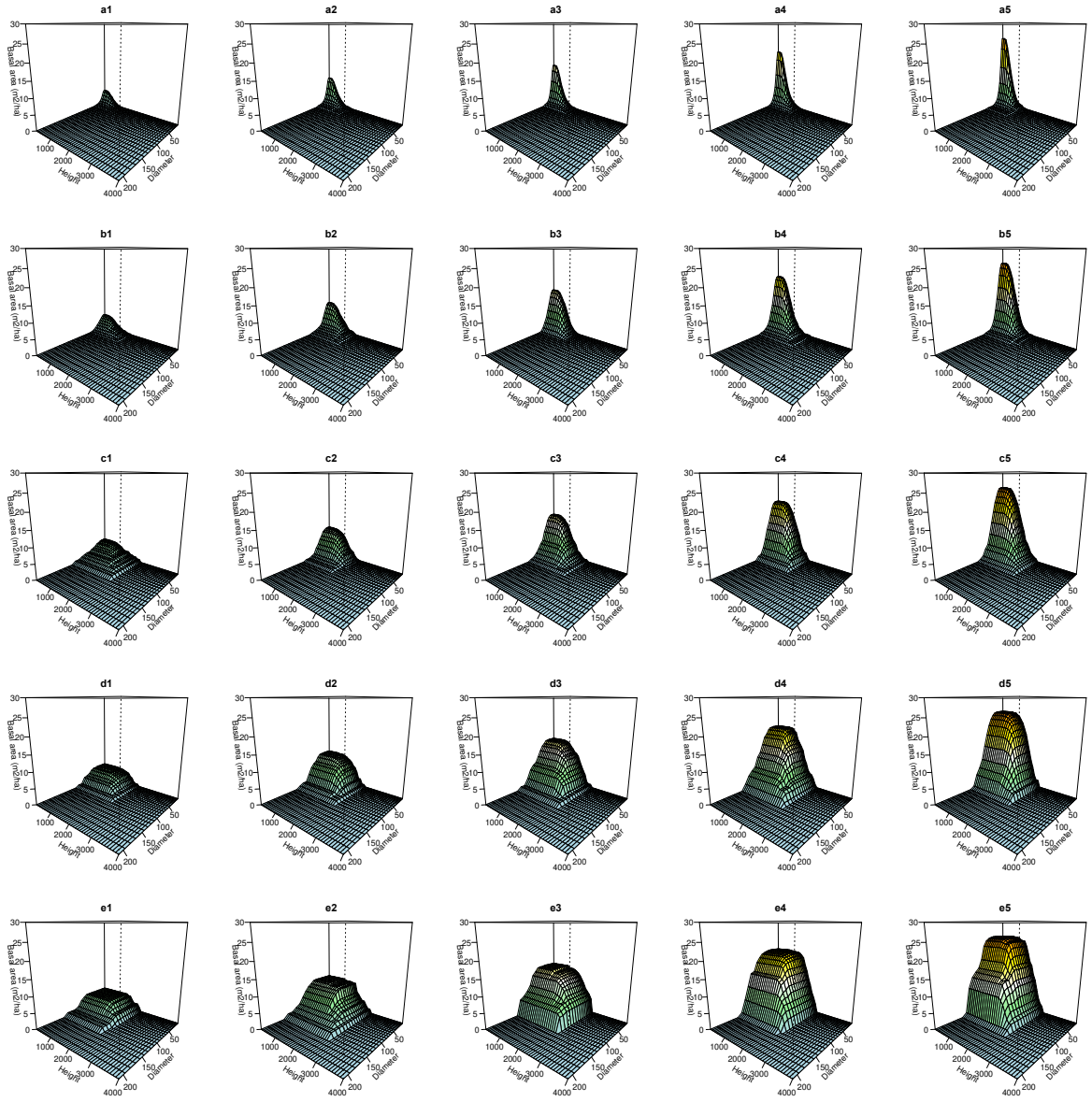

676
677

678 We then calculated the resemblance between all pairs of simulated stands using either D_{man} or
679 D_{bray}. We used Kruskal's non-metric multidimensional scaling (nMDS) to display each of the
680 resulting dissimilarity matrices in a two-dimensional scatter plot (see Fig. S1.3). Both coefficients

were responsive to changes in total basal area and tree size. However, in the dissimilarity matrix obtained using D_{man} the distances due to differences in tree size were smaller between stands with small basal area than between stands with large basal area (i.e., compare sequences a1-e1 and a5-e5 in Fig. S1.3). Similarly, the distances due to differences in basal area were smaller between stands composed of small individuals than between stands composed of large individuals (i.e., compare sequences a1-a5 and e1-e5 in Fig. S1.3a). These patterns did not occur in the case of D_{bray}. Contrastingly, with this coefficient the dissimilarity between a pair stands differing in basal area was somewhat larger when the two stands had 5 and 10 m^2/ha, respectively (i.e., a1 vs. a2, b1 vs. b2, …; Fig. S1.3b), than when they had 20 and 25 m^2/ha, respectively (i.e., a4 vs. a5, b4 vs. b5, …; Fig. S1.3b). Similarly, the dissimilarity between pairs of plots differing in tree distribution was larger between small tree treatments (i.e., a1 vs. b1, a2 vs. b2, …; Fig. S1.3b) than between large tree treatments (i.e., d1 vs. e1, d2 vs. e2, …; Fig. S1.3b).

Fig. S1.3 Non-metric multidimensional scaling (nMDS) of the dissimilarity matrix obtained using either D_{man} or D_{bray}. Edges indicate stands that are contiguous along treatment sequences.

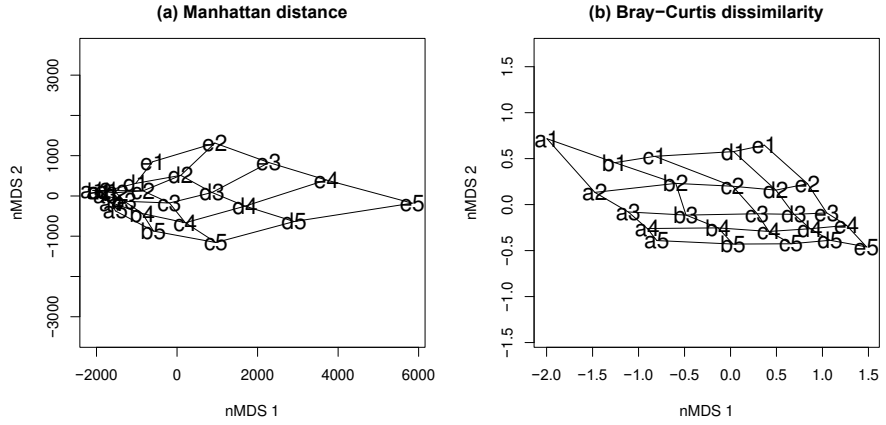

Second simulation experiment

In a second experiment we calculated the resemblance among stands having all the same basal area (25 m^2/ha) but differing in height distribution, diameter distribution, or both. In this case we generated stands by crossing the five treatments in diameter distribution (labeled ‘a’ to ‘e’) with the five treatments in tree size distribution (labeled ‘1’ to ‘5’). Thus, stands could be composed of short and thin trees, tall and thin trees, short and thick trees, or tall and thick trees; with intermediates situations being also covered. The CAS for each plot was built as before (Fig. S1.4).

Fig. S1.4 Cumulative abundance surfaces (CASs) of the 25 simulated forest stands of the second experiment. Each panel corresponds to a combination of diameter distribution (rows) and height distribution (columns) among those presented in Fig. S1.1. All stands have a basal area of 25 m^2/ha.

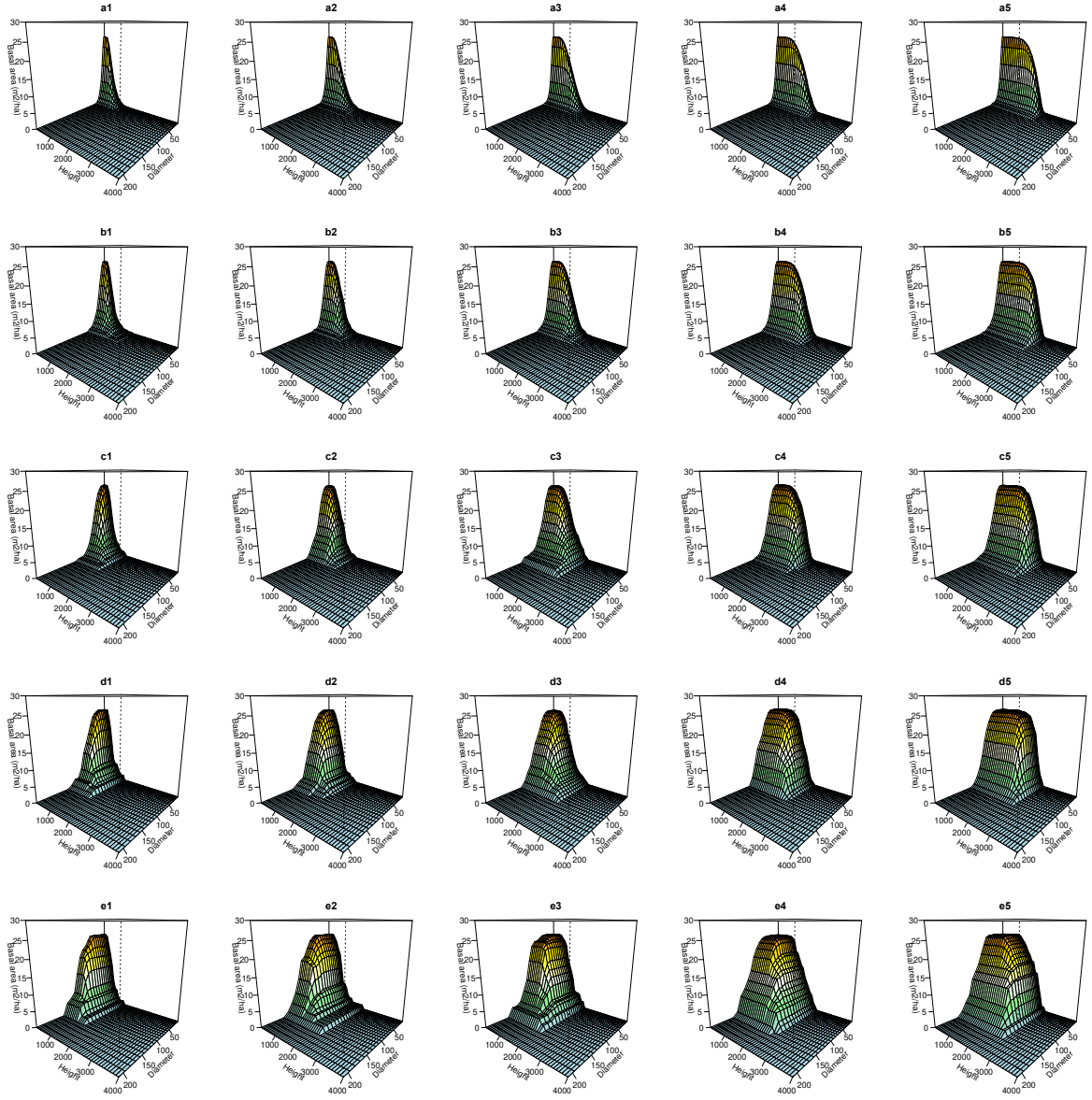

As with the first experiment, we calculated the resemblance between all pairs of simulated stands using either D_{man} or D_{bray} and displayed the resulting dissimilarity matrices using non-metric multidimensional scaling (Fig. S1.5).

Fig. S1.5 Non-metric multidimensional scaling (nMDS) of the dissimilarity matrix obtained using either D_{man} or D_{bray}. Labels indicate forest stands simulated using combinations of diameter distribution (a-e) and height distribution (1-5). Edges indicate stands that are contiguous along treatment sequences.

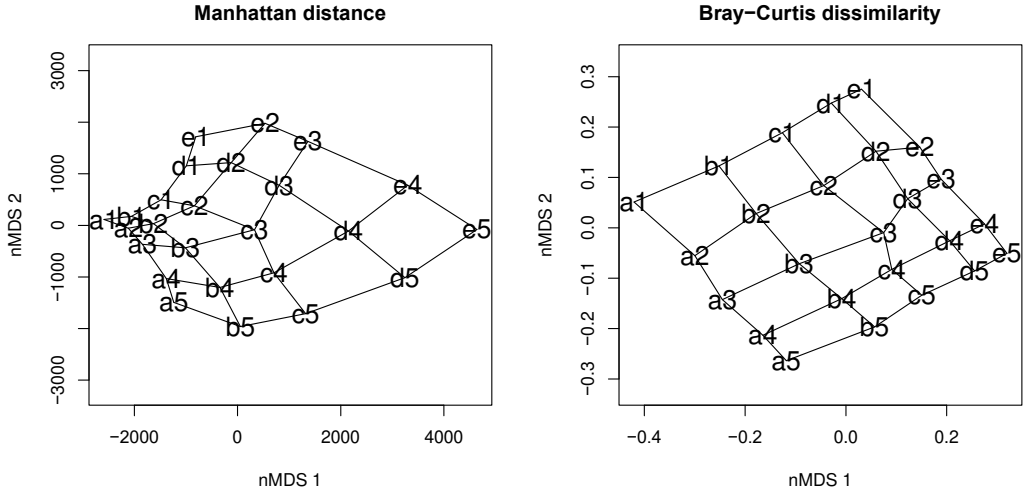

Both coefficients were responsive to changes in tree diameter and tree height. Although the effects where less obvious, the behavior of both indices was similar to the first experiment. With D_{man} the distances due to differences in diameter distribution were smaller between stands with short trees than between stands with tall trees and, similarly, the distances due to differences in tree height were smaller between stands composed of thin individuals than between stands composed of thick individuals (Fig. S1.5a). With D_{bray} the dissimilarity between stands differing in tree diameter was larger between thin tree treatments than between thick tree treatments and, similarly, the dissimilarity between plots differing in tree height was larger between short tree treatments than between tall tree treatments (Fig. S1.5b).

Literature cited

De Cáceres, M., Legendre, P., and F. He. 2013. Dissimilarity measurements and the size structure of ecological communities. *Methods in Ecology and Evolution* 4: 1167-1177.

Johnson, N.L. 1949. Bivariate distributions based on simple translation system. *Biometrika* 36: 297-304.

Schreuder, H.T. and W.L. Hafley. 1977. Bivariate distribution for describing stand structure of tree heights and diameters. *Biometrics* 33: 471-478.

Appendix S2. Additional table

Table S2.1 Linear correlation between the dissimilarity matrices obtained using D_{man} (eq. 2) on either CAS, CAP(d) or CAP(h), for each dominance-based forest type.

Forest type	$D_{CAP(d)}$ vs $D_{CAP(h)}$	$D_{CAP(d)}$ vs D_{CAS}	$D_{CAP(h)}$ vs D_{CAS}	Forest type	$D_{CAP(d)}$ vs $D_{CAP(h)}$	$D_{CAP(d)}$ vs D_{CAS}	$D_{CAP(h)}$ vs D_{CAS}
Single-species forests				**Two-species forests (cont.)**			
Pinus halepensis	0.938	0.926	0.951	*P. nigra – Q. ilex*	0.954	0.956	0.950
Pinus nigra	0.890	0.930	0.901	*P. nigra – Q. humilis*	0.902	0.882	0.927
Pinus sylvestris	0.889	0.916	0.915	*P. nigra – Q. faginea*	0.944	0.933	0.923
Pinus uncinata	0.865	0.886	0.928	*P. sylvestris – P. uncinata*	0.939	0.929	0.947
Pinus pinea	0.976	0.954	0.983	*P. sylvestris – A. alba*	0.977	0.950	0.970
Pinus pinaster	0.950	0.955	0.952	*P. sylvestris – Q. ilex*	0.914	0.921	0.944
Abies alba	0.942	0.900	0.935	*P. sylvestris – Q. humilis*	0.918	0.927	0.955
Quercus ilex	0.943	0.924	0.916	*P. sylvestris – Q. faginea*	0.862	0.878	0.965
Quercus suber	0.941	0.892	0.918	*P. sylvestris – F. sylvatica*	0.973	0.962	0.949
Quercus humilis	0.898	0.913	0.903	*P. uncinata – A. alba*	0.933	0.965	0.931
Quercus faginea	0.920	0.928	0.913	*P. pinea – P. pinaster*	0.983	0.975	0.973
Fagus sylvatica	0.732	0.871	0.888	*P. pinea – Q. ilex*	0.947	0.911	0.961
				P. pinea – Q. suber	0.949	0.946	0.958
Two-species forests				*P. pinaster – Q. ilex*	0.964	0.981	0.992
P. halepensis – P. nigra	0.917	0.921	0.936	*P. pinaster – Q. suber*	0.979	0.973	0.976
P. halepensis – P. pinea	0.938	0.935	0.968	*A. alba – F. sylvatica*	0.935	0.962	0.940
P. halepensis – Q. ilex	0.932	0.919	0.960	*Q. ilex – Q. suber*	0.929	0.934	0.921
P. halepensis – Q. humilis	0.954	0.925	0.976	*Q. ilex – Q. humilis*	0.883	0.899	0.952
P. halepensis – Q. faginea	0.862	0.840	0.880	*Q. ilex – Q. faginea*	0.949	0.930	0.880
P. nigra – P. sylvestris	0.909	0.924	0.901	*Q. suber – Q. humilis*	0.901	0.876	0.926

Appendix S3. Single-species forest types

Fig. S3.1 Twelve subtypes of forests dominated by *Pinus halepensis* (PH), ordered by increasing basal area. For each subtype we show the distribution of basal area (m^2/ha) among 1-m height classes and 5-cm diameter classes (first and second columns, respectively) and the distribution of density (ind./ha) among height and dbh classes (third and fourth columns, respectively).

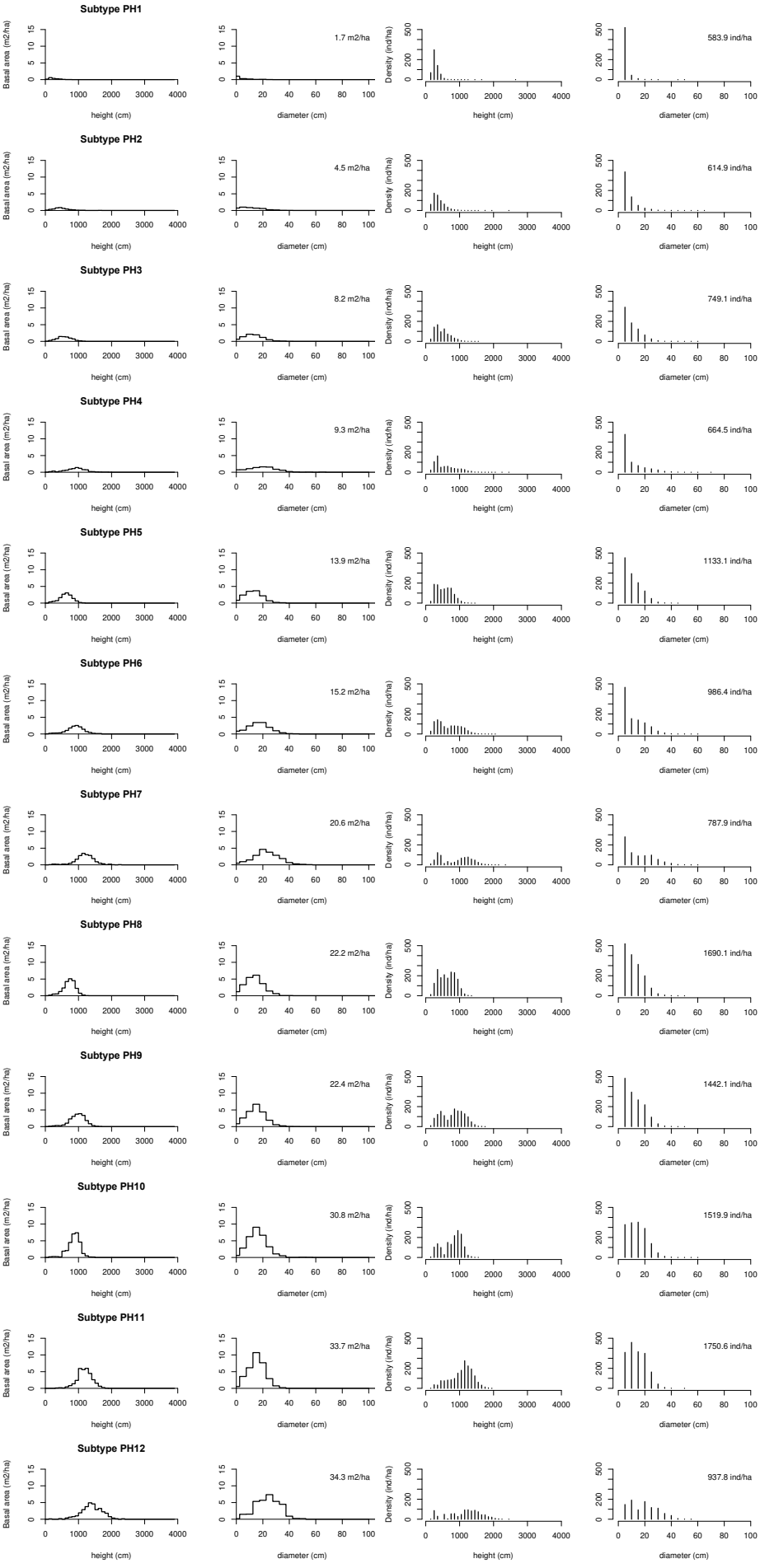
Subtype PH1
1.7 m2/ha
583.9 ind/ha
Subtype PH2
4.5 m2/ha
614.9 ind/ha
Subtype PH3
8.2 m2/ha
749.1 ind/ha
Subtype PH4
9.3 m2/ha
664.5 ind/ha
Subtype PH5
13.9 m2/ha
1133.1 ind/ha
Subtype PH6
15.2 m2/ha
986.4 ind/ha
Subtype PH7
20.6 m2/ha
787.9 ind/ha
Subtype PH8
22.2 m2/ha
1690.1 ind/ha
Subtype PH9
22.4 m2/ha
1442.1 ind/ha
Subtype PH10
30.8 m2/ha
1519.9 ind/ha
Subtype PH11
33.7 m2/ha
1750.6 ind/ha
Subtype PH12
34.3 m2/ha
937.8 ind/ha
Basal area (m2/ha)
Density (ind/ha)
height (cm)
diameter (cm)

746

747 **Table S3.1** Structural statistics of forests subtypes dominated by *Pinus halepensis* (PH), ordered by
748 increasing basal area. Av. N and S.d. N – Average and standard deviation of density (ind./ha); Av. BA
749 and S.d. BA – Average and standard deviation of basal area (m^2/ha); Av. D and S.d. D – Average and
750 standard deviation of dbh (cm); Av. H and S.d. H – Average and standard deviation of height (cm).

Subtype	Plots	Av. N	S.d. N	Av. BA	S.d. BA	Av. D	S.d. D	Av. H	S.d. H
PH1	258	584	945	1.7	2.1	5.6	2.4	319	98
PH2	226	615	1105	4.5	3.2	8.1	5.2	412	171
PH3	205	749	655	8.2	2.6	10.1	6.2	506	210
PH4	110	665	763	9.3	2.8	10.4	8.3	604	318
PH5	158	1133	834	13.9	3.2	10.8	6.3	567	224
PH6	109	986	641	15.2	2.2	11.5	8.0	686	332
PH7	42	788	506	20.6	3.3	15.0	10.4	896	446
PH8	72	1690	857	22.2	4.0	11.2	6.5	654	238
PH9	57	1442	757	22.4	3.2	12.2	7.0	819	329
PH10	30	1520	608	30.8	4.0	14.3	7.3	804	279
PH11	17	1751	620	33.7	6.8	14.0	7.0	1076	330
PH12	13	938	621	34.3	6.7	18.9	10.4	1173	473

751

752

Fig. S3.2 Five subtypes of forests dominated by *Pinus nigra* (PN), ordered by increasing basal area. For each subtype we show the distribution of basal area (m^2/ha) among 1-m height classes and 5-cm diameter classes (first and second columns, respectively) and the distribution of density (ind./ha) among height and dbh classes (third and fourth columns, respectively).

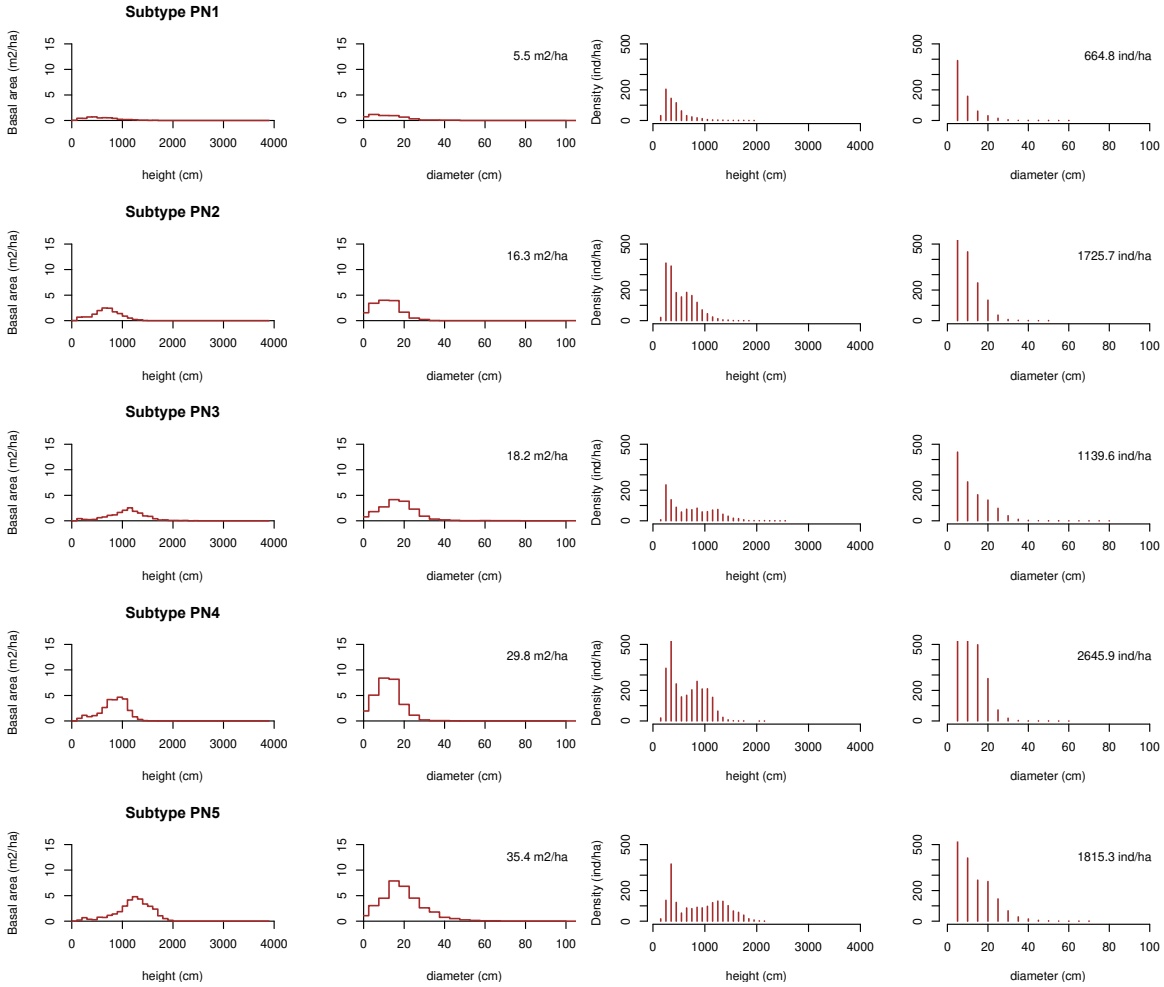

Table S3.2 Structural statistics of five subtypes of forests dominated by *Pinus nigra* (PN), ordered by increasing stand's basal area. Av. N and S.d. N – Average and standard deviation of density (ind./ha); Av. BA and S.d. BA – Average and standard deviation of basal area (m^2/ha); Av. D and S.d. D – Average and standard deviation of dbh (cm); Av. H and S.d. H – Average and standard deviation of height (cm).

Subtype	Plots	Av. N	S.d. N	Av. BA	S.d. BA	Av. D	S.d. D	Av. H	S.d. H
PN1	105	665	1234	5.5	4.6	8.5	5.6	449	231
PN2	116	1726	1360	16.3	5.6	9.4	5.6	551	259
PN3	81	1140	863	18.2	4.5	11.9	7.8	751	420
PN4	82	2646	1075	29.8	5.9	10.4	5.9	665	316
PN5	50	1815	1366	35.4	8.4	13.2	8.6	889	475

Fig. S3.3: Eight subtypes of forests dominated by *Pinus sylvestris* (PS), ordered by increasing basal area. For each subtype we show the distribution of basal area (m^2/ha) among 1-m height classes and 5-cm diameter classes (first and second columns, respectively) and the distribution of density (ind./ha) among height and dbh classes (third and fourth columns, respectively).

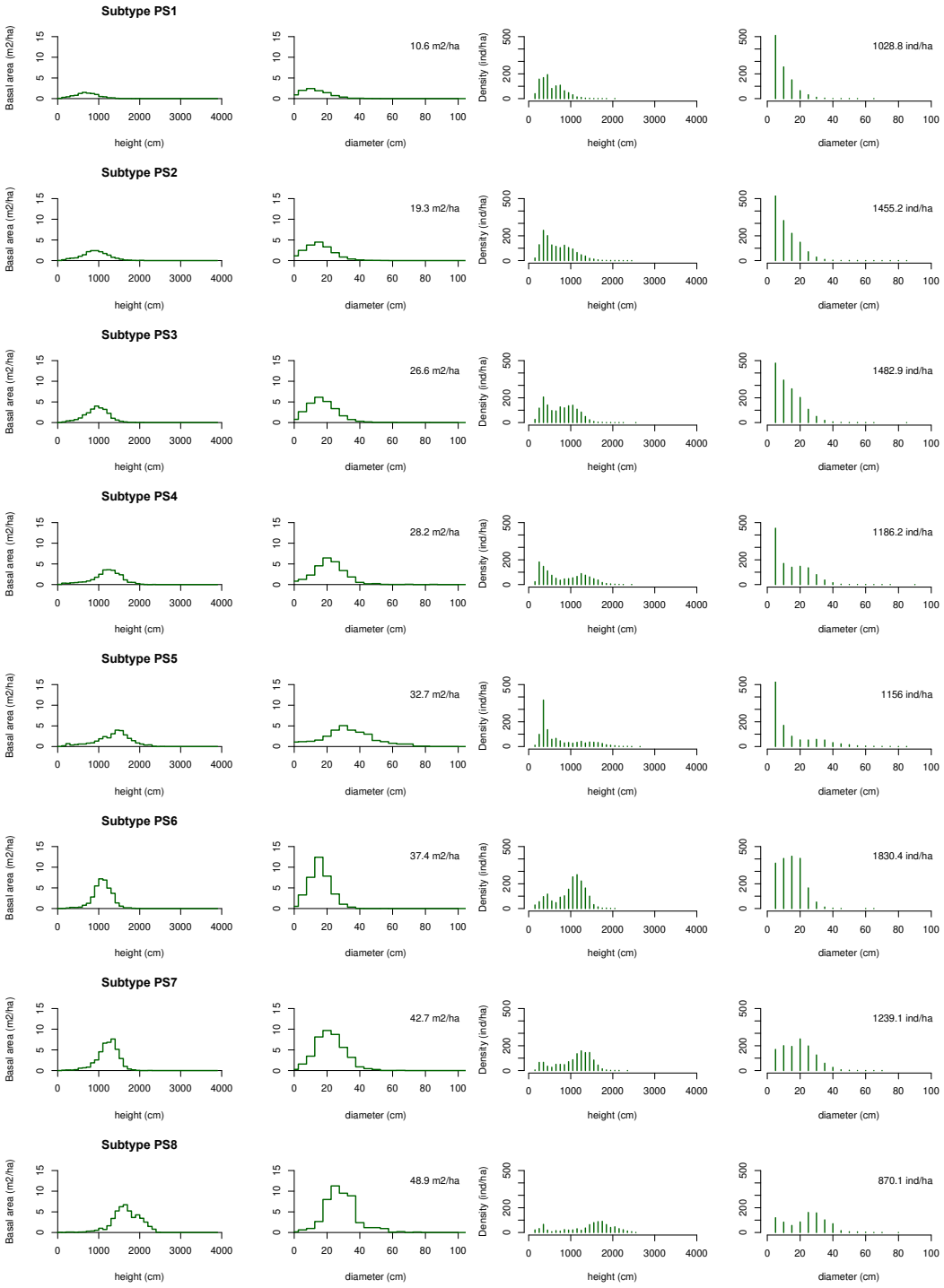

Table S3.3 Structural statistics of forests subtypes dominated by *Pinus sylvestris* (PS), ordered by increasing basal area. Av. N and S.d. N – Average and standard deviation of density (ind./ha); Av. BA and S.d. BA – Average and standard deviation of basal area (m^2/ha); Av. D and S.d. D – Average and standard deviation of dbh (cm); Av. H and S.d. H – Average and standard deviation of height (cm).

Subtype	Plots	Av. N	S.d. N	Av. BA	S.d. BA	Av. D	S.d. D	Av. H	S.d. H
PS1	160	1029	1335	10.6	7.1	9.7	6.1	563	261
PS2	184	1455	1257	19.3	5.5	10.9	7.1	698	340
PS3	116	1483	858	26.6	5.1	12.9	7.9	771	351
PS4	71	1186	800	28.2	4.6	14.3	10.0	842	484
PS5	29	1156	1146	32.7	5.9	13.7	13.1	738	496
PS6	50	1830	777	37.4	5.3	14.5	7.0	998	357
PS7	50	1239	578	42.7	5.1	18.7	9.4	1096	407
PS8	19	870	233	48.9	5.2	23.9	12.0	1417	598

777 **Fig. S3.4** Ten subtypes of forests dominated by *Pinus uncinata* (PU), ordered by increasing basal area.
778 For each subtype we show the distribution of basal area (m^2/ha) among 1-m height classes and 5-cm
779 diameter classes (first and second columns, respectively) and the distribution of density (ind./ha) among
780 height and dbh classes (third and fourth columns, respectively).

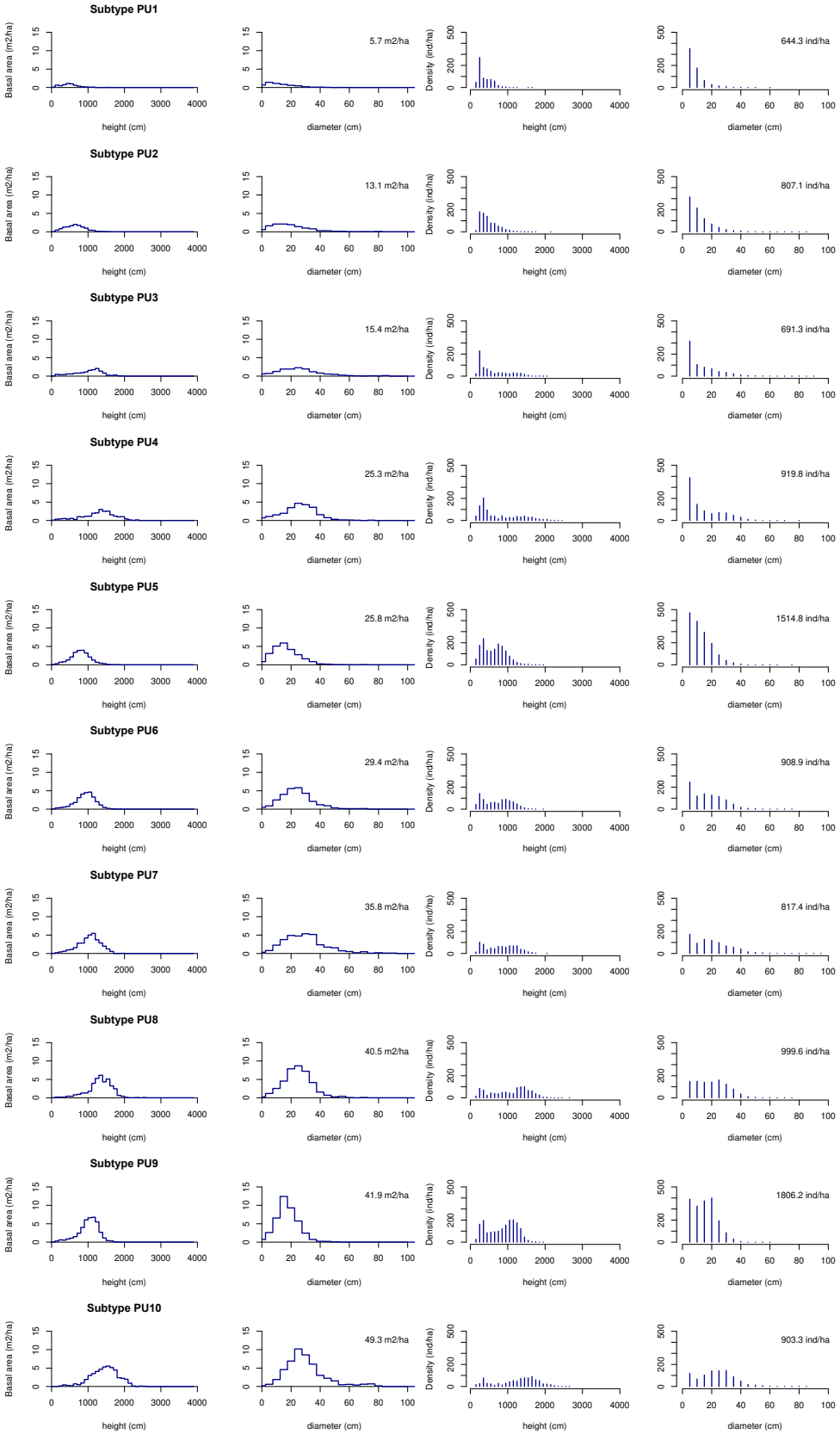
Subtype PU1
5.7 m2/ha
644.3 ind/ha
Subtype PU2
13.1 m2/ha
807.1 ind/ha
Subtype PU3
15.4 m2/ha
691.3 ind/ha
Subtype PU4
25.3 m2/ha
919.8 ind/ha
Subtype PU5
25.8 m2/ha
1514.8 ind/ha
Subtype PU6
29.4 m2/ha
908.9 ind/ha
Subtype PU7
35.8 m2/ha
817.4 ind/ha
Subtype PU8
40.5 m2/ha
999.6 ind/ha
Subtype PU9
41.9 m2/ha
1806.2 ind/ha
Subtype PU10
49.3 m2/ha
903.3 ind/ha
Basal area (m2/ha)
Density (ind/ha)
height (cm)
diameter (cm)

Table S3.4 Structural statistics of forests subtypes dominated by *Pinus uncinata* (PU), ordered by increasing basal area. Av. N and S.d. N – Average and standard deviation of density (ind./ha); Av. BA and S.d. BA – Average and standard deviation of basal area (m^2/ha); Av. D and S.d. D – Average and standard deviation of dbh (cm); Av. H and S.d. H – Average and standard deviation of height (cm).

Subtype	Plots	Av. N	S.d. N	Av. BA	S.d. BA	Av. D	S.d. D	Av. H	S.d. H
PU1	53	644	717	5.7	4.3	8.8	5.8	398	186
PU2	80	807	816	13.1	5.0	11.7	8.3	512	236
PU3	41	691	674	15.4	3.6	13.0	10.8	616	409
PU4	26	920	678	25.3	4.0	14.6	11.7	767	535
PU5	79	1515	986	25.8	6.5	12.6	7.6	655	302
PU6	41	909	486	29.4	4.6	17.1	11.0	738	369
PU7	28	817	593	35.8	7.2	19.9	12.8	836	405
PU8	24	1000	532	40.5	6.8	20.0	10.8	1085	501
PU9	44	1806	791	41.9	7.0	15.2	8.0	865	382
PU10	15	903	339	49.3	6.4	23.4	12.2	1277	545

Fig. S3.5 Three subtypes of forests dominated by *Pinus pinea* (PPI), ordered by increasing basal area. For each subtype we show the distribution of basal area (m^2/ha) among 1-m height classes and 5-cm diameter classes (first and second columns, respectively) and the distribution of density (ind./ha) among height and dbh classes (third and fourth columns, respectively).

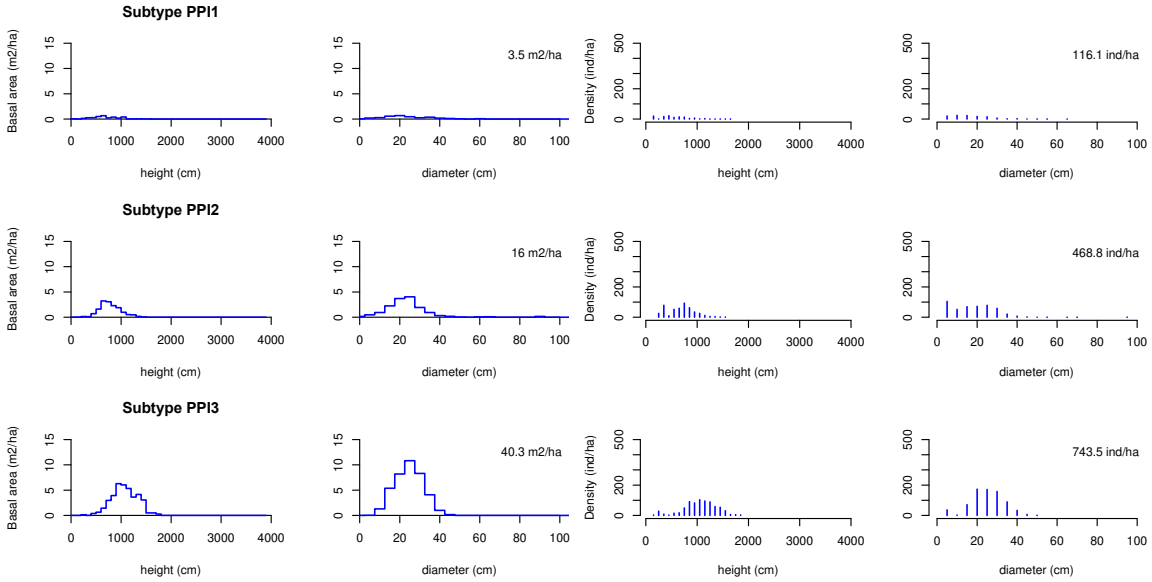

Table S3.5 Structural statistics of forests subtypes dominated by *Pinus pinea* (PPI), ordered by increasing basal area. Av. N and S.d. N – Average and standard deviation of density (ind./ha); Av. BA and S.d. BA – Average and standard deviation of basal area (m^2/ha); Av. D and S.d. D – Average and standard deviation of dbh (cm); Av. H and S.d. H – Average and standard deviation of height (cm).

Subtype	Plots	Av. N	S.d. N	Av. BA	S.d. BA	Av. D	S.d. D	Av. H	S.d. H
PPI1	26	116	207	3.5	3.6	17.0	9.8	561	276
PPI2	22	469	412	16.0	4.5	18.2	10.2	709	264
PPI3	12	744	416	40.3	13.4	25.0	8.1	1080	309

Fig. S3.6 Two subtypes of forests dominated by *Pinus pinaster* (PPS), ordered by increasing basal area. For each subtype we show the distribution of basal area (m^2/ha) among 1-m height classes and 5-cm diameter classes (first and second columns, respectively) and the distribution of density (ind./ha) among height and dbh classes (third and fourth columns, respectively).

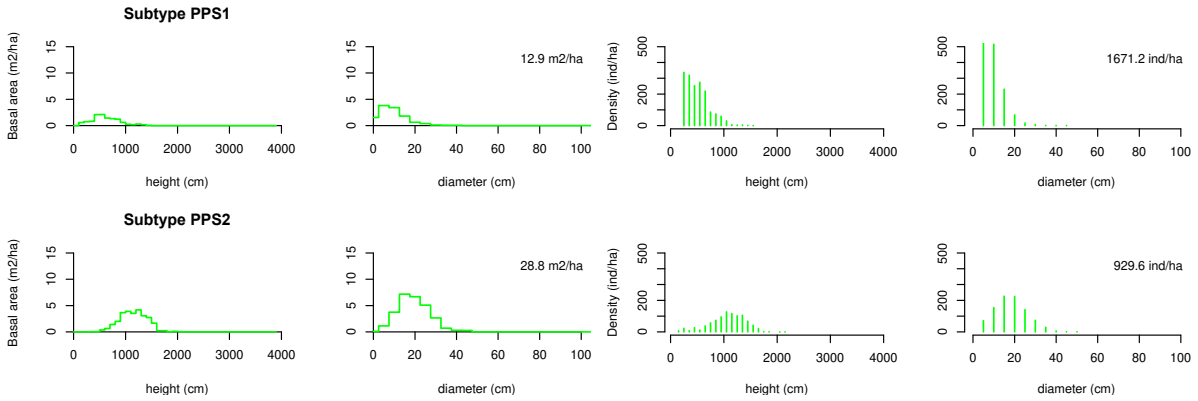

Table S3.6 Structural statistics of forests subtypes dominated by *Pinus pinaster* (PPS), ordered by increasing basal area. Av. N and S.d. N – Average and standard deviation of density (ind./ha); Av. BA and S.d. BA – Average and standard deviation of basal area (m^2/ha); Av. D and S.d. D – Average and standard deviation of dbh (cm); Av. H and S.d. H – Average and standard deviation of height (cm).

Subtype	Plots	Av. N	S.d. N	Av. BA	S.d. BA	Av. D	S.d. D	Av. H	S.d. H
PPS1	21	1671	1577	12.9	7.4	8.7	4.8	530	213
PPS2	19	930	629	28.8	10.3	18.3	7.8	1090	326

Fig. S3.7 Two subtypes of forests dominated by *Abies alba* (AA), ordered by increasing basal area. For each subtype we show the distribution of basal area (m^2/ha) among 1-m height classes and 5-cm diameter classes (first and second columns, respectively) and the distribution of density (ind./ha) among height and dbh classes (third and fourth columns, respectively).

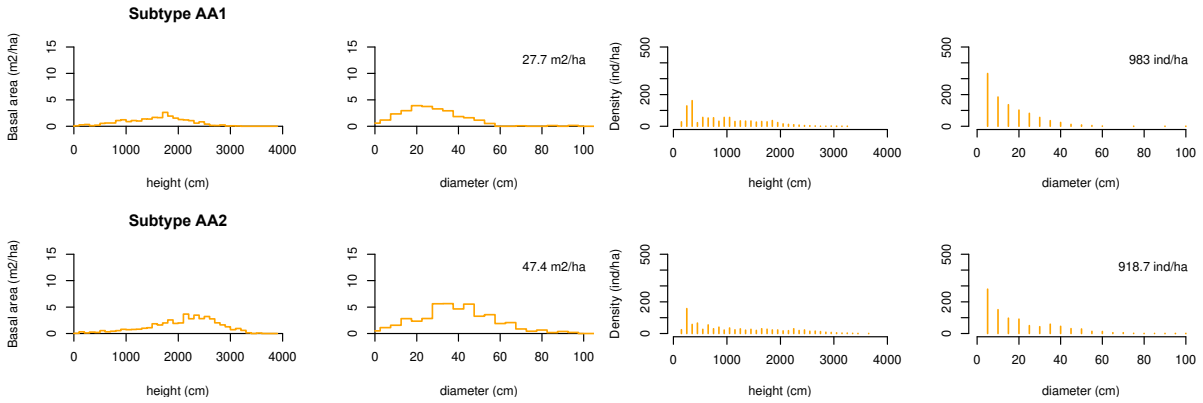

Table S3.7 Structural statistics of forests subtypes dominated by *Abies alba* (AA), ordered by increasing basal area. Av. N and S.d. N – Average and standard deviation of density (ind./ha); Av. BA and S.d. BA – Average and standard deviation of basal area (m^2/ha); Av. D and S.d. D – Average and standard deviation of dbh (cm); Av. H and S.d. H – Average and standard deviation of height (cm).

Subtype	Plots	Av. N	S.d. N	Av. BA	S.d. BA	Av. D	S.d. D	Av. H	S.d. H
AA1	24	983	736	27.7	12.8	15.1	11.5	944	626
AA2	18	919	468	47.4	12.4	19.7	16.4	1157	835

Fig. S3.8 Eleven subtypes of forests dominated by *Quercus ilex* (QI), ordered by increasing basal area. For each subtype we show the distribution of basal area (m^2/ha) among 1-m height classes and 5-cm diameter classes (first and second columns, respectively) and the distribution of density (ind./ha) among height and dbh classes (third and fourth columns, respectively).

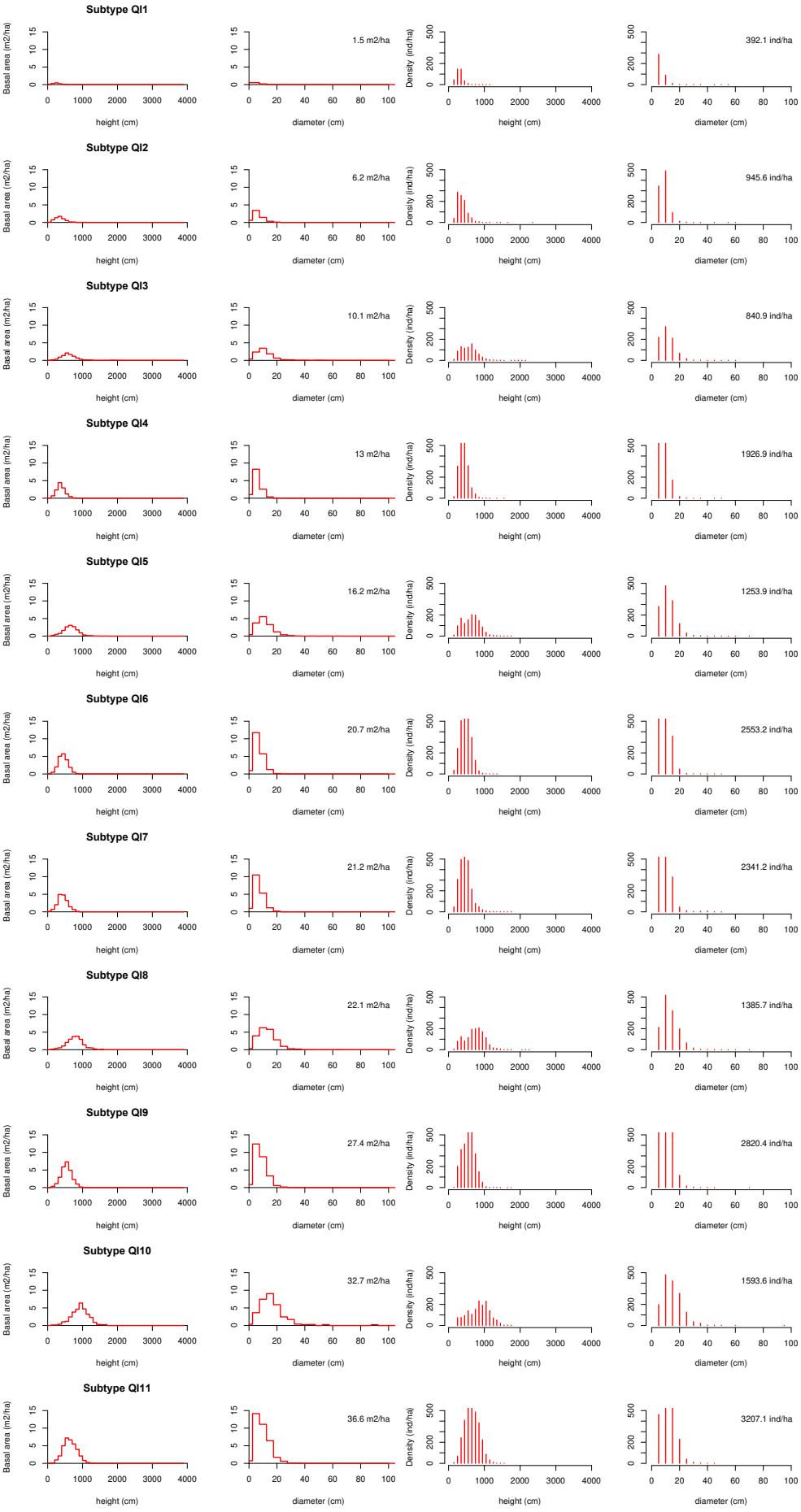
Subtype QI1
1.5 m2/ha
392.1 ind/ha
Subtype QI2
6.2 m2/ha
945.6 ind/ha
Subtype QI3
10.1 m2/ha
840.9 ind/ha
Subtype QI4
13 m2/ha
1926.9 ind/ha
Subtype QI5
16.2 m2/ha
1253.9 ind/ha
Subtype QI6
20.7 m2/ha
2553.2 ind/ha
Subtype QI7
21.2 m2/ha
2341.2 ind/ha
Subtype QI8
22.1 m2/ha
1385.7 ind/ha
Subtype QI9
27.4 m2/ha
2820.4 ind/ha
Subtype QI10
32.7 m2/ha
1593.6 ind/ha
Subtype QI11
36.6 m2/ha
3207.1 ind/ha
Basal area (m2/ha)
Density (ind/ha)
height (cm)
diameter (cm)

Table S3.8 Structural statistics of forests subtypes dominated by *Quercus ilex* (QI), ordered by increasing basal area. Av. N and S.d. N – Average and standard deviation of density (ind./ha); Av. BA and S.d. BA – Average and standard deviation of basal area (m^2/ha); Av. D and S.d. D – Average and standard deviation of dbh (cm); Av. H and S.d. H – Average and standard deviation of height (cm).

Subtype	Plots	Av. N	S.d. N	Av. BA	S.d. BA	Av. D	S.d. D	Av. H	S.d. H
QI1	161	392	464	1.5	1.4	6.3	2.8	336	98
QI2	139	946	560	6.2	2.1	8.5	3.5	400	135
QI3	66	841	471	10.1	3.0	11.1	5.5	587	220
QI4	108	1927	835	13.0	3.5	8.7	3.2	444	124
QI5	78	1254	525	16.2	3.1	11.6	5.4	646	234
QI6	87	2553	775	20.7	3.7	9.6	3.5	496	142
QI7	11	2341	895	21.2	6.3	9.8	4.4	487	168
QI8	54	1386	526	22.1	4.1	12.9	6.0	752	265
QI9	50	2820	735	27.4	3.9	10.4	4.0	580	167
QI10	18	1594	692	32.7	6.3	14.6	7.0	861	295
QI11	26	3207	828	36.6	5.3	11.2	4.4	672	193

Fig. S3.9 Seven subtypes of forests dominated by *Quercus suber* (QS), ordered by increasing basal area. For each subtype we show the distribution of basal area (m^2/ha) among 1-m height classes and 5-cm diameter classes (first and second columns, respectively) and the distribution of density (ind./ha) among height and dbh classes (third and fourth columns, respectively).

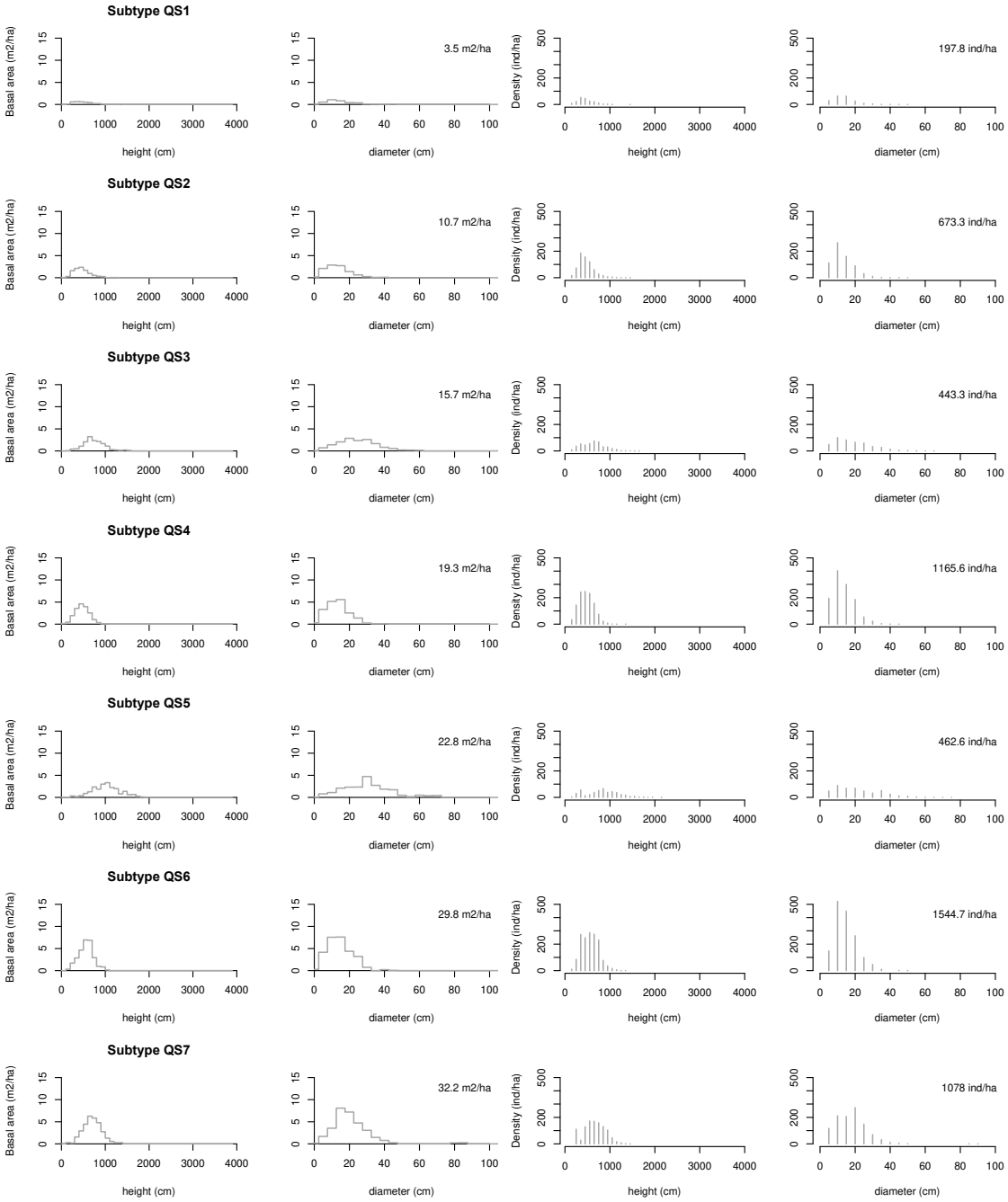

Table S3.9 Structural statistics of forests subtypes dominated by *Quercus suber* (QS), ordered by increasing basal area. Av. N and S.d. N – Average and standard deviation of density (ind./ha); Av. BA and S.d. BA – Average and standard deviation of basal area (m^2/ha); Av. D and S.d. D – Average and standard deviation of dbh (cm); Av. H and S.d. H – Average and standard deviation of height (cm).

Subtype	Plots	Av. N	S.d. N	Av. BA	S.d. BA	Av. D	S.d. D	Av. H	S.d. H
QS1	45	198	211	3.5	2.4	13.6	6.3	476	180
QS2	46	673	448	10.7	3.3	12.8	6.1	486	172
QS3	23	443	244	15.7	3.7	18.4	10.5	644	257
QS4	30	1166	585	19.3	4.1	13.2	6.0	496	164
QS5	10	463	222	22.8	5.6	21.7	12.5	843	366
QS6	12	1545	389	29.8	4.3	14.4	6.2	586	187
QS7	12	1078	655	32.2	9.0	17.6	8.5	681	229

845 **Fig. S3.10** Three subtypes of forests dominated by *Quercus humilis* (QH), ordered by increasing basal
846 area. For each subtype we show the distribution of basal area (m^2/ha) among 1-m height classes and 5-
847 cm diameter classes (first and second columns, respectively) and the distribution of density (ind./ha)
848 among height and dbh classes (third and fourth columns, respectively).

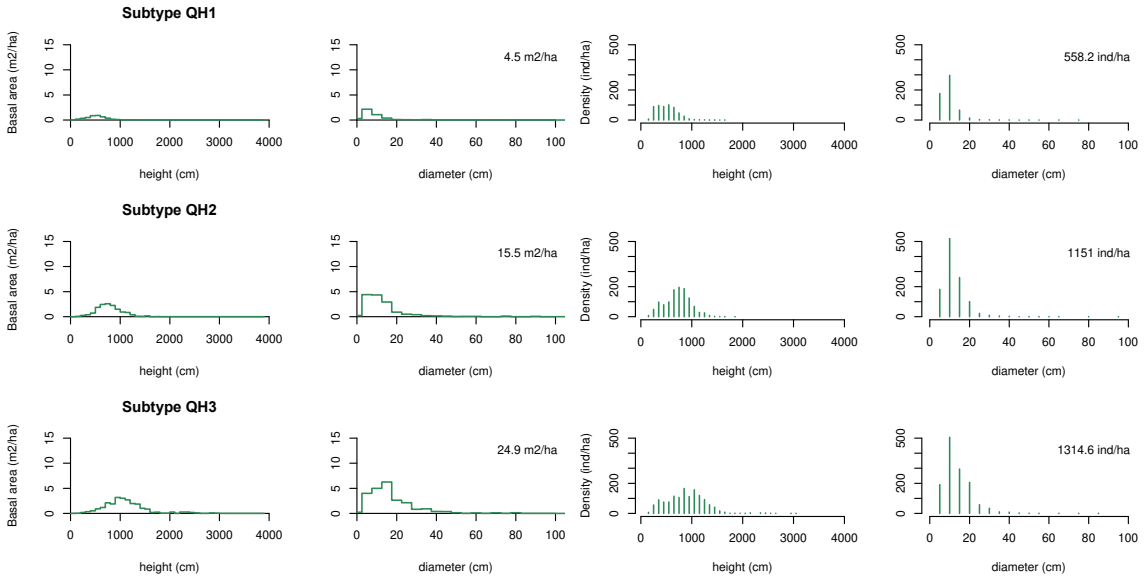

849

850 **Table S3.10** Structural statistics of forests subtypes dominated by *Quercus humilis* (QH), ordered by
851 increasing basal area. Av. N and S.d. N – Average and standard deviation of density (ind./ha); Av. BA
852 and S.d. BA – Average and standard deviation of basal area (m^2/ha); Av. D and S.d. D – Average and
853 standard deviation of dbh (cm); Av. H and S.d. H – Average and standard deviation of height (cm).

Subtype	Plots	Av. N	S.d. N	Av. BA	S.d. BA	Av. D	S.d. D	Av. H	S.d. H
QH1	124	558	633	4.5	4.5	9.2	4.2	529	199
QH2	46	1151	796	15.5	5.2	11.8	5.7	737	246
QH3	19	1315	747	24.9	7.8	13.7	7.3	912	375

854

855

Fig. S3.11 Two subtypes of forests dominated by *Quercus faginea* (QF), ordered by increasing basal area. For each subtype we show the distribution of basal area (m^2/ha) among 1-m height classes and 5-cm diameter classes (first and second columns, respectively) and the distribution of density (ind./ha) among height and dbh classes (third and fourth columns, respectively).

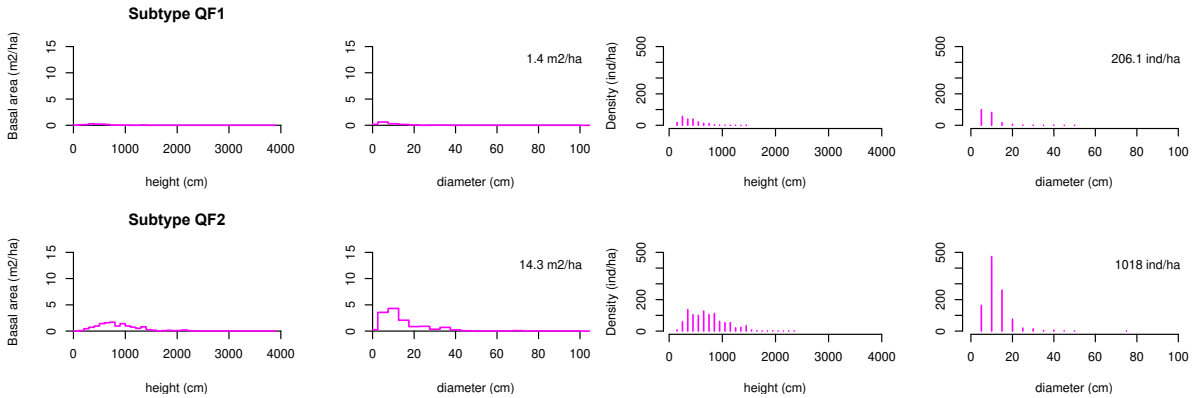

Table S3.11 Structural statistics of forests subtypes dominated by *Quercus faginea* (QF), ordered by increasing basal area. Av. N and S.d. N – Average and standard deviation of density (ind./ha); Av. BA and S.d. BA – Average and standard deviation of basal area (m^2/ha); Av. D and S.d. D – Average and standard deviation of dbh (cm); Av. H and S.d. H – Average and standard deviation of height (cm).

Subtype	Plots	Av. N	S.d. N	Av. BA	S.d. BA	Av. D	S.d. D	Av. H	S.d. H
QF1	71	206	351	1.4	2.5	8.4	4.4	433	186
QF2	24	1018	635	14.3	6.7	12.0	6.0	745	341

Fig. S3.12 Three subtypes of forests dominated by *Fagus sylvatica* (FS), ordered by increasing basal area. For each subtype we show the distribution of basal area (m^2/ha) among 1-m height classes and 5-cm diameter classes (first and second columns, respectively) and the distribution of density (ind./ha) among height and dbh classes (third and fourth columns, respectively).

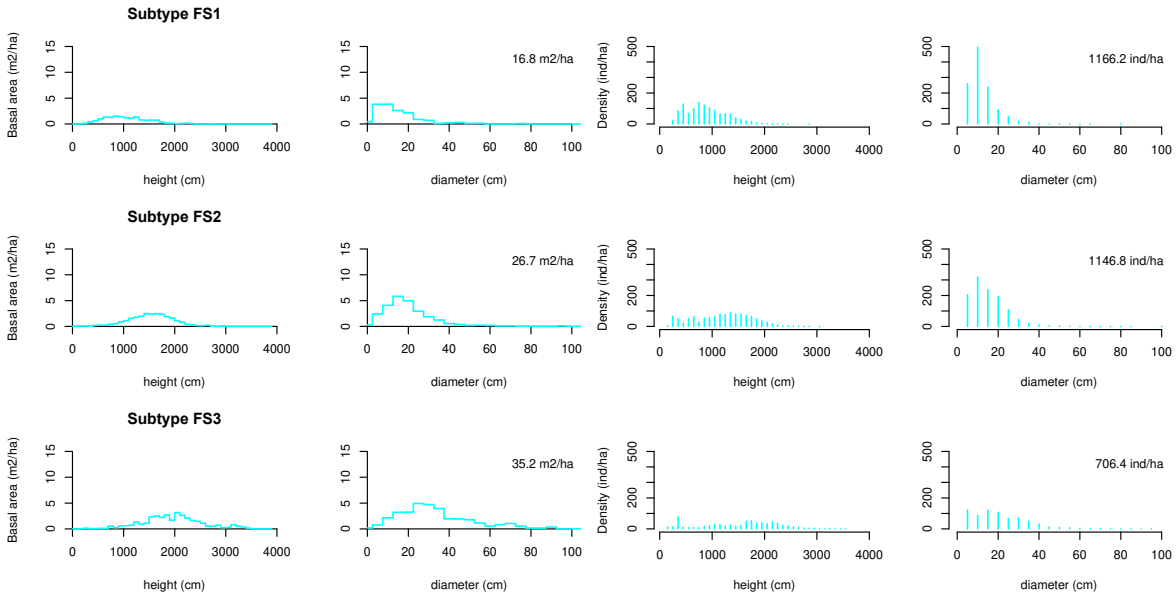

Table S3.12 Structural statistics of forests subtypes dominated by *Fagus sylvatica* (FS), ordered by increasing basal area. Av. N and S.d. N – Average and standard deviation of density (ind./ha); Av. BA and S.d. BA – Average and standard deviation of basal area (m^2/ha); Av. D and S.d. D – Average and standard deviation of dbh (cm); Av. H and S.d. H – Average and standard deviation of height (cm).

Subtype	Plots	Av. N	S.d. N	Av. BA	S.d. BA	Av. D	S.d. D	Av. H	S.d. H
FS1	29	1166	890	16.8	6.8	11.9	6.6	897	384
FS2	46	1147	491	26.7	5.0	15.0	8.5	1227	531
FS3	19	706	387	35.2	9.4	21.0	13.9	1548	745

Appendix S4. Two-species forest types

Fig. S4.1 Three subtypes of forests co-dominated by *Pinus halepensis* (PH) and *P. nigra* (PN), ordered by increasing basal area. For each subtype and species we show the distribution of basal area (m^2/ha) among 1 m height classes and 5 cm diameter classes (first and second columns, respectively) and the distribution of density (ind./ha) among height and dbh classes (third and fourth columns, respectively).

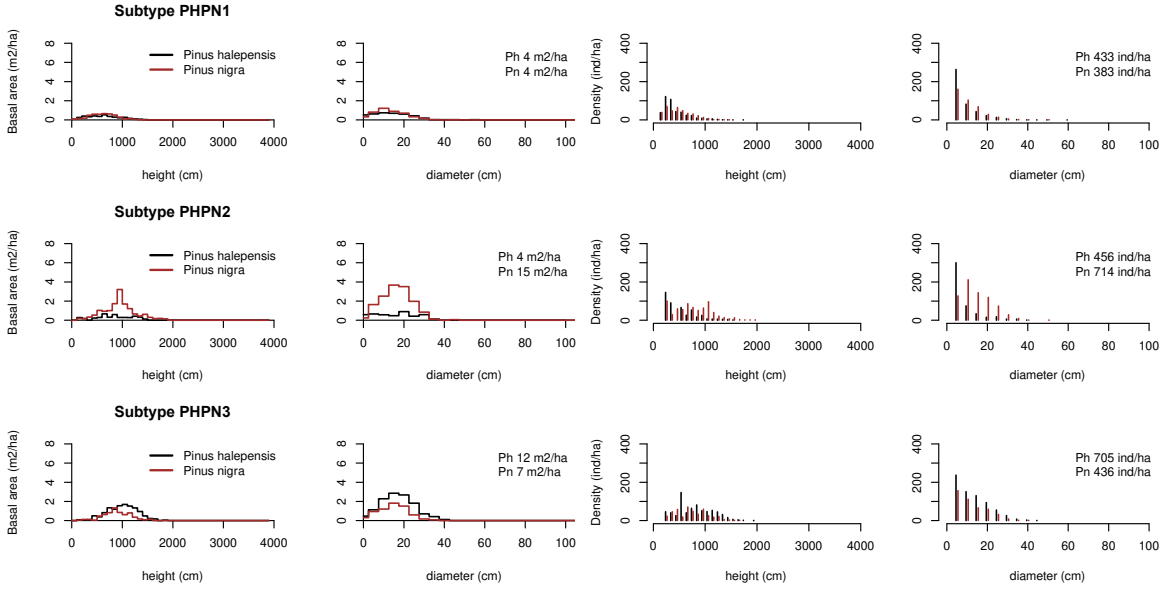

Table S4.1 Structural statistics of the forests subtypes co-dominated by *Pinus halepensis* (PH) and *P. nigra* (PN), ordered by increasing basal area. Av. N1 and Av. N2 – Average density (ind./ha) for PH and PN, respectively; Av. BA1 and Av. BA2 – Average basal area (m^2/ha) for PH and PN, respectively; Av. D1, S.d. D1, Av. D2 and S.d. D2 – Average and standard deviation of dbh (cm) for PH and PN, respectively; Av. H1, S.d. H1, Av. H1 and S.d. H1 – Average and standard deviation of height (cm) for PH and PN, respectively.

Subtype	Plots	Av. N1	Av. N2	Av. BA1	Av. BA2	Av. D1	S.d. D1	Av. H1	S.d. H1	Av. D2	S.d. D2	Av. H2	S.d. H2
PHPN1	58	433	383	3.9	4.5	8.7	6.2	455	245	10.4	6.3	510	244
PHPN2	14	456	714	4.3	14.6	8.7	6.6	552	295	14.3	7.4	782	347
PHPN3	22	705	436	12.4	6.6	12.8	7.9	822	340	12.0	7.1	757	298

Fig. S4.2 Four subtypes of forests co-dominated by *Pinus halepensis* (PH) and *P. pinea* (PPI), ordered by increasing basal area. For each subtype and species we show the distribution of basal area (m^2/ha) among 1 m height classes and 5 cm diameter classes (first and second columns, respectively) and the distribution of density (ind./ha) among height and dbh classes (third and fourth columns, respectively).

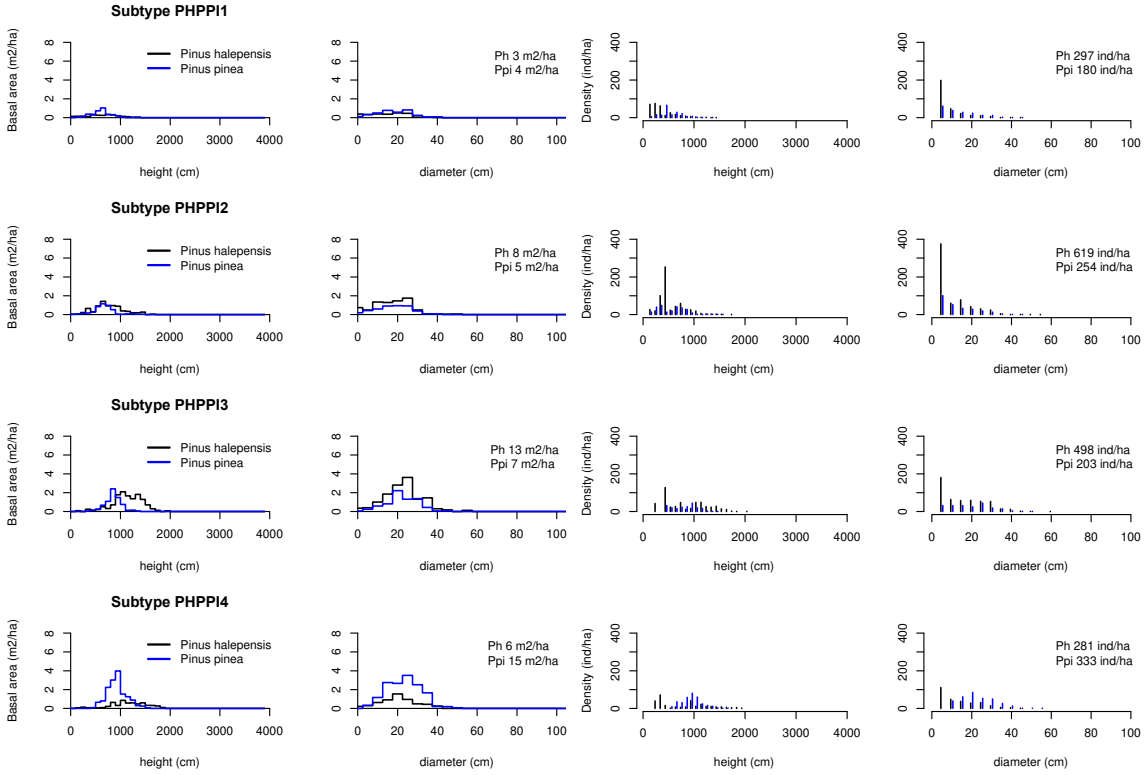

Table S4.2 Structural statistics of the forests subtypes co-dominated by *Pinus halepensis* (PH) and *P. pinea* (PPI), ordered by increasing basal area.

Subtype	Plots	Av. N1	Av. N2	Av. BA1	Av. BA2	Av. D1	S.d. D1	Av. H1	S.d. H1	Av. D2	S.d. D2	Av. H2	S.d. H2
PHPPI1	27	297	180	2.6	3.5	8.4	6.3	410	235	13.3	8.5	563	198
PHPPI2	19	619	254	7.8	4.5	10.0	7.7	553	250	12.5	8.4	565	246
PHPPI3	12	498	203	13.4	7.2	15.2	10.6	853	398	18.9	9.8	814	241
PHPPI4	16	281	333	5.7	15.1	13.1	9.3	794	471	22.5	8.3	954	197

Fig. S4.3 Six subtypes of forests co-dominated by *Pinus halepensis* (PH) and *Quercus ilex* (QI), ordered by increasing basal area. For each subtype and species we show the distribution of basal area (m^2/ha) among 1 m height classes and 5 cm diameter classes (first and second columns, respectively) and the distribution of density (ind./ha) among height and dbh classes (third and fourth columns, respectively).

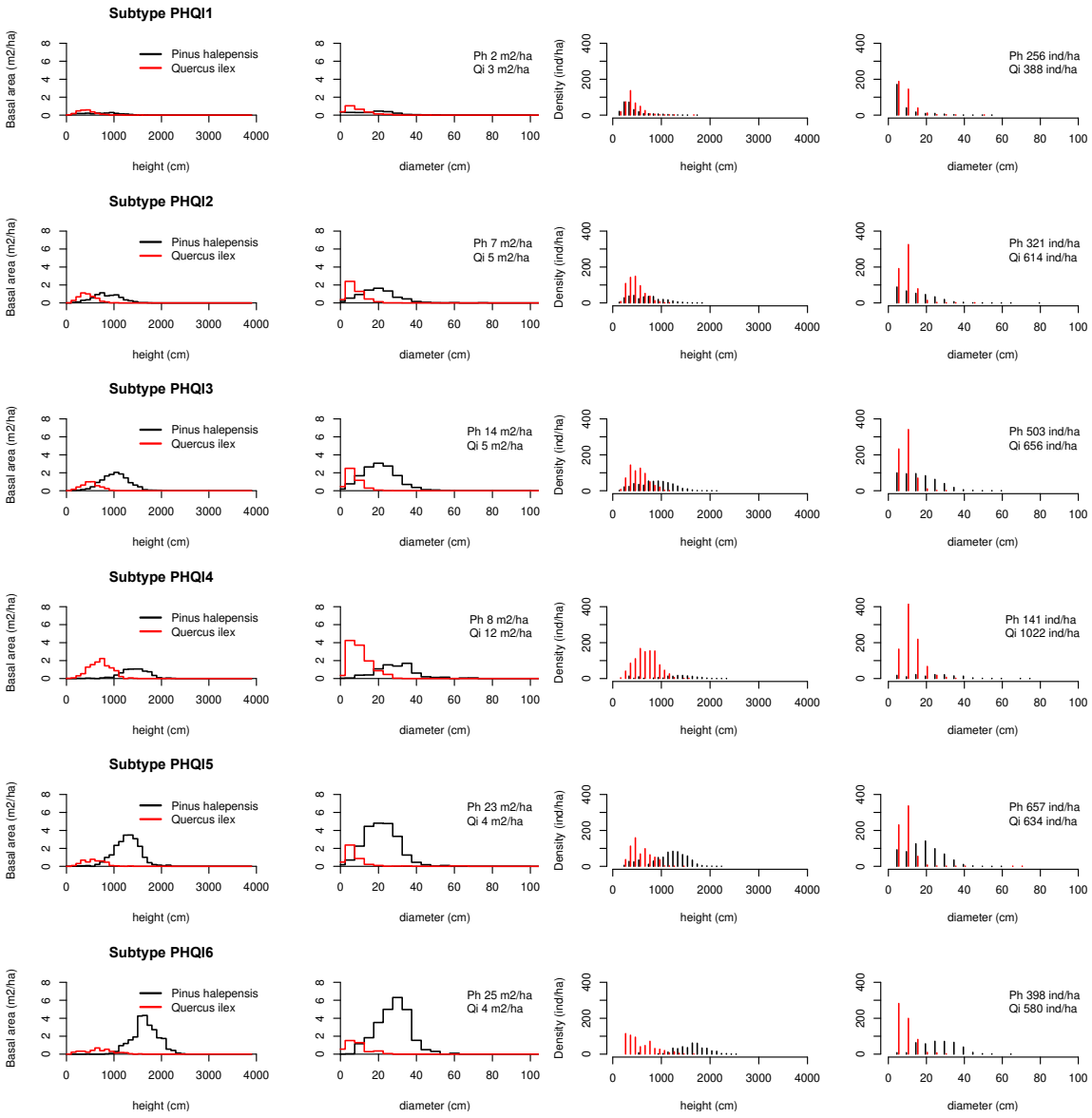

Table S4.3 Structural statistics of the forests subtypes co-dominated by *Pinus halepensis* (PH) and *Quercus ilex* (QI), ordered by increasing basal area. Av. N1 and Av. N2 – Average density (ind./ha) for PH and QI, respectively; Av. BA1 and Av. BA2 – Average basal area (m^2/ha) for PH and QI, respectively; Av. D1, S.d. D1, Av. D2 and S.d. D2 – Average and standard deviation of dbh (cm) for PH and QI, respectively; Av. H1, S.d. H1, Av. H1 and S.d. H1 – Average and standard deviation of height (cm) for PH and QI, respectively.

Subtype	Plots	Av. N1	Av. N2	Av. BA1	Av. BA2	Av. D1	S.d. D1	Av. H1	S.d. H1	Av. D2	S.d. D2	Av. H2	S.d. H2
PHQI1	73	256	388	2.5	2.7	8.7	7.0	441	248	8.3	4.3	426	154
PHQI2	98	321	614	7.5	4.7	14.6	9.0	713	312	9.1	3.8	472	162
PHQI3	78	503	656	14.1	4.5	16.5	9.2	901	340	8.7	3.5	532	180
PHQI4	29	141	1022	7.8	11.6	23.6	12.2	1271	444	11.1	4.6	690	223
PHQI5	47	657	634	22.5	4.2	18.8	9.2	1175	368	8.5	3.6	579	197
PHQI6	16	298	580	25.3	4.0	26.8	9.6	1649	316	8.4	4.2	578	274

Fig. S4.4 Subtype of forests co-dominated by *Pinus halepensis* (PH) and *Quercus humilis* (QH). For each subtype and species we show the distribution of basal area (m^2/ha) among 1 m height classes and 5 cm diameter classes (first and second columns, respectively) and the distribution of density (ind./ha) among height and dbh classes (third and fourth columns, respectively).

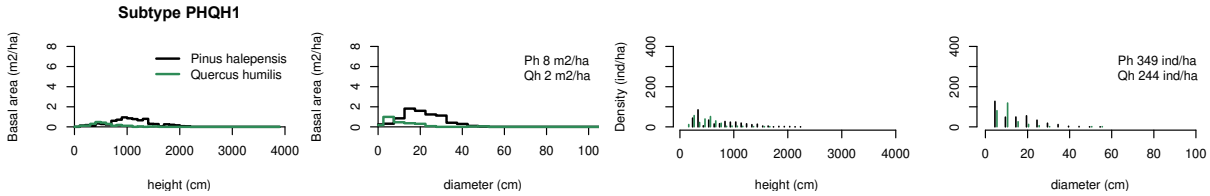

Table S4.4 Structural statistics of the forest subtype co-dominated by *Pinus halepensis* (PH) and *Quercus humilis* (QH).

Subtype	Plots	Av. N1	Av. N2	Av. BA1	Av. BA2	Av. D1	S.d. D1	Av. H1	S.d. H1	Av. D2	S.d. D2	Av. H2	S.d. H2
PHQH1	29	349	244	8.1	2.4	14.2	9.6	768	433	10.0	5.1	511	224

Fig. S4.5 Two subtypes of forests co-dominated by *Pinus halepensis* (PH) and *Quercus faginea* (QF), ordered by increasing basal area. For each subtype and species we show the distribution of basal area (m^2/ha) among 1 m height classes and 5 cm diameter classes (first and second columns, respectively) and the distribution of density (ind./ha) among height and dbh classes (third and fourth columns, respectively).

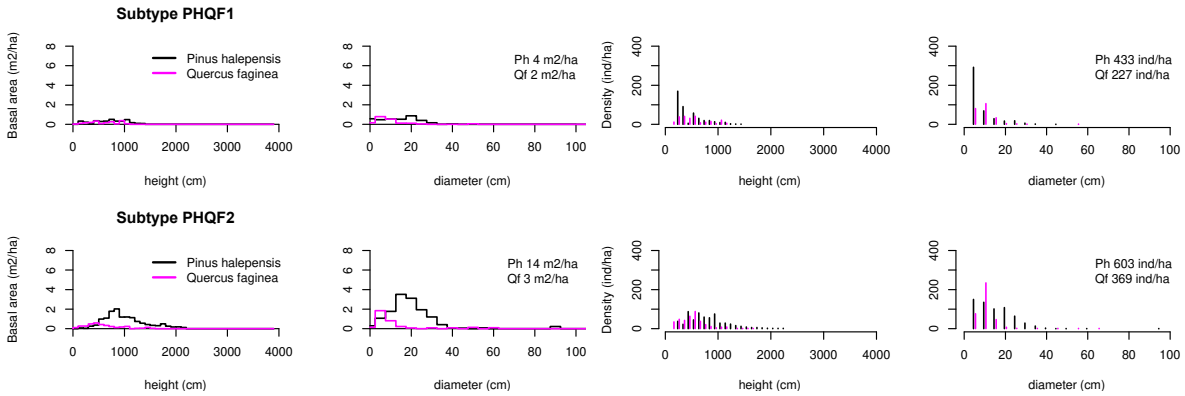

Table S4.5 Structural statistics of forests subtypes co-dominated by *Pinus halepensis* (PH) and *Quercus faginea* (QF), ordered by increasing basal area.

Subtype	Plots	Av. N1	Av. N2	Av. BA1	Av. BA2	Av. D1	S.d. D1	Av. H1	S.d. H1	Av. D2	S.d. D2	Av. H2	S.d. H2
PHQF1	24	433	227	3.6	1.8	8.2	6.1	478	267	9.1	4.3	547	263
PHQF2	17	604	369	13.7	3.5	14.7	8.6	832	362	10.0	4.6	515	236

Fig. S4.6 Five subtypes of forests co-dominated by *Pinus nigra* (PN) and *P. sylvestris* (PS), ordered by increasing basal area. For each subtype and species we show the distribution of basal area (m^2/ha) among 1 m height classes and 5 cm diameter classes (first and second columns, respectively) and the distribution of density (ind./ha) among height and dbh classes (third and fourth columns, respectively).

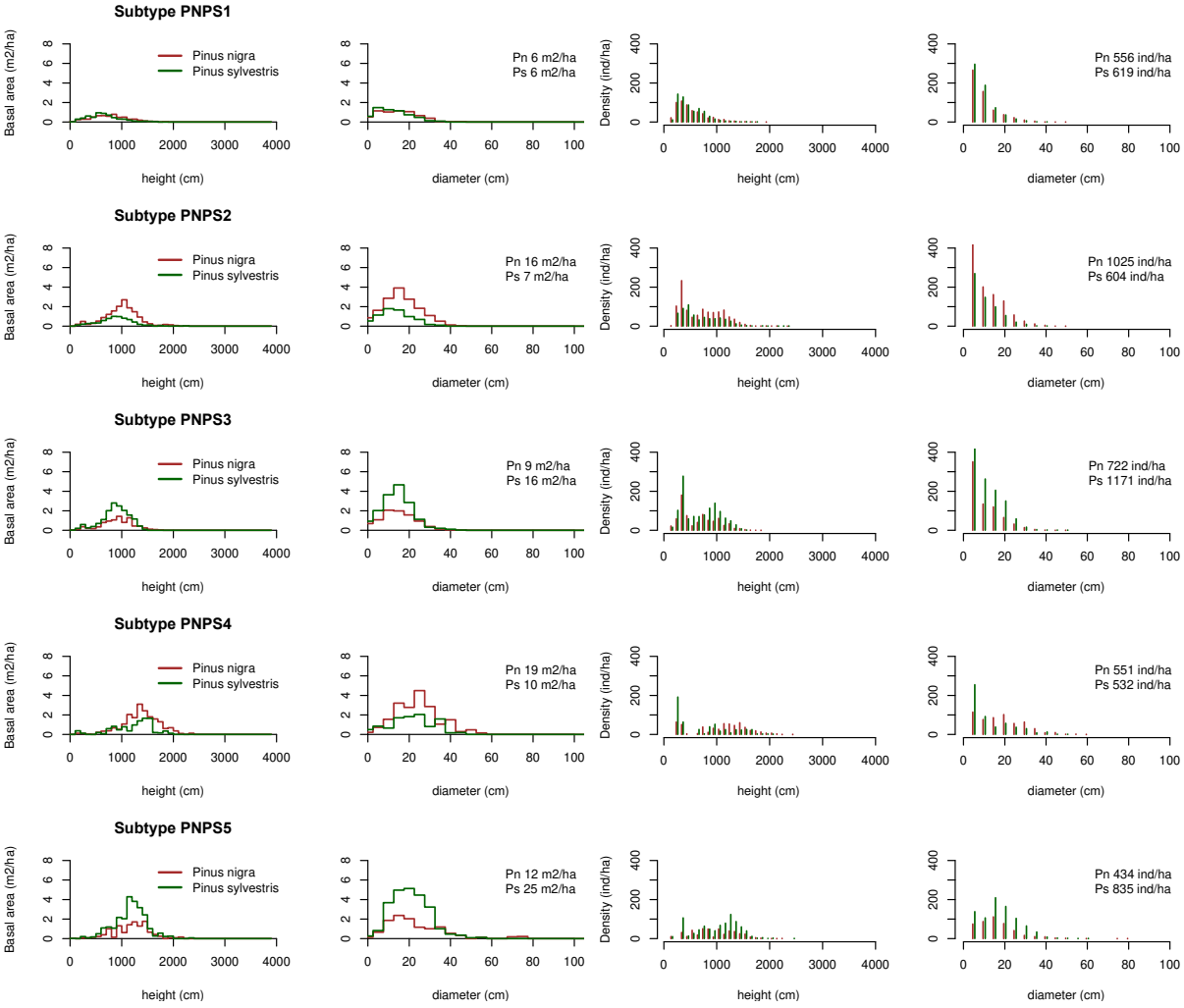

Table S4.6 Structural statistics of the forest subtypes co-dominated by *Pinus nigra* (PN) and *P. sylvestris* (PS), ordered by increasing basal area.

Subtype	Plots	Av. N1	Av. N2	Av. BA1	Av. BA2	Av. D1	S.d. D1	Av. H1	S.d. H1	Av. D2	S.d. D2	Av. H2	S.d. H2
PNPS1	59	556	619	6.1	5.9	9.8	6.5	550	285	9.4	5.8	523	248
PNPS2	52	1025	604	15.6	7.1	11.7	7.6	741	377	10.4	6.4	695	337
PNPS3	41	722	1171	8.9	15.9	10.5	6.9	675	341	11.2	6.8	718	330
PNPS4	10	550	532	19.3	10.4	18.3	10.6	1104	503	12.5	9.6	769	508
PNPS5	12	434	835	11.8	24.6	16.0	9.5	983	399	17.2	8.9	1030	395

Fig. S4.7 Four subtypes of forests co-dominated by *Pinus nigra* (PN) and *Quercus ilex* (QI), ordered by increasing basal area. For each subtype and species we show the distribution of basal area (m^2/ha) among 1 m height classes and 5 cm diameter classes (first and second columns, respectively) and the distribution of density (ind./ha) among height and dbh classes (third and fourth columns, respectively).

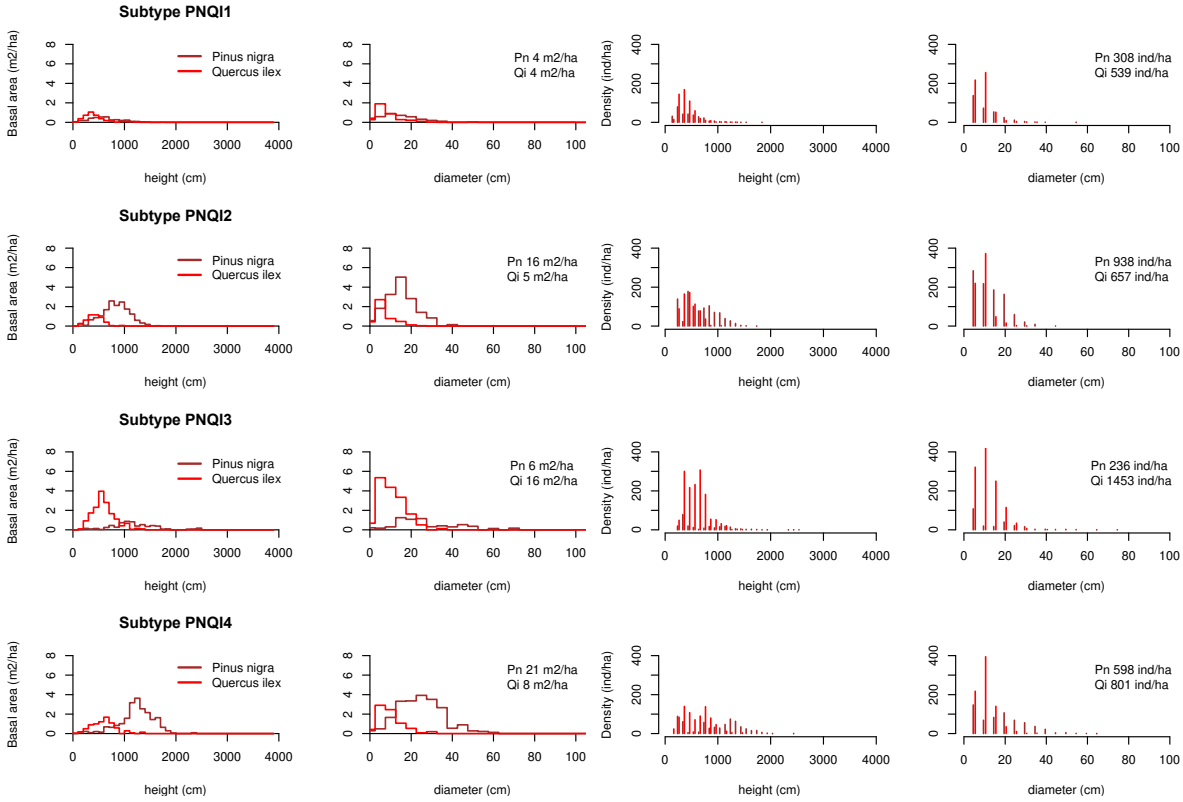

Table S4.7 Structural statistics of the forest subtypes co-dominated by *Pinus nigra* (PN) and *Quercus ilex* (QI), ordered by increasing basal area.

Subtype	Plots	Av. N1	Av. N2	Av. BA1	Av. BA2	Av. D1	S.d. D1	Av. H1	S.d. H1	Av. D2	S.d. D2	Av. H2	S.d. H2
PNQI1	62	308	539	3.7	3.8	10.4	6.6	479	251	8.6	4.0	420	154
PNQI2	22	938	657	15.8	4.6	12.8	7.1	699	292	8.7	3.5	479	144
PNQI3	13	236	1453	6.4	16.0	14.6	11.5	732	439	10.7	5.0	597	212
PNQI4	13	598	801	21.3	7.7	18.2	11.1	978	474	10.0	4.6	595	243

Fig. S4.8 Three subtypes of forests co-dominated by *Pinus nigra* (PN) and *Quercus humilis* (QH), ordered by increasing basal area. For each subtype and species we show the distribution of basal area (m^2/ha) among 1 m height classes and 5 cm diameter classes (first and second columns, respectively) and the distribution of density (ind./ha) among height and dbh classes (third and fourth columns, respectively).

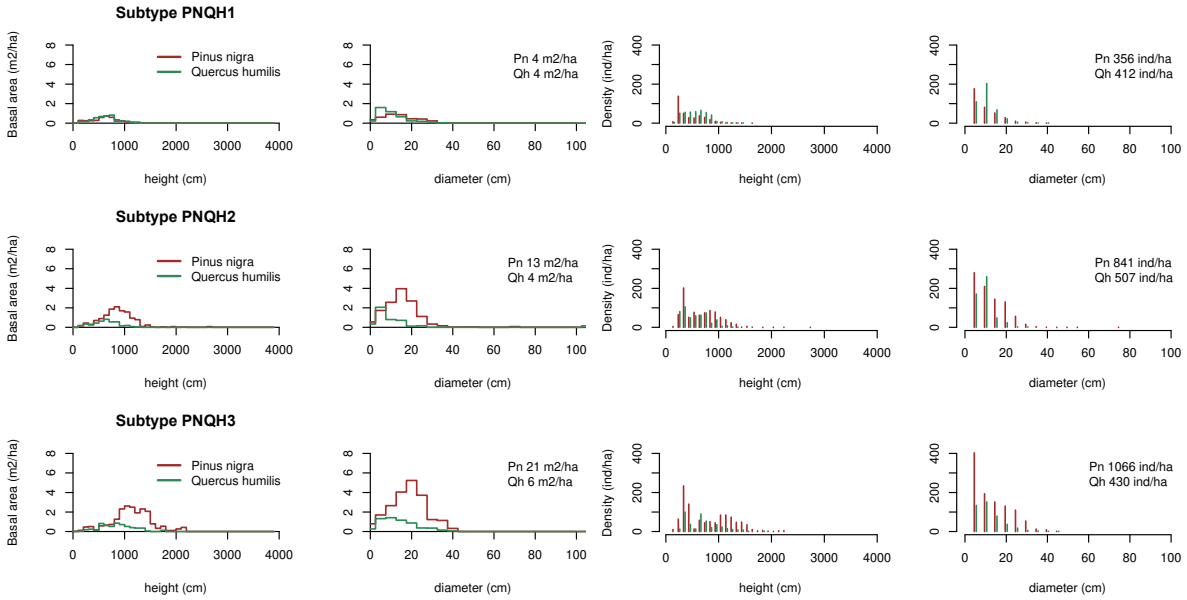

Table S4.8 Structural statistics of the forest subtypes co-dominated by *Pinus nigra* (PN) and *Quercus humilis* (QH), ordered by increasing basal area.

Subtype	Plots	Av. N1	Av. N2	Av. BA1	Av. BA2	Av. D1	S.d. D1	Av. H1	S.d. H1	Av. D2	S.d. D2	Av. H2	S.d. H2
PNQH1	47	356	412	3.9	4.2	9.9	6.5	485	244	10.3	4.8	591	231
PNQH2	31	840	507	13.3	4.3	12.3	7.1	692	320	9.4	4.6	580	239
PNQH3	12	1066	430	20.8	6.0	13.2	8.6	825	453	11.6	6.5	696	310

Fig. S4.9 Two subtypes of forests co-dominated by *Pinus nigra* (PN) and *Quercus faginea* (QF), ordered by increasing basal area. For each subtype and species we show the distribution of basal area (m^2/ha) among 1 m height classes and 5 cm diameter classes (first and second columns, respectively) and the distribution of density (ind./ha) among height and dbh classes (third and fourth columns, respectively).

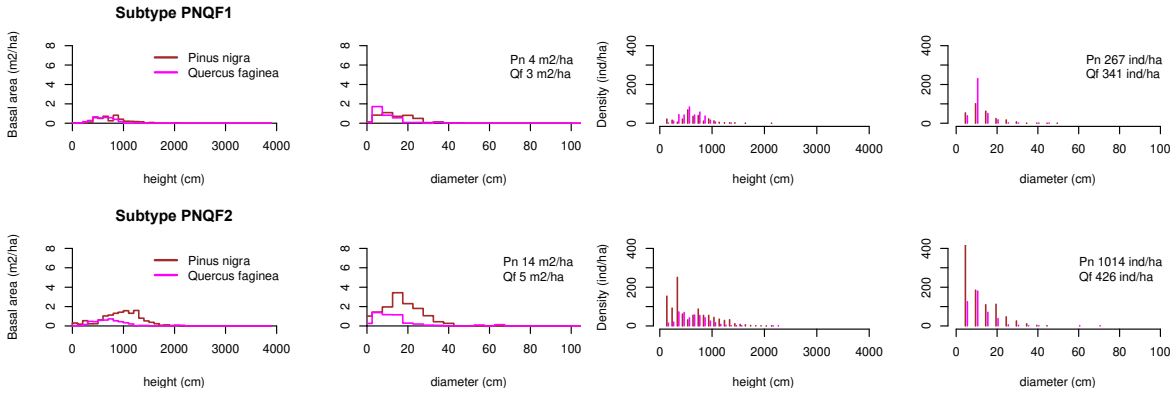

Table S4.9 Structural statistics of the forest subtypes co-dominated by *Pinus nigra* (PN) and *Quercus faginea* (QF), ordered by increasing basal area.

Subtype	Plots	Av. N1	Av. N2	Av. BA1	Av. BA2	Av. D1	S.d. D1	Av. H1	S.d. H1	Av. D2	S.d. D2	Av. H2	S.d. H2
PNQF1	24	267	340	4.3	3.4	12.8	6.5	667	270	10.6	4.1	631	191
PNQF2	29	1014	426	13.7	4.8	10.7	7.6	601	394	10.6	5.7	630	248

Fig. S4.10 Four subtypes of forests co-dominated by *Pinus sylvestris* (PS) and *P. uncinata* (PU), ordered by increasing basal area. For each subtype and species we show the distribution of basal area (m^2/ha) among 1 m height classes and 5 cm diameter classes (first and second columns, respectively) and the distribution of density (ind./ha) among height and dbh classes (third and fourth columns, respectively).

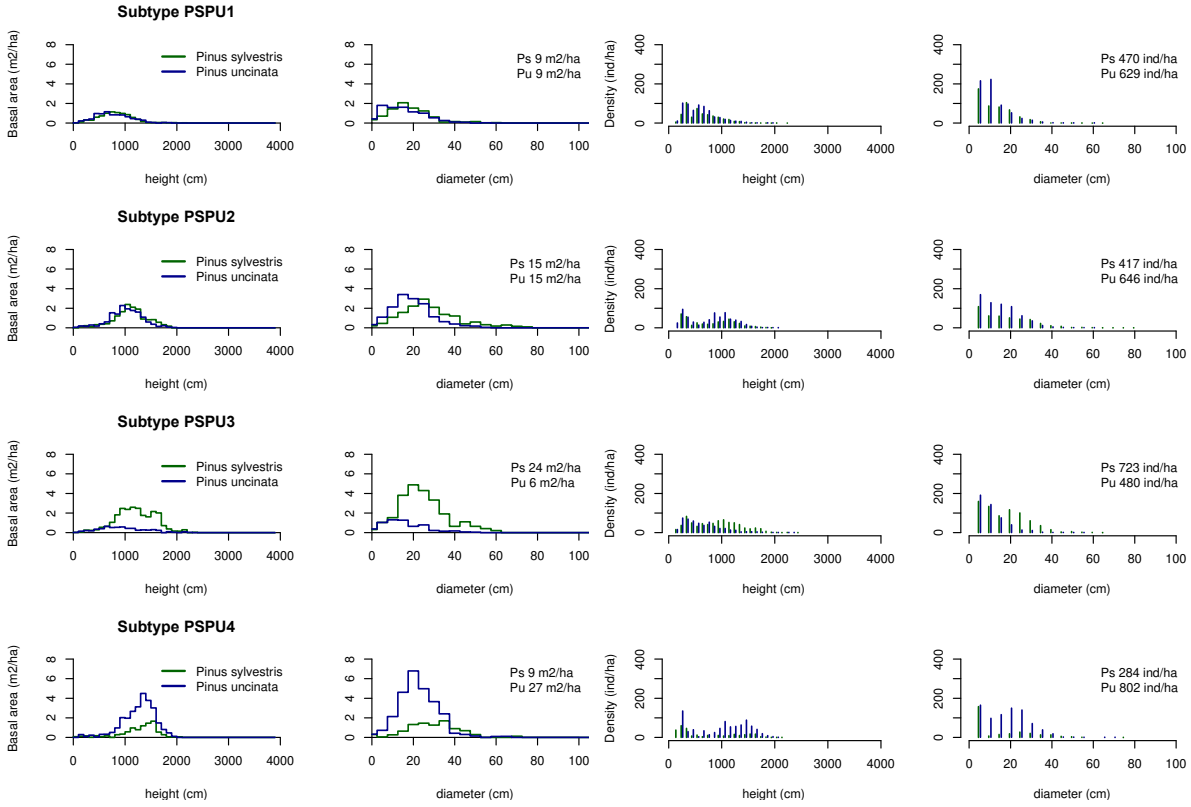

Table S4.10 Structural statistics of the forest subtypes co-dominated by *Pinus sylvestris* (PS) and *P. uncinata* (PU), ordered by increasing basal area. Av. N1 and Av. N2 – Average density (ind./ha) for PS and PU, respectively; Av. BA1 and Av. BA2 – Average basal area (m^2/ha) for PS and PU, respectively; Av. D1, S.d. D1, Av. D2 and S.d. D2 – Average and standard deviation of dbh (cm) for PS and PU, respectively; Av. H1, S.d. H1, Av. H1 and S.d. H1 – Average and standard deviation of height (cm) for PS and PU, respectively.

Subtype	Plots	Av. N1	Av. N2	Av. BA1	Av. BA2	Av. D1	S.d. D1	Av. H1	S.d. H1	Av. D2	S.d. D2	Av. H2	S.d. H2
PSPU1	49	470	629	8.5	8.6	12.7	8.3	641	297	11.2	6.9	602	283
PSPU2	27	417	646	15.2	15.0	17.8	12.1	818	435	14.8	8.8	816	397
PSPU3	24	723	480	24.1	6.1	17.5	10.8	922	442	10.7	6.9	643	347
PSPU4	17	284	802	9.0	26.7	15.1	13.2	758	539	18.0	9.9	1036	486

Fig. S4.11 Subtype of forests co-dominated by *Pinus sylvestris* (PS) and *Abies alba* (AA). For each subtype and species we show the distribution of basal area (m^2/ha) among 1 m height classes and 5 cm diameter classes (first and second columns, respectively) and the distribution of density (ind./ha) among height and dbh classes (third and fourth columns, respectively).

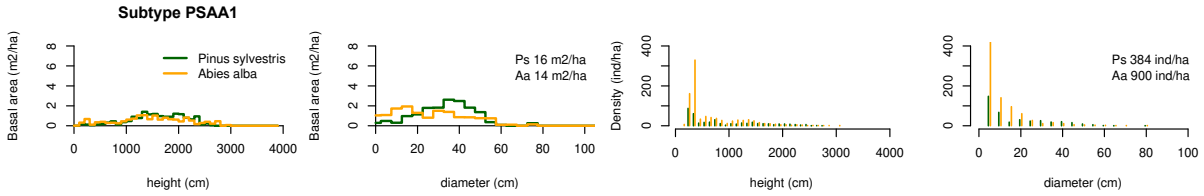

Table S4.11 Structural statistics of the forest subtype co-dominated by *Pinus sylvestris* (PS) and *Abies alba* (AA).

Subtype	Plots	Av. N1	Av. N2	Av. BA1	Av. BA2	Av. D1	S.d. D1	Av. H1	S.d. H1	Av. D2	S.d. D2	Av. H2	S.d. H2
PSAA1	19	384	900	15.8	14.4	17.4	14.8	910	669	10.6	9.6	677	513

Fig. S4.12 Three subtypes of forests co-dominated by *Pinus sylvestris* (PS) and *Quercus ilex* (QI), ordered by increasing basal area. For each subtype and species we show the distribution of basal area (m^2/ha) among 1 m height classes and 5 cm diameter classes (first and second columns, respectively) and the distribution of density (ind./ha) among height and dbh classes (third and fourth columns, respectively).

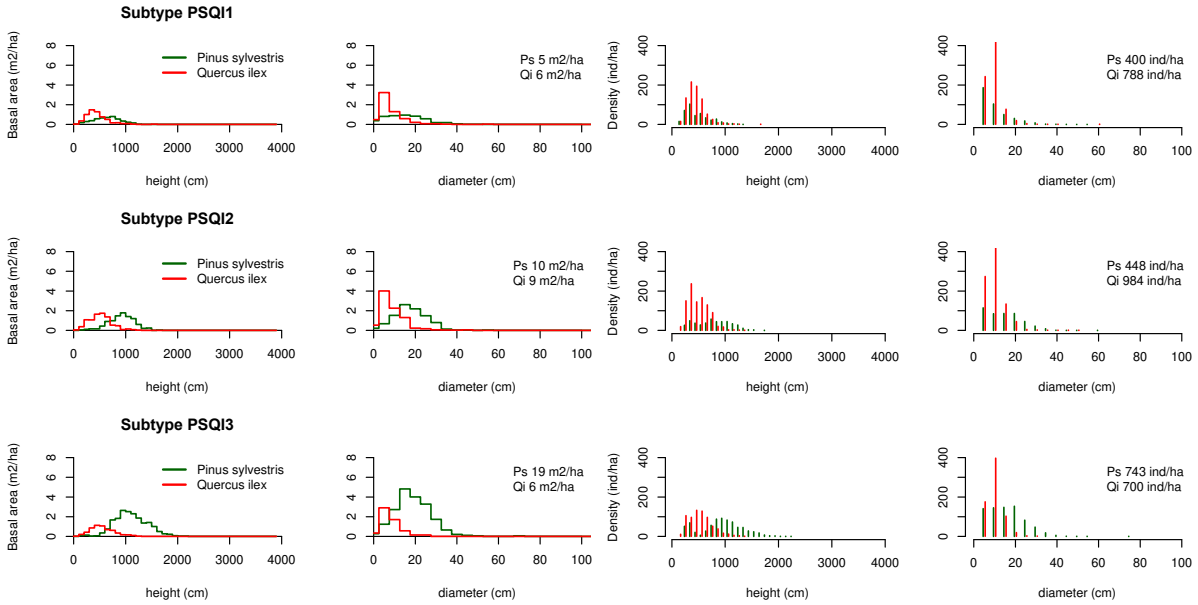

Table S4.12 Structural statistics of the forest subtypes co-dominated by *Pinus sylvestris* (PS) and *Quercus ilex* (QI), ordered by increasing basal area.

Subtype	Plots	Av. N1	Av. N2	Av. BA1	Av. BA2	Av. D1	S.d. D1	Av. H1	S.d. H1	Av. D2	S.d. D2	Av. H2	S.d. H2
PSQI1	67	400	788	4.9	6.0	10.4	6.9	512	231	9.0	3.9	454	155
PSQI2	39	448	984	9.8	8.7	14.6	8.1	799	311	9.7	4.3	508	183
PSQI3	37	743	700	19.2	5.8	16.1	8.4	960	384	9.5	3.9	546	207

Fig. S4.13 Two subtypes of forests co-dominated by *Pinus sylvestris* (PS) and *Quercus humilis* (QH), ordered by increasing basal area. For each subtype and species we show the distribution of basal area (m^2/ha) among 1 m height classes and 5 cm diameter classes (first and second columns, respectively) and the distribution of density (ind./ha) among height and dbh classes (third and fourth columns, respectively).

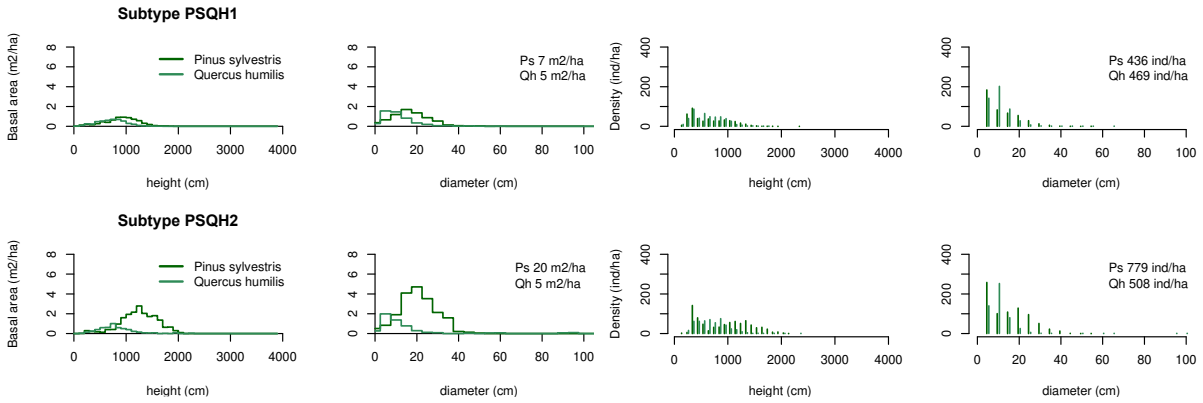

Table S4.13 Structural statistics of the forest subtypes co-dominated by *Pinus sylvestris* (PS) and *Quercus humilis* (QH), ordered by increasing basal area.

Subtype	Plots	Av. N1	Av. N2	Av. BA1	Av. BA2	Av. D1	S.d. D1	Av. H1	S.d. H1	Av. D2	S.d. D2	Av. H2	S.d. H2
PSQH1	89	436	469	6.9	4.8	11.9	7.8	676	350	10.2	5.1	642	271
PSQH2	45	779	508	19.7	5.3	15.2	9.6	962	461	10.2	5.3	708	261

Fig. S4.14 Two subtypes of forests co-dominated by *Pinus sylvestris* (PS) and *Quercus faginea* (QF), ordered by increasing basal area. For each subtype and species we show the distribution of basal area (m^2/ha) among 1 m height classes and 5 cm diameter classes (first and second columns, respectively) and the distribution of density (ind./ha) among height and dbh classes (third and fourth columns, respectively).

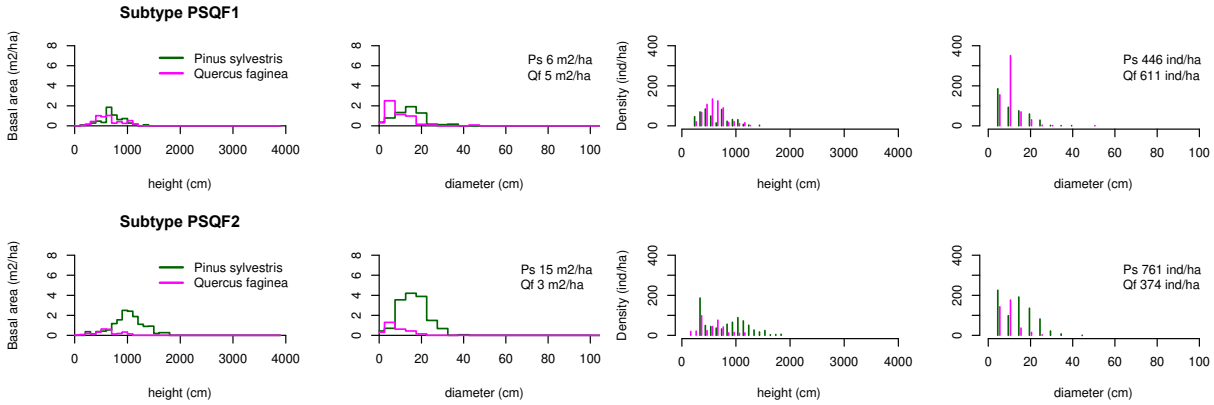

Table S4.14 Structural statistics of the forest subtypes co-dominated by *Pinus sylvestris* (PS) and *Quercus faginea* (QF), ordered by increasing basal area.

Subtype	Plots	Av. N1	Av. N2	Av. BA1	Av. BA2	Av. D1	S.d. D1	Av. H1	S.d. H1	Av. D2	S.d. D2	Av. H2	S.d. H2
PSQF1	11	446	610	6.2	5.3	11.4	6.9	626	267	9.6	4.3	623	194
PSQF2	13	761	374	15.0	2.8	13.9	7.6	852	384	8.9	4.0	586	231

Fig. S4.15 Subtype of forests co-dominated by *Pinus sylvestris* (PS) and *Fagus sylvatica* (FS). For each subtype and species we show the distribution of basal area (m^2/ha) among 1 m height classes and 5 cm diameter classes (first and second columns, respectively) and the distribution of density (ind./ha) among height and dbh classes (third and fourth columns, respectively).

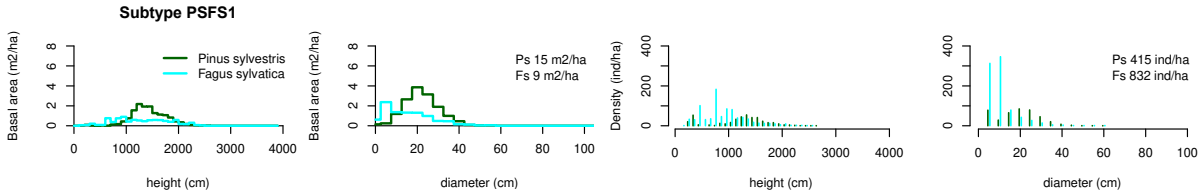

Table S4.15 Structural statistics of the forest subtype co-dominated by *Pinus sylvestris* (PS) and *Fagus sylvatica* (FS).

Subtype	Plots	Av. N1	Av. N2	Av. BA1	Av. BA2	Av. D1	S.d. D1	Av. H1	S.d. H1	Av. D2	S.d. D2	Av. H2	S.d. H2
PSFS1	31	415	832	14.8	9.3	19.0	9.6	1215	508	10.0	6.5	918	404

Fig. S4.16 Subtypes of forests co-dominated by *Pinus uncinata* (PU) and *Abies alba* (AA). For each subtype and species we show the distribution of basal area (m^2/ha) among 1 m height classes and 5 cm diameter classes (first and second columns, respectively) and the distribution of density (ind./ha) among height and dbh classes (third and fourth columns, respectively).

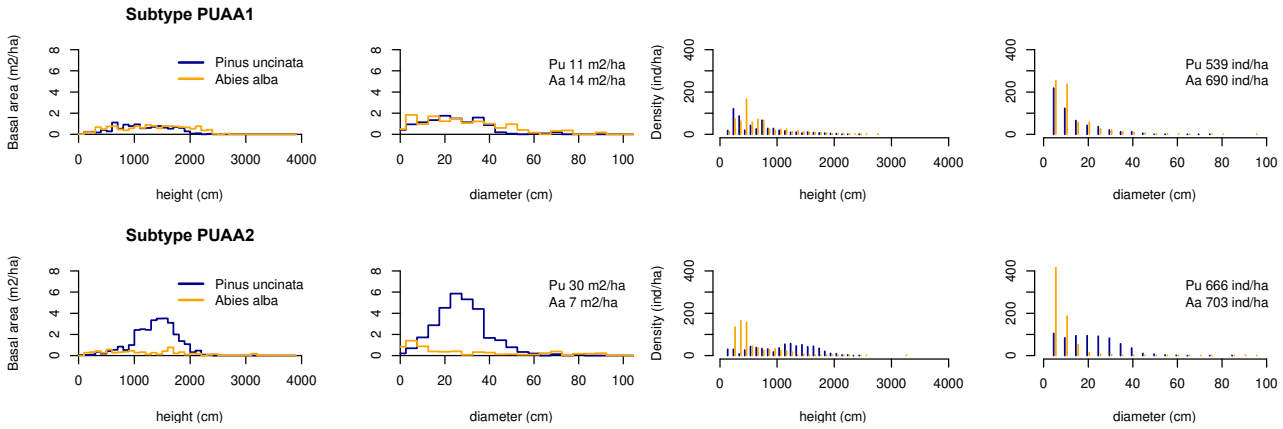

Table S4.16 Structural statistics of the forest subtype co-dominated by *Pinus uncinata* (PU) and *Abies alba* (AA).

Subtype	Plots	Av. N1	Av. N2	Av. BA1	Av. BA2	Av. D1	S.d. D1	Av. H1	S.d. H1	Av. D2	S.d. D2	Av. H2	S.d. H2
PUAA1	21	539	690	11.3	14.1	12.9	10.1	688	450	12.4	10.3	716	440
PUAA2	17	666	703	30.3	7.0	21.0	11.8	1124	506	8.3	7.5	565	346

Fig. S4.17 Subtype of forests co-dominated by *Pinus pinea* (PPI) and *P. pinaster* (PPS). For each subtype and species we show the distribution of basal area (m^2/ha) among 1 m height classes and 5 cm diameter classes (first and second columns, respectively) and the distribution of density (ind./ha) among height and dbh classes (third and fourth columns, respectively).

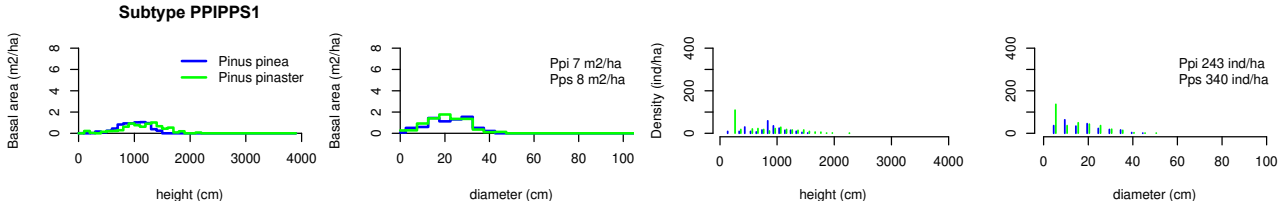

Table S4.17 Structural statistics of the forest subtype co-dominated by *Pinus pinea* (PPI) and *P. pinaster* (PPS).

Subtype	Plots	Av. N1	Av. N2	Av. BA1	Av. BA2	Av. D1	S.d. D1	Av. H1	S.d. H1	Av. D2	S.d. D2	Av. H2	S.d. H2
PPIPPS1	14	243	340	7.3	8.0	17.1	9.6	877	299	14.2	9.8	792	463

Fig. S4.18 Subtypes of forests co-dominated by *Pinus pinea* (PPI) and *Quercus ilex* (QI). For each subtype and species we show the distribution of basal area (m^2/ha) among 1 m height classes and 5 cm diameter classes (first and second columns, respectively) and the distribution of density (ind./ha) among height and dbh classes (third and fourth columns, respectively).

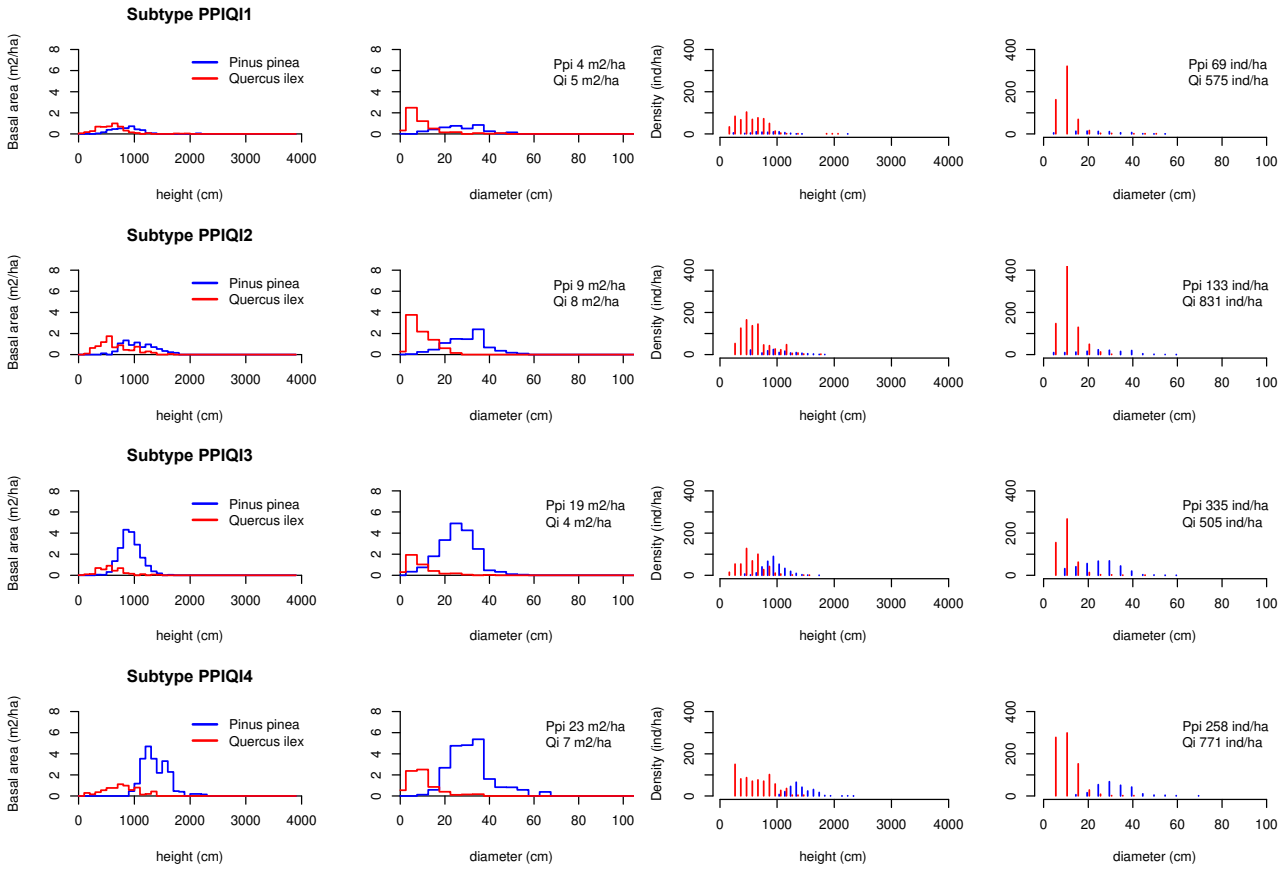

Table S4.18 Structural statistics of the forest subtypes co-dominated by *Pinus pinea* (PPI) and *Quercus ilex* (QI).

Subtype	Plots	Av. N1	Av. N2	Av. BA1	Av. BA2	Av. D1	S.d. D1	Av. H1	S.d. H1	Av. D2	S.d. D2	Av. H2	S.d. H2
PPIQI1	25	69	574	3.9	5.0	24.6	10.2	845	273	9.6	4.4	545	222
PPIQI2	13	133	830	8.6	8.4	26.1	11.7	1031	305	10.5	4.3	625	257
PPIQI3	21	335	504	18.9	4.1	25.4	8.6	979	186	9.3	4.2	557	202
PPIQI4	10	258	771	22.6	7.1	32.3	8.4	1443	200	9.7	4.8	639	291

Fig. S4.19 Subtypes of forests co-dominated by *Pinus pinea* (PPI) and *Quercus suber* (QS). For each subtype and species we show the distribution of basal area (m^2/ha) among 1 m height classes and 5 cm diameter classes (first and second columns, respectively) and the distribution of density (ind./ha) among height and dbh classes (third and fourth columns, respectively).

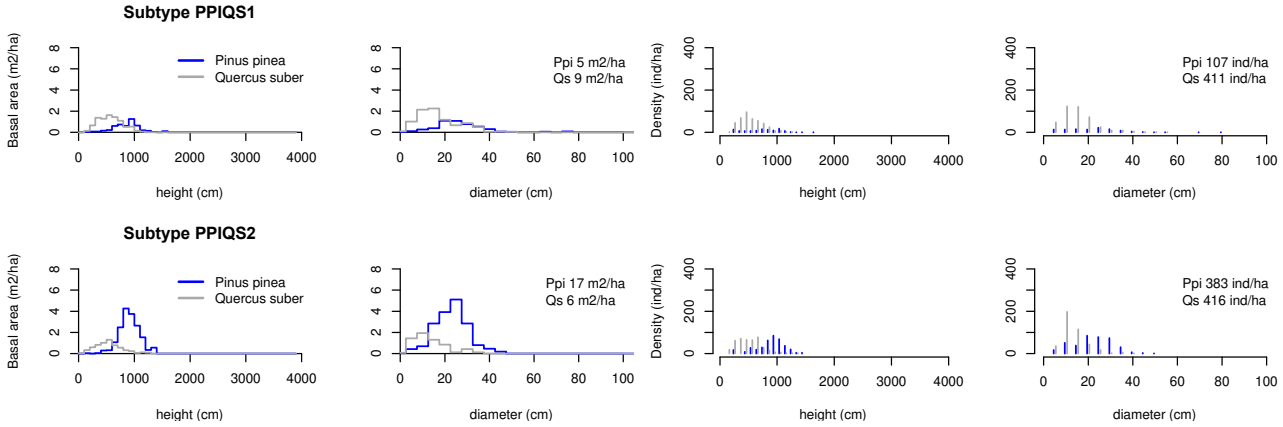

Table S4.19 Structural statistics of the forest subtypes co-dominated by *Pinus pinea* (PPI) and *Quercus suber* (QS).

Subtype	Plots	Av. N1	Av. N2	Av. BA1	Av. BA2	Av. D1	S.d. D1	Av. H1	S.d. H1	Av. D2	S.d. D2	Av. H2	S.d. H2
PPIQS1	29	107	411	4.9	8.9	21.4	11.0	775	305	14.9	7.3	551	195
PPIQS2	15	383	416	17.3	6.3	22.4	8.7	918	242	12.7	5.6	527	207

Fig. S4.20 Subtypes of forests co-dominated by *Pinus pinaster* (PPS) and *Quercus ilex* (QI). For each subtype and species we show the distribution of basal area (m^2/ha) among 1 m height classes and 5 cm diameter classes (first and second columns, respectively) and the distribution of density (ind./ha) among height and dbh classes (third and fourth columns, respectively).

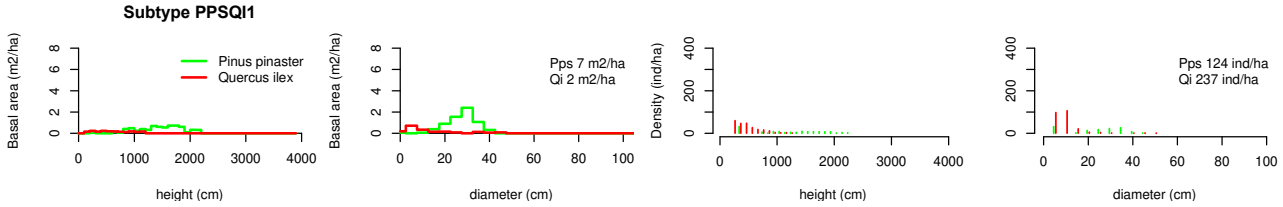

Table S4.20 Structural statistics of the forest subtype co-dominated by *Pinus pinaster* (PPS) and *Quercus ilex* (QI).

Subtype	Plots	Av. N1	Av. N2	Av. BA1	Av. BA2	Av. D1	S.d. D1	Av. H1	S.d. H1	Av. D2	S.d. D2	Av. H2	S.d. H2
PPSQI1	12	124	237	6.8	1.9	23.3	12.2	1210	590	8.7	5.2	493	212

Fig. S4.21 Subtype of forests co-dominated by *Pinus pinaster* (PPS) and *Quercus suber* (QS). For each subtype and species we show the distribution of basal area (m^2/ha) among 1 m height classes and 5 cm diameter classes (first and second columns, respectively) and the distribution of density (ind./ha) among height and dbh classes (third and fourth columns, respectively).

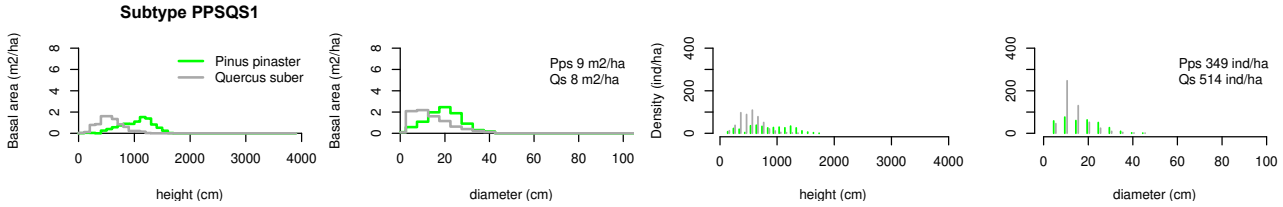

Table S4.21 Structural statistics of the forest subtype co-dominated by *Pinus pinaster* (PPS) and *Quercus suber* (QS).

Subtype	Plots	Av. N1	Av. N2	Av. BA1	Av. BA2	Av. D1	S.d. D1	Av. H1	S.d. H1	Av. D2	S.d. D2	Av. H2	S.d. H2
PPSQS1	33	385	514	9.5	8.5	16.5	8.6	885	365	13.2	6.0	547	194

Fig. S4.22 Subtypes of forests co-dominated by *Abies alba* (AA) and *Fagus sylvatica* (FS). For each subtype and species we show the distribution of basal area (m^2/ha) among 1 m height classes and 5 cm diameter classes (first and second columns, respectively) and the distribution of density (ind./ha) among height and dbh classes (third and fourth columns, respectively).

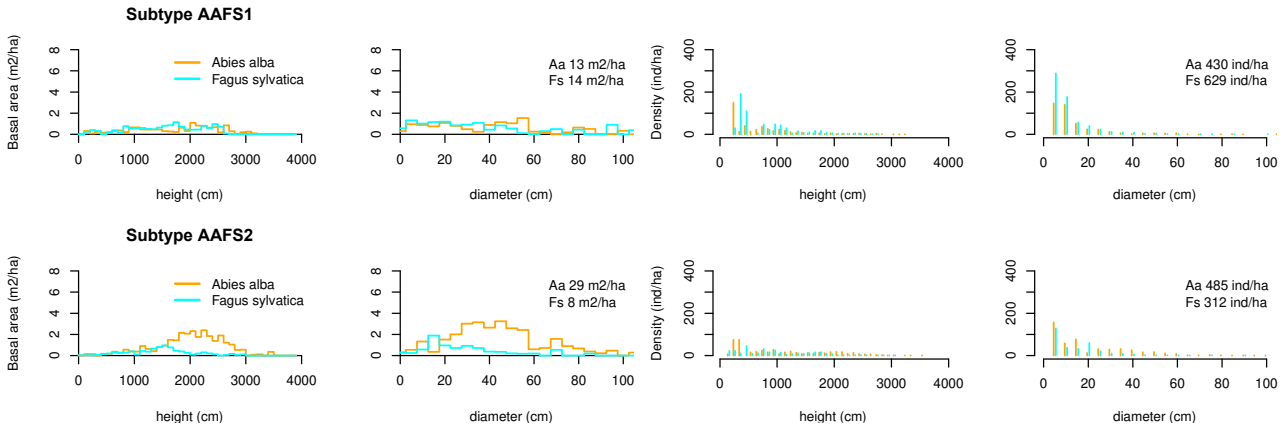

Table S4.22 Structural statistics of the forest subtypes co-dominated by *Abies alba* (AA) and *Fagus sylvatica* (FS).

Subtype	Plots	Av. N1	Av. N2	Av. BA1	Av. BA2	Av. D1	S.d. D1	Av. H1	S.d. H1	Av. D2	S.d. D2	Av. H2	S.d. H2
AAFS1	13	430	629	12.7	13.9	13.8	13.7	768	595	11.8	11.9	813	528
AAFS2	17	485	312	28.9	8.3	20.9	18.0	1131	780	14.4	11.6	971	605

Fig. S4.23 Subtypes of forests co-dominated by *Quercus ilex* (QI) and *Q. suber* (QS). For each subtype and species we show the distribution of basal area (m^2/ha) among 1 m height classes and 5 cm diameter classes (first and second columns, respectively) and the distribution of density (ind./ha) among height and dbh classes (third and fourth columns, respectively).

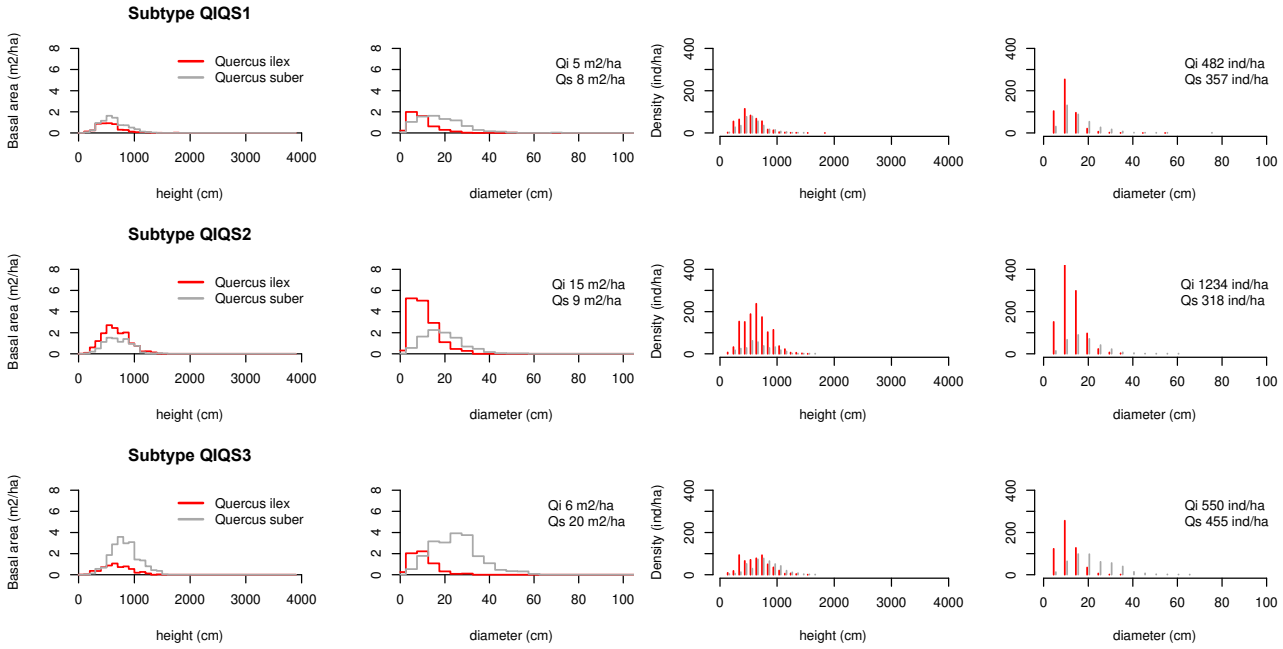

Table S4.23 Structural statistics of the forest subtypes co-dominated by *Quercus ilex* (QI) and *Q. suber* (QS).

Subtype	Plots	Av. N1	Av. N2	Av. BA1	Av. BA2	Av. D1	S.d. D1	Av. H1	S.d. H1	Av. D2	S.d. D2	Av. H2	S.d. H2
QIQS1	58	482	357	4.9	8.1	10.5	4.4	554	197	15.1	7.6	593	206
QIQS2	33	1234	318	15.4	9.5	11.7	4.6	668	222	17.9	7.6	702	237
QIQS3	22	550	455	6.1	20.3	10.9	4.7	644	232	21.8	9.7	795	250

Fig. S4.24 Subtypes of forests co-dominated by *Quercus ilex* (QI) and *Q. humilis* (QH). For each subtype and species we show the distribution of basal area (m^2/ha) among 1 m height classes and 5 cm diameter classes (first and second columns, respectively) and the distribution of density (ind./ha) among height and dbh classes (third and fourth columns, respectively).

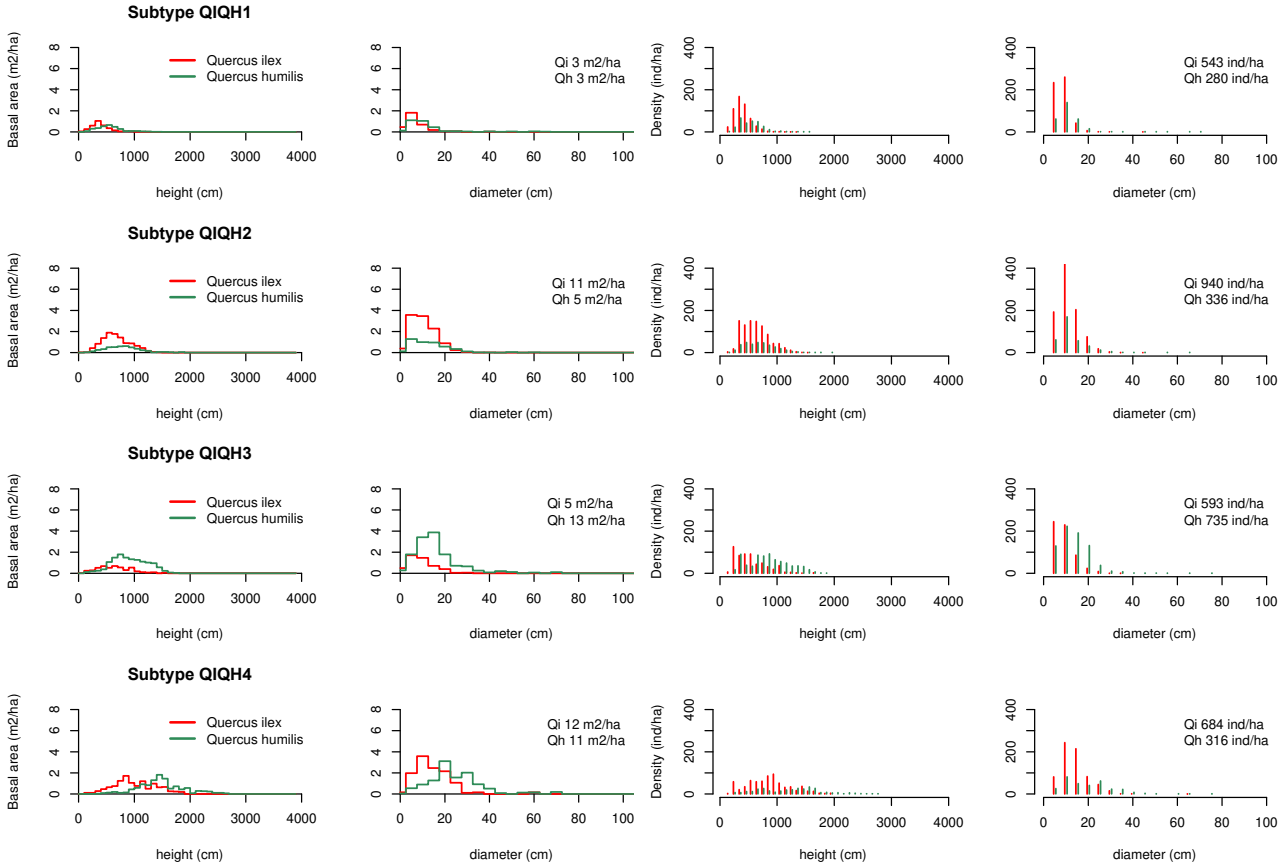

Table S4.24 Structural statistics of the forest subtypes co-dominated by *Quercus ilex* (QI) and *Q. humilis* (QH).

Subtype	Plots	Av. N1	Av. N2	Av. BA1	Av. BA2	Av. D1	S.d. D1	Av. H1	S.d. H1	Av. D2	S.d. D2	Av. H2	S.d. H2
QIQH1	70	543	280	3.3	3.1	8.1	3.5	423	139	10.7	5.0	550	199
QIQH2	51	940	336	10.9	4.5	11.1	4.8	657	232	11.7	5.9	705	272
QIQH3	20	593	734	4.9	13.4	9.1	4.6	566	264	13.6	6.8	866	346
QIQH4	11	684	316	11.8	11.5	13.5	6.1	883	364	18.9	10.2	1242	516

Fig. S4.25 Subtype of forests co-dominated by *Quercus ilex* (QI) and *Q. faginea* (QF). For each subtype and species we show the distribution of basal area (m^2/ha) among 1 m height classes and 5 cm diameter classes (first and second columns, respectively) and the distribution of density (ind./ha) among height and dbh classes (third and fourth columns, respectively).

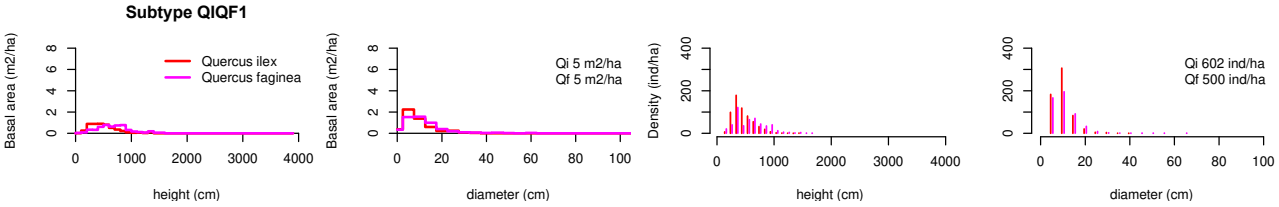

Table S4.25 Structural statistics of the forest subtype co-dominated by *Quercus ilex* (QI) and *Q. faginea* (QF).

Subtype	Plots	Av. N1	Av. N2	Av. BA1	Av. BA2	Av. D1	S.d. D1	Av. H1	S.d. H1	Av. D2	S.d. D2	Av. H2	S.d. H2
QIQF1	45	602	500	5.2	5.4	9.5	4.4	482	183	10.3	5.5	603	261

Fig. S4.26 Subtype of forests co-dominated by *Quercus suber* (QI) and *Q. humilis* (QH). For each subtype and species we show the distribution of basal area (m^2/ha) among 1 m height classes and 5 cm diameter classes (first and second columns, respectively) and the distribution of density (ind./ha) among height and dbh classes (third and fourth columns, respectively).

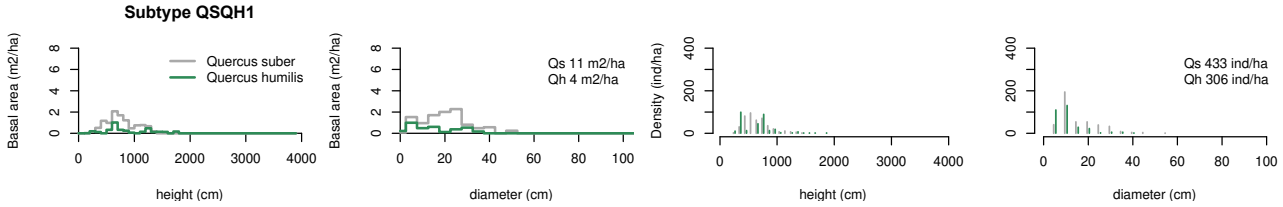

Table S4.26 Structural statistics of the forest subtype co-dominated by *Quercus suber* (QI) and *Q. humilis* (QH).

Subtype	Plots	Av. N1	Av. N2	Av. BA1	Av. BA2	Av. D1	S.d. D1	Av. H1	S.d. H1	Av. D2	S.d. D2	Av. H2	S.d. H2
QSQH1	10	432	306	10.7	3.5	15.4	8.8	679	229	10.3	6.4	655	282